OAK RIDGE NATIONAL LABORATORY LIBRARIES

3 4456 0550627 1

ORNL-TM-4917

Cy 2

Conceptual Design of the Special Nuclear Material Nondestructive Assay and Accountability System for the HTGR Fuel Refabrication Pilot Plant

J. D. Jenkins
S. R. McNeany
J. E. Rushton

OAK RIDGE NATIONAL LABORATORY
CENTRAL RESEARCH LIBRARY
DOCUMENT COLLECTION
LIBRARY LOAN COPY
DO NOT TRANSFER TO ANOTHER PERSON
If you wish someone else to see this document, send in name with document and the library will arrange a loan.

OAK RIDGE NATIONAL LABORATORY
OPERATED BY UNION CARBIDE CORPORATION • FOR THE U.S. ATOMIC ENERGY COMMISSION

Printed in the United States of America. Available from
National Technical Information Service
U.S. Department of Commerce
5285 Port Royal Road, Springfield, Virginia 22161
Price: Printed Copy $5.45; Microfiche $2.25

This report was prepared as an account of work sponsored by the United States Government. Neither the United States nor the Energy Research and Development Administration, nor any of their employees, nor any of their contractors, subcontractors, or their employees, makes any warranty, express or implied, or assumes any legal liability or responsibility for the accuracy, completeness or usefulness of any information, apparatus, product or process disclosed, or represents that its use would not infringe privately owned rights.

ORNL-TM-4917
UC-77 — Gas-Cooled
Reactor Technology

Contract No. W-7405-eng-26

Metals and Ceramics Division

Reactor Division

CONCEPTUAL DESIGN OF THE SPECIAL NUCLEAR MATERIAL NONDESTRUCTIVE ASSAY AND ACCOUNTABILITY SYSTEM FOR THE HTGR FUEL REFABRICATION PILOT PLANT

J. D. Jenkins*
S. R. McNeany*
J. E. Rushton*

July 1975

*On loan to the Metals and Ceramics Division from Reactor Division.

NOTICE This document contains information of a preliminary nature and was prepared primarily for internal use at the Oak Ridge National Laboratory. It is subject to revision or correction and therefore does not represent a final report.

OAK RIDGE NATIONAL LABORATORY
Oak Ridge, Tennessee 37830
operated by
UNION CARBIDE CORPORATION
for the
ENERGY RESEARCH AND DEVELOPMENT ADMINISTRATION

OAK RIDGE NATIONAL LABORATORY LIBRARIES
3 4456 0550627 1

Contents

Page

Abstract xi

1. Introduction 1
   1.1 HTGR Refabrication Pilot Plant Accountability and Safeguards Objectives 1
   1.2 Contents and Motivation for this Document 1

2. Overall System Description 3
   2.1 Plant Description and System Functions 3
   2.2 Material Flow Description 5
   2.3 Special Features Affecting Safeguards 24

3. Description of Material — Nuclear Characteristics Affecting Heavy Metal Assay 27
   3.1 Introduction 27
   3.2 Thorium-Uranium Loading Range and Uranium Isotopic Variation 27
   3.3 Uranium-232 and Uranium-233 Daughters: Concentrations and Effects 28
   3.4 Gamma Sources and Intensities 33
   3.5 Neutron Sources and Intensities 46
      3.5.1 Spontaneous Fission 46
      3.5.2 (α, n) Neutrons 47
   3.6 Thermal Emissions 49
   3.7 Neutron Response Characteristics 51
      3.7.1 Neutron Cross Sections and Fission Thresholds 51
      3.7.2 Gamma Yield 56

4. Physical Characteristics of Materials that Affect Heavy-Metal Assay 59
   4.1 Introduction 59
   4.2 Solutions 59
   4.3 Loaded Resin 60
   4.4 Bare and Coated Particles 60
   4.5 Green and Carbonized Rods 63
      4.5.1 Description of Green and Carbonized Fuel Rods 63
      4.5.2 Physical Aspects Affecting Assay 63
   4.6 Loaded Fuel Blocks 70
      4.6.1 Introduction 70
      4.6.2 Physical Characteristics Affecting Assay 70
   4.7 Waste Streams 77

5. Assay System Description 83
   5.1 Assay Philosophy 83
   5.2 Assay System Description 84

Page

5.3 Specific Conceptual Design Solutions 85
5.3.1 On-line Assay Machine 85
5.3.2 On-line Gamma-Scan Machine 92
5.3.3 High-Uranium-Content Waste Assay System 94
5.3.4 Low-level Waste Assay System 98
5.3.5 Sample Inspection Station Radioassay Unit 100
5.4 Standards 111

6. Data Flow and Data Handling 114
6.1 Hardware Description 114
6.2 Software Description and Data Flow 114
6.3 Real-Time Dynamic System Model 117

LIST OF FIGURES

Figure		Page
2.1	Floor plan of HTGR fuel refabrication pilot plant	6
2.2	Equipment Layout for cell D (TURF)	7
2.3	Pilot plant material flowsheet number 1	9
2.4	Pilot plant material flowsheet number 2	11
2.5	Pilot plant material flowsheet number 3	13
2.6	Pilot plant material flowsheet number 4	15
2.7	Pilot plant material flowsheet number 5	18
2.8	Pilot plant material flowsheet number 6	20
2.9	Material flows through major assay points in the HTGR-FRPP	23
3.1	Decay chains of ^{232}Th and ^{232}U	29
3.2	Uranium-232 daughters radioactivity vs time for initially pure ^{232}U	31
3.3	Effect of postseparation time and type of separation on the radioactivity of ^{208}Tl per unit initial radioactivity of ^{232}U	32
3.4	Lead-212 number density vs time during and after 2-hr ^{220}Rn removal	34
3.5	Thallium-208 number density vs time during and after 2-hr ^{220}Rn removal	35
3.6	Uranium-233 decay chain	40
3.7	Gamma-ray spectrum ^{233}U with high-ppm ^{232}U content	41
3.8	Effect of postpurification time on the activity of ^{208}Tl for a typical sequence of operations in Kilorod Facility	44
3.9	Heat generation of 1g of ^{233}U containing 400, 800, and 1200 ppm ^{232}U as a function of time after uranium cleanup	52
3.10	Fission cross sections of the fissile nuclides ^{233}U and ^{235}U	53

Figure		Page
3.11	Fission cross sections for the fertile nuclides	54
4.1	Preparation of fuel particles from weak-acid resins	61
4.2	Photomicrograph at sectioned TRISO particle	64
4.3	Neutron self-shielding factors for weak-acid resin-derived ^{233}U kernels as a function of ^{233}U fuel rod loading for four diameters	71
4.4	Neutron self-shielding factors for weak-acid resin-derived ^{233}U kernels as a function of fissile kernel diameter for three kernel densities	72
4.5	Neutron self-shielding factors for weak-acid resin-derived ^{233}U kernels as a function of fissile kernel density for four kernel diameters	73
4.6	Ft. St. Vrain reactor fuel element	74
4.7	Typical 1160-MW(e) HTGR fuel element	75
4.8	HTGR-FRPP system 9 reject fissile and fertile material storage can conceptual design	79
5.1	Overall plant material flow and assay points	86
5.2	Specific neutron count rates and count rate ratios of ^{233}U and ^{232}Th irradiated in the ^{252}Cf assay device	89
5.3	HTGR fuel rod assay system	90
5.4	Californium-252 shuffler	96
5.5	Sample inspection station radioassay unit option 1 — californium-source device	104
5.6	Sample inspection station radioassay unit option 2 — californium-source multiplier device	105
5.7	Twin-bridge calorimeter for active HTGR fuel rod assay	108
5.8	Rabbit for assay of loose particles	110

Figure | Page

6.1 Schematic of the proposed plant accountability data handling system and the types of data available from each station 115

6.2 Schematic of on-line assay machine and data flow 116

List of Tables

Table		Page
2.1	Description of pilot plant systems	4
2.2	Calculated material flow rates corresponding to flowsheet number 1	10
2.3	Calculated material flow rates corresponding to flowsheet number 2	12
2.4	Calculated material flow rates corresponding to flowsheet number 3	14
2.5	Calculated material flow rates corresponding to flowsheet number 4	16
2.6	Calculated material flow rates corresponding to flowsheet number 5	19
2.7	Calculated material flow rates corresponding to flowsheet number 6	21
2.8	Summary of material flow rate calculations	22
2.9	Maximum percent error of assay measurements on input and output streams to remain within ±0.5% LEMUF standard	25
3.1	Recycle fuel block loading ranges for the commercial HTGR	28
3.2	Uranium isotopic composition for commercial HTGR recycle fuel	30
3.3	Gamma rays, energies, and yields from ^{233}U, ^{232}U, and ^{232}Th and their daughters	37
3.4	Dose rates in millirem per hour for a 1-g source of ^{233}U with 500-ppm ^{232}U (without shielding)	45
3.5	Dose rates in millirem per hour for a 1-g source of ^{233}U with 500-ppm ^{232}U (with 5-cm lead shield)	45
3.6	Time windows for handling ^{233}U-^{232}U fuels in a sample inspection laboratory	46
3.7	Specific activities and neutron-emission rates for spontaneous fission	47

Table		Page
3.8	Calculated yields of (α, n) neutrons from HTGR recycle fuel	48
3.9	Energy release of U-233, U-232, and U-232 daughters from radioactive decay	50
3.10	Thermal cross sections (barns) and resonance integrals for the uranium and thorium nuclides	55
3.11	Prompt fission neutron yields for thermal fission	55
3.12	Delayed neutron yields for thermal and fast fission	56
4.1	Dry loaded resin beads (average physical parameter values)	62
4.2	Calculated average composition of dry loaded resin beads	62
4.3	Carbonized resin beads (average physical parameter values)	65
4.4	Calculated average composition of carbonized resin beads	65
4.5	TRISO-coated particles (average physical parameter values)	66
4.6	Calculated average atom densities of TRISO-coated particles	67
4.7	Elemental composition of green fuel rods, wt%	68
4.8	Nuclear number densities of green fuel rods, atom/b-cm	68
4.9	Estimated average daily production of high-uranium-content solid-waste material	78
4.10	Estimated daily production of combustible and noncombustible low-level waste	81
5.1	Estimated daily nondestructive assay sample load during pilot plant operation	101
5.2	Performance and design characteristics of ^{252}Cf multiplier (CFX)	106

Table		Page
6.1	Proposed material accountability summary data sheet	118
6.2	Information type and application in calculating accountability data	120

ABSTRACT

The conceptual design of the fissile material assay and accountability system for the HTGR refabrication pilot plant has been established. The primary feature affecting the design is the high, time varying, gamma activity of the process material due to the unavoidable presence of uranium-232. This imposes stringent requirements for remote operation and remote maintainability of system components. At the same time, the remote operation lends itself to implementation of an automated data collection and processing system for real-time accountability. The high time-varying gamma activity of the material also precludes application of a number of techniques presently employed for light-water reactor fuel assay. The techniques selected for application in the refabrication facility are (1) active thermal neutron interrogation with fast-fission or delayed-neutron counting for fuel-rod and small-sample assay, (2) calorimetry for high-level waste assay, and (3) passive gamma scanning for low-level waste assay, and rapid on-line relative rod-loading measurements. The principal nondestructive assay subsystems are identified as (1) on-line devices for 100% product fuel rod assay and quality control, (2) a multipurpose device in the sample inspection laboratory for small-sample assay and secondary standards calibration, and (3) equipment for assay of high- and low-uranium content scrap and waste materials. A data processing system, which coordinates data from these subsystems with information from other process control sensors, is included to provide real-time material balance information.

1. INTRODUCTION

1.1 HTGR REFABRICATION PILOT PLANT ACCOUNTABILITY AND SAFEGUARDS OBJECTIVES

The objective behind the design and operation of the HTGR Refabrication Prototype Plant is the development of refabrication processes, equipment, practices, and procedures required to allow the establishment of a commercial HTGR fuel recycle operation. As part of this program accountability and safeguards equipment and procedures will be required to demonstrate that the information necessary to ensure the amount of material unaccounted for (MUF) during the refabrication operation and the associated limits of error (LEMUF) can be defined at levels suitable for commercial plant operation. In addition, nondestructive assay equipment will be required to provide quality control and quality assurance information on in-process and final-product material to provide process control data and to provide information for criticality safety. Actual operation of the pilot plant will be in accordance with ORNL standards for material accountability and will be governed by the requirements specified in ORNL-2800.[1]

It must be emphasized that the objectives of the accountability and safeguards program for the prototype plants are developmental in nature. Resasonable and achievable values for MUF and LEMUF for the ^{232}Th-^{233}U fuel, with its attendant problems of high ^{232}U daughter activity and the requirement for remote operation, are currently poorly defined. One objective of the prototype plant operation will be to establish these values and develop and demonstrate the equipment and techniques for implementing the material control program. Operation of the prototype plant will serve to check the methods and equipment and the adequacy of the material control program. Where necessary, equipment or procedures will be modified during plant operation to improve accountability techniques and meet design objectives.

1.2 CONTENTS AND MOTIVATION FOR THIS DOCUMENT

The purposes of this document are fivefold. First, it is intended to present a unified picture of the fissile material assay and accountability system as currently conceptualized for the HTGR refabrication pilot plant to be constructed in the TURF facility. Several components of the assay system are described in a number of the System Design Descriptions (SDDs),[2] which are a portion of the conceptual design package of the pilot plant. However, no systematic description of the overall assay system previously existed to describe the proposed integrated functioning of these devices in conjunction with a centralized plant data processing system. This document is designed to fulfill that function.

Second, this document presents (under one cover) a description of those nuclear and physical characteristics of the product and waste materials peculiar to the HTGR ^{233}U-^{232}Th fuel which strongly influence the selection and design of nondestructive assay techniques and devices.

Third, the document identifies the principal assay points for the plant and describes the current conceptual design solutions to achieve fissile material assay at those locations and the rationale behind their selection. The physics and mechanical constraints and desired performance characteristics of each proposed device is discussed in as much detail as is presently available, and, in some cases, alternative solutions are presented.

Fourth, it is intended to serve a programmatic function by defining areas of additional analytical and experimental work that are required before a final design solution to the pilot plant assay problem can be developed.

Fifth and finally, the document is intended to serve as a basis for a technical review by nonproject personnel of the overall conceptual design of the pilot plant assay and accountability system.

REFERENCES FOR SECTION 1

1. *Source and Special Nuclear Materials Procedures Manual*, ORNL-2800 (May 15, 1963).

2. *HTGR Fuel Refabrication Pilot Plant — Conceptual Design Report*, GCR: 74-30, vols 1 through 4, (Nov. 1, 1974).

2. OVERALL SYSTEM DESCRIPTION

2.1 PLANT DESCRIPTION AND SYSTEM FUNCTIONS

The purpose of the HTGR refabrication pilot plant is to develop and demonstrate the processes, equipment, and procedures necessary to allow establishment of a commercial-sized HTGR fuel recycle facility. In keeping with this objective, the plant is envisioned as a fully integrated facility in which all aspects of operation including material handling, waste handling, system interfacing, and plant control can be demonstrated on prototypic or scalable equipment. The design objective of the pilot plant is the production of approximately two and one-half reactor-grade fuel elements per day. This output corresponds to the successful processing of ∿25 kg of heavy metal per day, of which about 2.5 kg is ^{233}U. By comparison, a commercial facility designed to support a 20,000 MW(e) HTGR economy would, at equilibrium, be required to process ∿400 kg of heavy metal or 40 kg of ^{233}U per day, assuming a 60% plant availability factor. As a matter of interest, this quantity of material translates to $\sim 1.6 \times 10^5$ fuel rods (or ∿1,600,000,000 coated particles) per day.

Despite these disparities in total capacity, the requirement for a demonstration of prototypic equipment can be achieved in the pilot plant, since much of the equipment is limited in size either by criticality considerations or for process reasons.

The plant is divided into ten systems. These are enumerated in Table 2.1. Six of the systems encompass specific pieces of equipment which perform the operations necessary to transmute the product from one well defined form to another as it progresses through the plant. The quality control and quality assurance functions are performed in a sample inspection laboratory designated system 7, and the integrated plant data management system that interfaces with all seven operating systems is designated system 8. The assay equipment does not exist as a separate system (in the vernacular of the pilot plant conceptual design documentation) but is incorporated as subcomponents in several systems throughout the plant.

Detailed descriptions of the functioning and conceptual design of the specific pilot plant systems are available from a number of sources.[1-3] Only sufficient detail is included here to familiarize the reader with the general functioning of the plant and to provide a framework for understanding the fissile material flow description and flow diagrams which follow in Sect. 2.2.

The fissile material will enter the Thorium-Uranium Fuel Cycle Development Facility in the form of clean uranyl nitrate solution (125 g/liter) stripped of fission products and uranium daughter product activity. Preparation of the feed solution by solvent extraction and ion exchange will have been done in system 1, Uranium Feed Preparation,

Table 2.1. Description of pilot plant systems

System number	System name
1	Uranium feed preparation
2	Resin loading
3	Resin carbonization
4	Microsphere coating
5	Fuel rod fabrication
6	Fuel element assembly
7	Sample inspection
8	Process control and data handling
9	Waste handling
10	Materials handling

which is located at ORNL but outside the TURF facility. The fresh feed solution will be prepared in three batches to produce a lot containing a total of ∿45 kg of uranium, sufficient for approximately ten days sustained operation of the pilot plant, and shipped to TURF in three 15-kg shipments.

In system 2, Resin Loading, the uranium will be loaded onto weak-acid resin kernels by contacting the resin with the uranium-containing solution. Four batches containing ∿1 kg of uranium will be prepared daily. The loaded resin will be dried and passed to system 3, Resin Carbonization, where the entire day's supply will be carbonized by heating to 800°C to decompose the constituent hydrocarbons and drive off the hydrogen component.

The carbonized resin is then passed to system 4, Microsphere Coating, where, in sequential operations in the same coating furnace, the material is converted to $UC_2 + UO_2$ and four layers of coating are deposited on the individual fuel kernels.

The coatings, from inside out, are: (1) a low-density buffer layer of pyrolytic carbon ∿50 μm thick, (2) a high-density isotropic layer of pyrolytic carbon ∿35 μm thick, (3) a silicon carbide layer ∿30 μm thick, and (4) a second high-density isotopic pyrolytic carbon layer.

Following coating, the particles pass to system 5, Fuel Rod Fabrication, where they are blended with the fertile ThO_2-coated particles and inert graphite shim and dispensed into molds. These are then injected

with a matrix of heated pitch and graphite filler that percolates through the interstices between particles to form a solid "green" fuel rod. An on-line assay machine (see Sect. 5.3.1) is included as part of the system 5 equipment. A 100% assay of the green rods will be performed as they emerge from the rod fabrication equipment and are passed to system 6, Element Assembly.

In system 6 the rods are loaded into fuel blocks and carbonized in place by passing the blocks through a whole-block carbonization and annealing furnace. Final processes performed in system 6 include cleaning, the insertion of indexing dowels, and canning of the element for shipment.

The entire process, from system 2 through system 6, will be housed in three contiguous hot cells in the TURF and will be operated remotely. Figure 2.1 is a plan view of the facility. Figure 2.2 a layout of cell D which houses systems 3 through 5, indicates the mechanical complexity of the process equipment.

Throughout the process, samples will be extracted from the process line and diverted to system 7, Sample Inspection, for quality control and quality assurance purposes. In addition, substantial quantities of reject material are anticipated from a number of the process steps. This material, plus samples returned from the sample inspection station and other contaminated wastes, will be routed to system 9, Waste Handling, for appropriate segregation, canning, assay, and disposal.

A detailed material flow analysis and process flow charts depicting the material flow through each of the separate systems are given in the following section.

2.2 MATERIAL FLOW DESCRIPTION

The design of an efficient assay system requires accurate estimates of the quantities of fissionable material that will be passing through the assay machines. To generate this data, a computer program, NOMUF,[4] has been developed. The code requires that flow sheets of the refabrication process steps be prepared according to a certain generalized format. Data describing these flow sheets must be supplied as input for the code.

The flow sheets for the currently proposed facility appear in Figs. 2.3 through 2.8. Each figure describes in detail the material flow through one subsystem of the total process. The first figure, entitled Material Receiving (TURF), is supplied merely as a starting point for flows into the plant. Examination of the flow sheets reveals that each process box is a junction point for either two or three flows. These are a main input flow, a main output flow, and, in some cases, a secondary output removal flow. The removal flow contains samples, rejects, or waste. Estimates have been made for the expected average removal percentages at each point involving samples, rejects, or waste. The

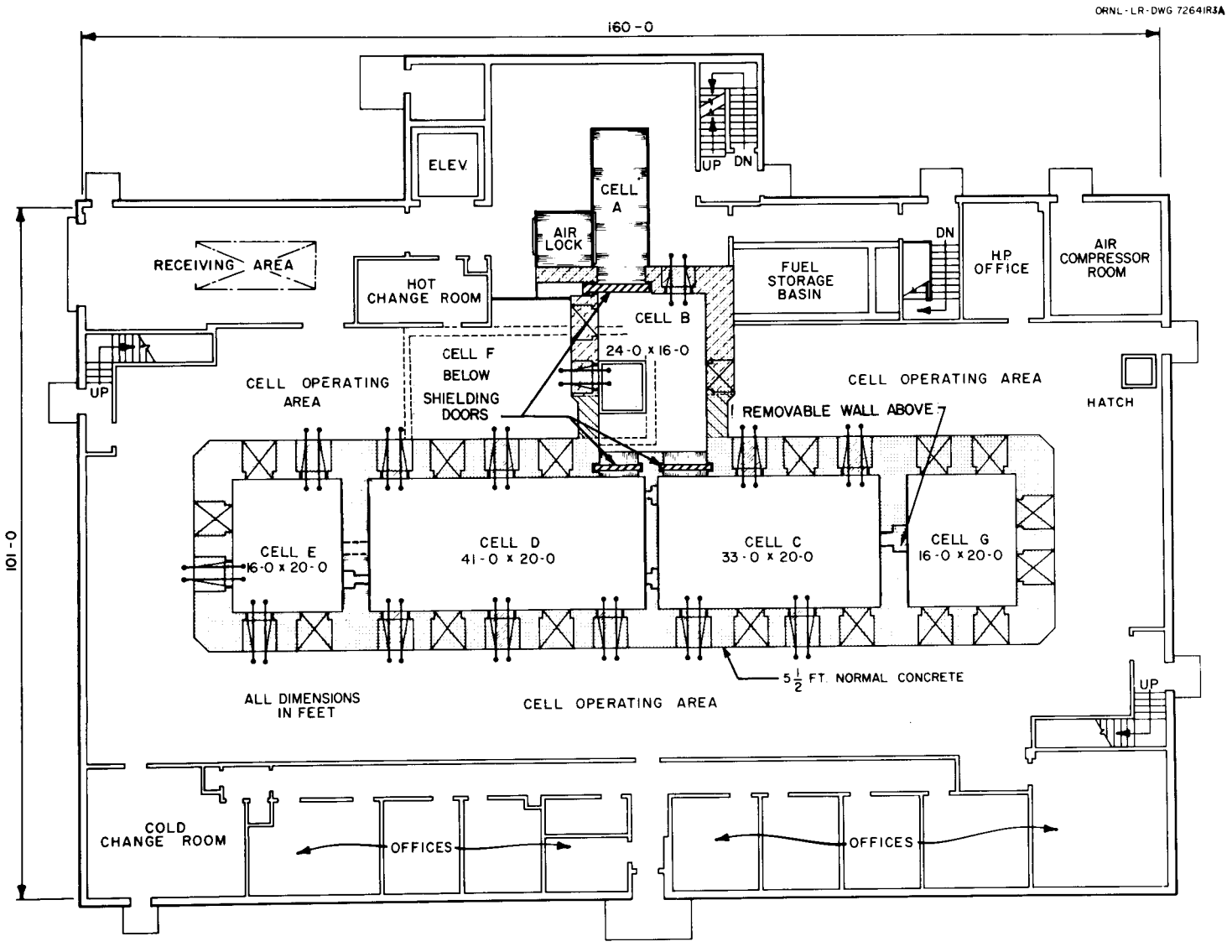

Fig. 2.1. Floor plan of HTGR fuel refabrication pilot plant.

ORNL-DWG 75-4453

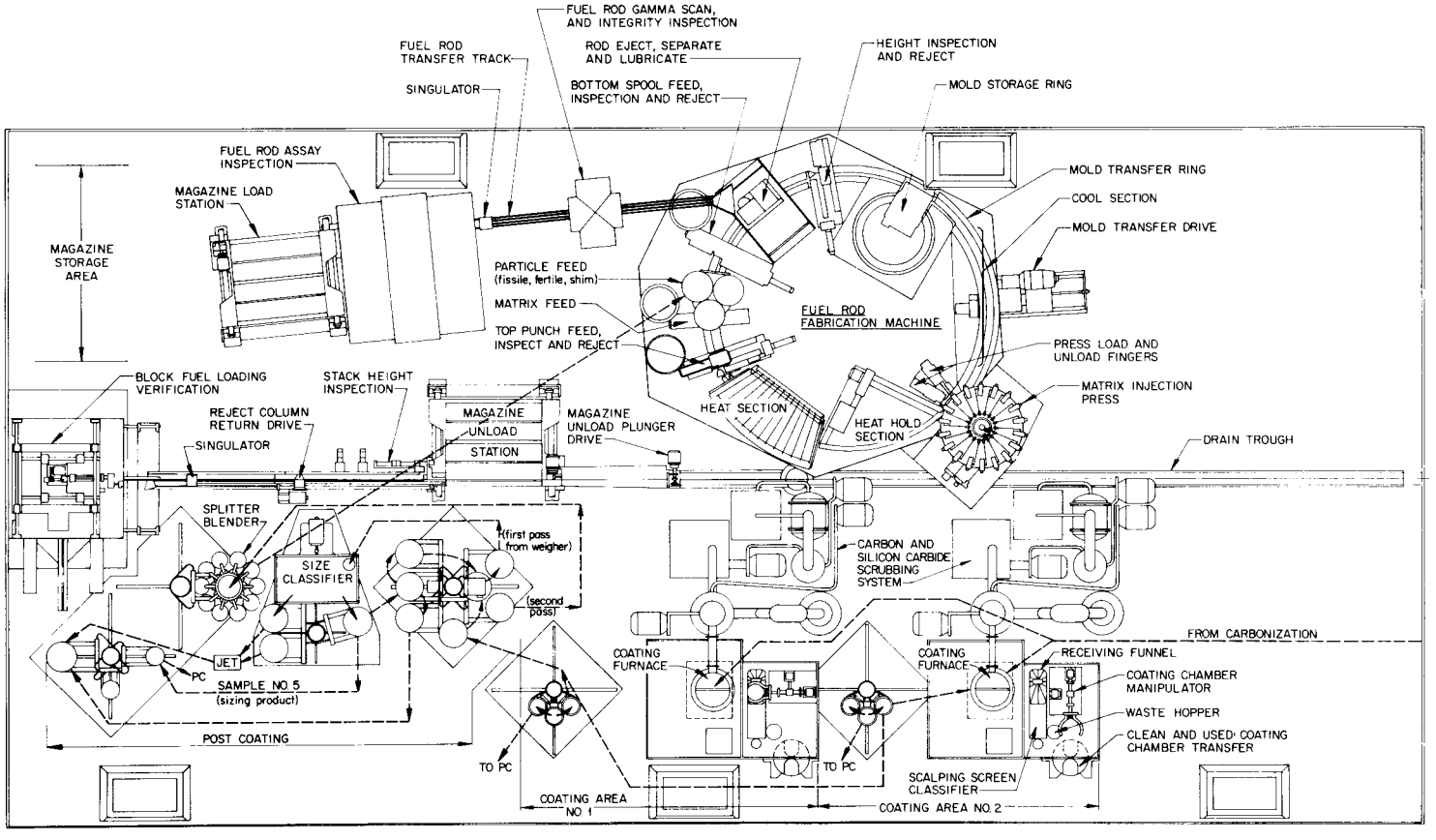

Fig. 2.2. Equipment layout for cell D (TURF).

current limiting factor on the maximum flows through the plant occurs in the conversion and coating system. Here, the coating furnace is being designed to handle 3.0 kg of uranium per day.

All of the above information along with a typical thorium-to-uranium ratio in the product elements for the Fort St. Vrain reactor is input to the code, which in turn calculates the expected average flow rates of uranium and thorium through each step in the process. The results of the calculations are output in tabular form. Tables 2.2 through 2.8 give the results of a calculation corresponding to the maximum uranium flow rate through the coating furnace. The step numbers in the tables refer to blocks on the flow sheets.

The calculated material flows are useful in making a determination of the approximate assay precision needed on the plant input and output streams to meet LEMUF requirements. As an example, Fig. 2.9 shows what the relative flows would be through the major assay points in the HTGR-FRPP, based on the previous calculations. Ideally, all input and output streams should be assayed at the plant boundaries; however, the plant product is more amenable to assay just before final assembly, which is why the figure shows product assay before the end of the refabrication process. Two known samples are taken after the product assay, and they eventually end up as waste, contributing to redundancy in assay. A loading verification is made after the final assembly, and the fissile content of the removed samples is accounted for in the uranium content of the finished element; hence, the absolute error in the uranium content of the product element should be no greater than the absolute error in the assay of the rods filling it.

Assuming that the beginning inventory and final inventory are zero at accounting times, the total LEMUF in this example will be determined by the assay precision at the indicated points. Using an LEMUF of ±0.5% and a plant input of 100 units, one writes the following inequality.

$$\sqrt{E_1^2 + E_2^2 + E_3^2 + E_4^2} \leqslant 0.5 \ , \qquad (1)$$

where

E_1 = absolute error (in a 95% confidence interval) on the input stream,

E_2 = absolute error (95% confidence interval) on the product stream,

E_3 = absolute error (95% confidence interval) on the high uranium content waste stream,

E_4 = absolute error (95% confidence interval) on the low uranium content waste stream.

ORNL DWG 74-10168

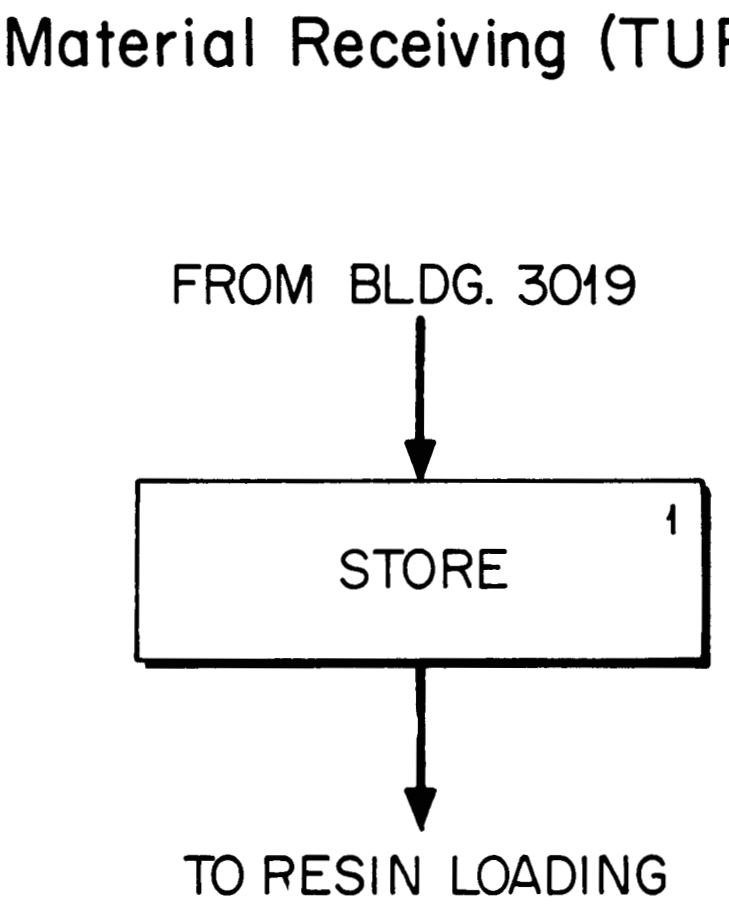

Fig. 2.3. Pilot plant material flowsheet number 1.

Table 2.2. Calculated material flow rates corresponding to flow sheet number 1

MATERIAL RECEIVING

STEP NO.	INPUT FLOW (KG. HEAVY METAL PER DAY)		REMOVAL FLOW (IF NON-ZERO) (KG. HEAVY METAL PER DAY)		PERCENT REMOVED
	URANIUM	THORIUM	URANIUM	THORIUM	
1	3.480	0.0			

PROCESS SUMMARY

URANIUM INPUT = 3.480 KGHM/DAY URANIUM OUTPUT = 3.480 KGHM/DAY TOTAL URANIUM REMOVED = 0.0 KGHM/DAY

THORIUM INPUT = 0.0 KGHM/DAY THORIUM OUTPUT = 0.0 KGHM/DAY TOTAL THORIUM REMOVED = 0.0 KGHM/DAY

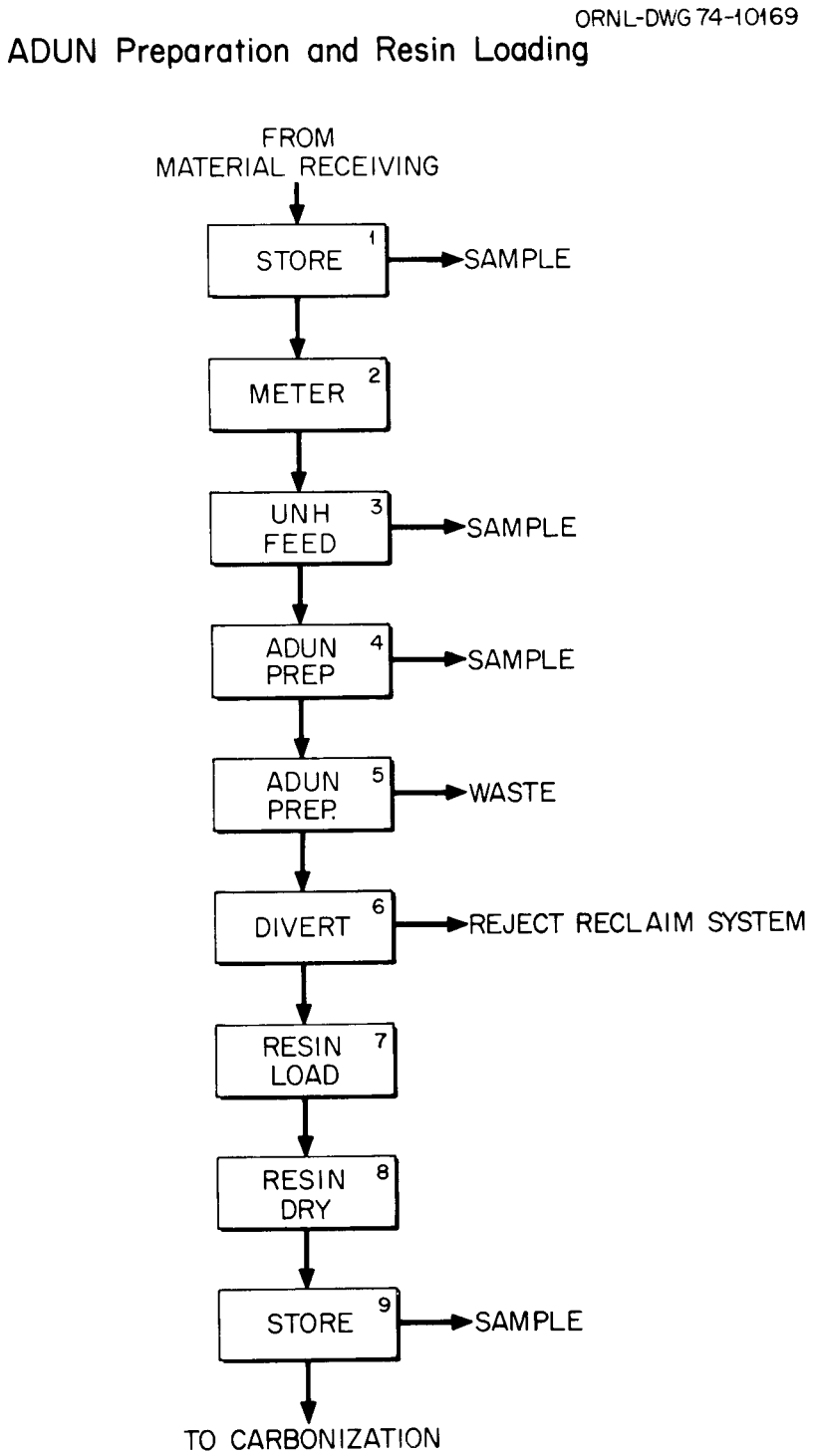

Fig. 2.4. Pilot plant material flowsheet number 2.

Table 2.3. Calculated material flow rates corresponding to flow sheet number 2
ADUN PREP. RESIN LOADING

STEP NO.	INPUT FLOW (KG. HEAVY METAL PER DAY) URANIUM	THORIUM	REMOVAL FLOW (IF NON-ZERO) (KG. HEAVY METAL PER DAY) URANIUM	THORIUM	PERCENT REMOVED
1	3.480	0.0	0.0001	0.0	0.002
2	3.480	0.0			
3	3.480	0.0	0.0010	0.0	0.030
4	3.479	0.0	0.0024	0.0	0.068
5	3.476	0.0	0.0014	0.0	0.040
6	3.475	0.0	0.0347	0.0	1.000
7	3.440	0.0			
8	3.440	0.0			
9	3.440	0.0	0.0010	0.0	0.030

PROCESS SUMMARY

URANIUM INPUT = 3.480 KGHM/DAY URANIUM OUTPUT = 3.439 KGHM/DAY TOTAL URANIUM REMOVED = 0.041 KGHM/DAY

THORIUM INPUT = 0.0 KGHM/DAY THORIUM OUTPUT = 0.0 KGHM/DAY TOTAL THORIUM REMOVED = 0.0 KGHM/DAY

ORNL-DWG 74-10170

Carbonization

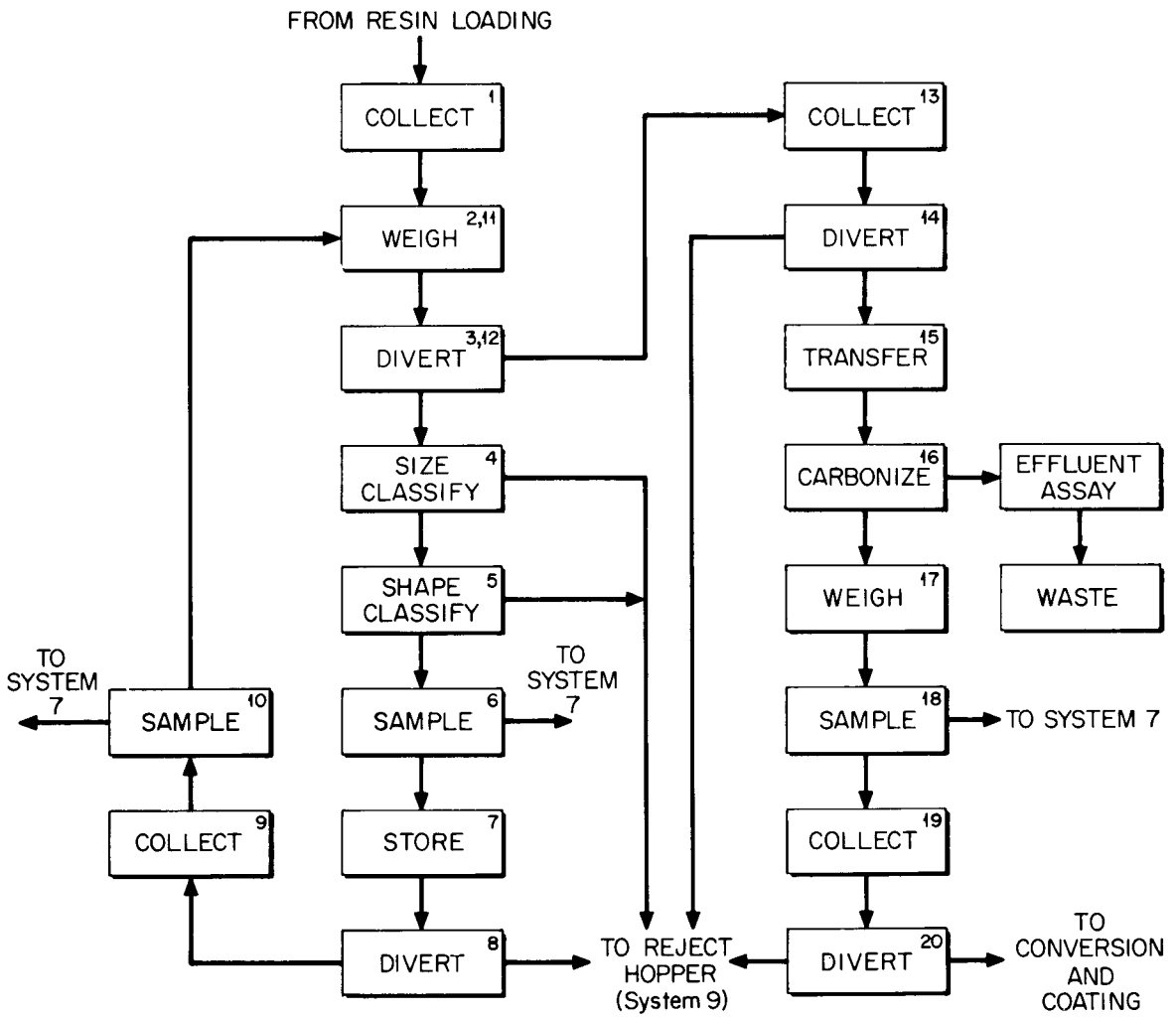

Fig. 2.5. Pilot plant material flowsheet number 3.

Table 2.4. Calculated material flow rates corresponding to flow sheet number 3

CARBONIZATION

STEP NO.	INPUT FLOW (KG. HEAVY METAL PER DAY) URANIUM	THORIUM	REMOVAL FLOW (IF NON-ZERO) (KG. HEAVY METAL PER DAY) URANIUM	THORIUM	PERCENT REMOVED
1	3.439	0.0			
2	3.439	0.0			
3	3.439	0.0			
4	3.439	0.0	0.0344	0.0	1.000
5	3.405	0.0	0.0340	0.0	1.000
6	3.371	0.0	0.0034	0.0	0.100
7	3.367	0.0			
8	3.367	0.0	0.1684	0.0	5.000
9	3.199	0.0			
10	3.199	0.0	0.0032	0.0	0.100
11	3.196	0.0			
12	3.196	0.0			
13	3.196	0.0			
14	3.196	0.0	0.0032	0.0	0.100
15	3.193	0.0			
16	3.193	0.0	0.0319	0.0	1.000
17	3.161	0.0			
18	3.161	0.0	0.0032	0.0	0.100
19	3.158	0.0			
20	3.158	0.0	0.1579	0.0	5.000

PROCESS SUMMARY

URANIUM INPUT = 3.439 KGHM/DAY URANIUM OUTPUT = 3.000 KGHM/DAY TOTAL URANIUM REMOVED = 0.440 KGHM/DAY

THORIUM INPUT = 0.0 KGHM/DAY THORIUM OUTPUT = 0.0 KGHM/DAY TOTAL THORIUM REMOVED = 0.0 KGHM/DAY

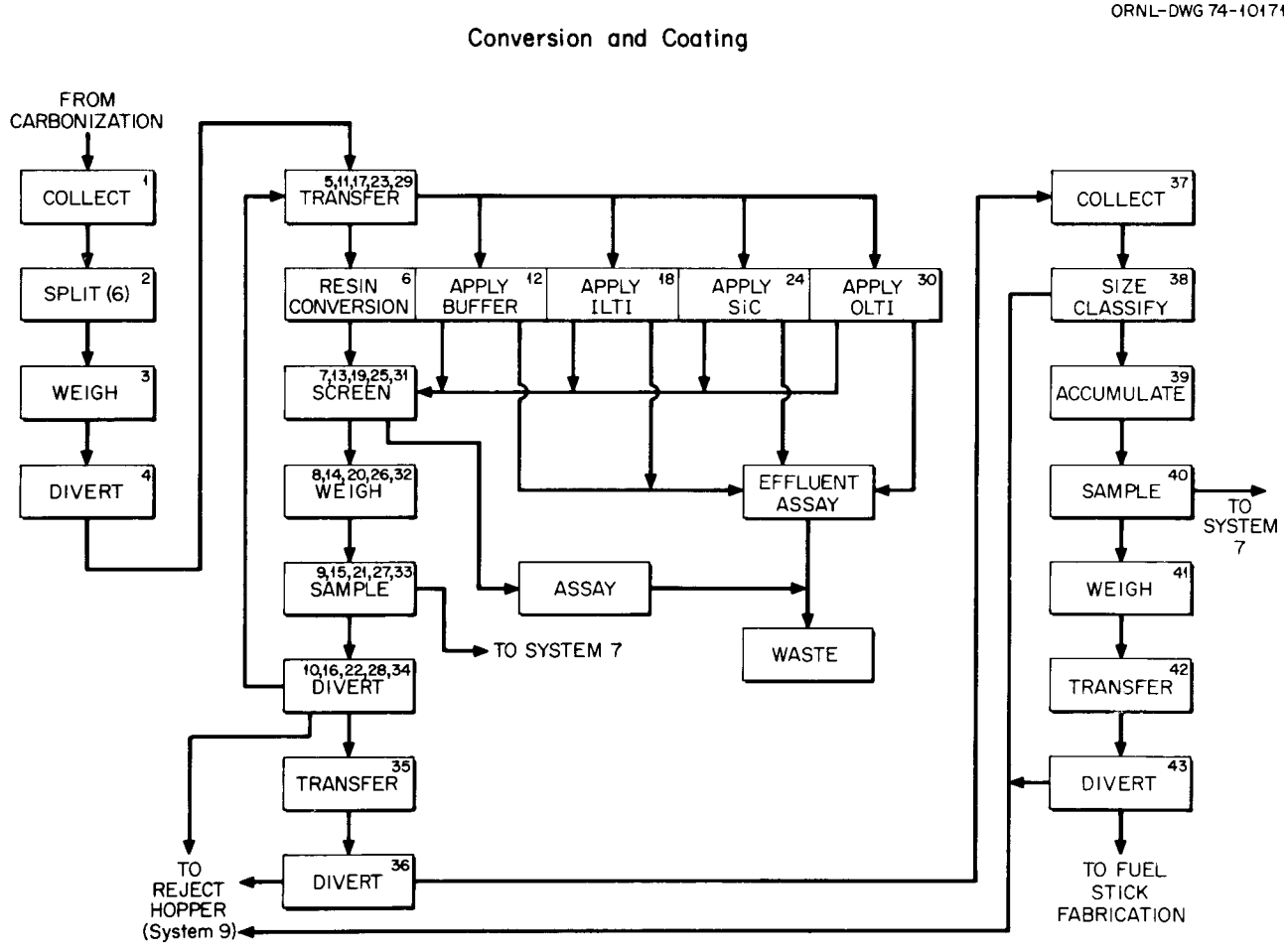

Fig. 2.6. Pilot plant material flowsheet number 4.

Table 2.5. Calculated material flow rates corresponding to flow sheet number 4
CONVERSION AND COATING

STEP NO.	INPUT FLOW (KG. HEAVY METAL PER DAY) URANIUM	THORIUM	REMOVAL FLOW (IF NON-ZERO) (KG. HEAVY METAL PER DAY) URANIUM	THORIUM	PERCENT REMOVED
1	3.000	0.0			
2	3.000	0.0			
3	3.000	0.0			
4	3.000	0.0			
5	3.000	0.0			
6	3.000	0.0	0.0030	0.0	0.100
7	2.997	0.0	0.0030	0.0	0.100
8	2.994	0.0			
9	2.994	0.0	0.0030	0.0	0.100
10	2.991	0.0			
11	2.991	0.0			
12	2.991	0.0	0.0030	0.0	0.100
13	2.988	0.0	0.0030	0.0	0.100
14	2.985	0.0			
15	2.985	0.0	0.0030	0.0	0.100
16	2.982	0.0	0.0596	0.0	2.000
17	2.922	0.0			
18	2.922	0.0	0.0029	0.0	0.100
19	2.919	0.0	0.0029	0.0	0.100
20	2.916	0.0			
21	2.916	0.0	0.0029	0.0	0.100
22	2.913	0.0	0.0583	0.0	2.000
23	2.855	0.0			

Table 2.5 (continued)

CONVERSION AND COATING

STEP NO.	INPUT FLOW (KG. HEAVY METAL PER DAY) URANIUM	THORIUM	REMOVAL FLOW (IF NON-ZERO) (KG. HEAVY METAL PER DAY) URANIUM	THORIUM	PERCENT REMOVED
24	2.855	0.0	0.0029	0.0	0.100
25	2.852	0.0	0.0029	0.0	0.100
26	2.849	0.0			
27	2.849	0.0	0.0028	0.0	0.100
28	2.846	0.0	0.0569	0.0	2.000
29	2.790	0.0			
30	2.790	0.0	0.0028	0.0	0.100
31	2.787	0.0	0.0028	0.0	0.100
32	2.784	0.0			
33	2.784	0.0	0.0028	0.0	0.100
34	2.781	0.0	0.0556	0.0	2.000
35	2.726	0.0			
36	2.726	0.0	0.0545	0.0	2.000
37	2.671	0.0			
38	2.671	0.0	0.0801	0.0	3.000
39	2.591	0.0			
40	2.591	0.0	0.0026	0.0	0.100
41	2.588	0.0			
42	2.588	0.0			
43	2.588	0.0	0.1294	0.0	5.000

PROCESS SUMMARY

URANIUM INPUT = 3.000 KGHM/DAY URANIUM OUTPUT = 2.459 KGHM/DAY TOTAL URANIUM REMOVED = 0.541 KGHM/DAY

THORIUM INPUT = 0.0 KGHM/DAY THORIUM OUTPUT = 0.0 KGHM/DAY TOTAL THORIUM REMOVED = 0.0 KGHM/DAY

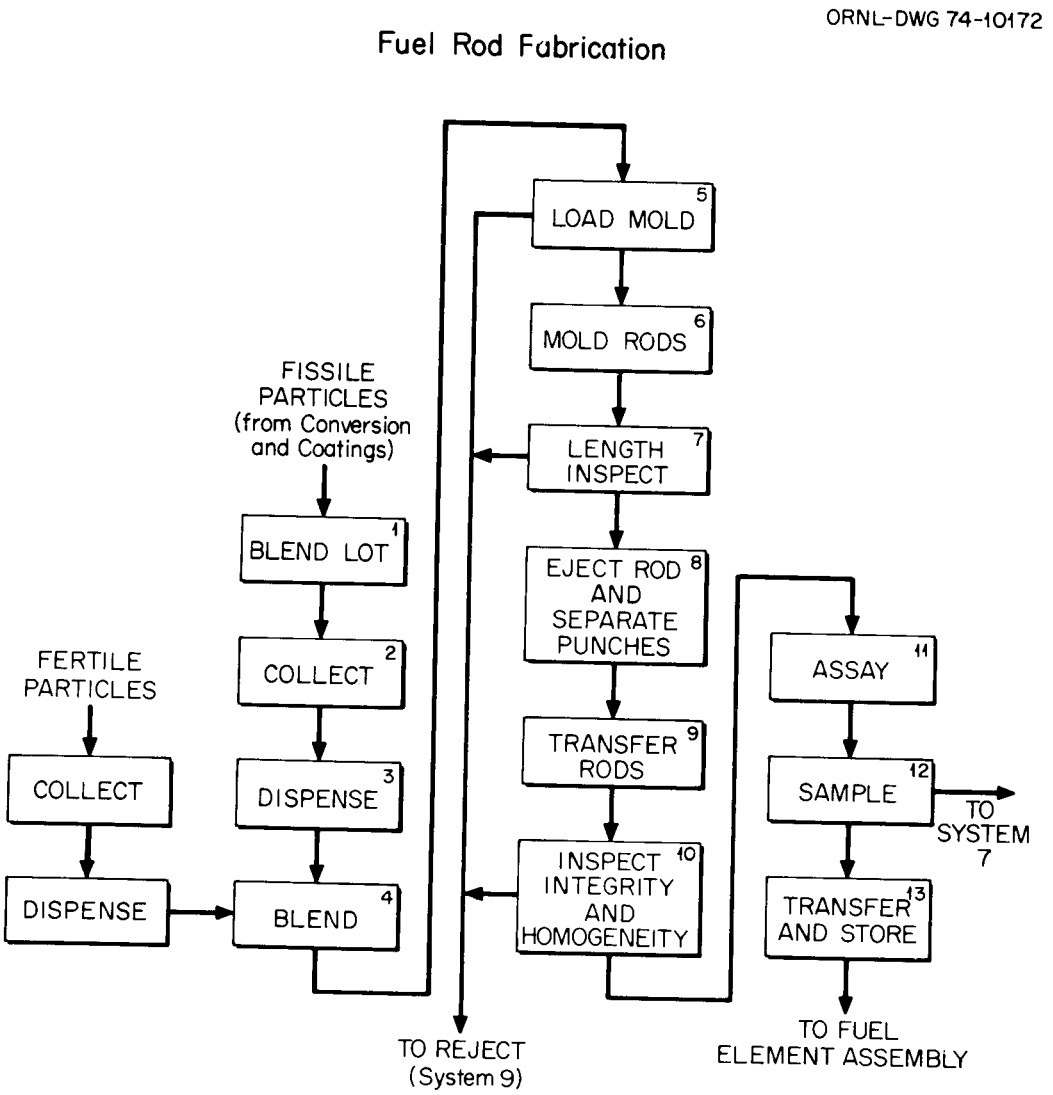

Fig. 2.7. Pilot plant material flowsheet number 5.

Table 2.6. Calculated material flow rates corresponding to flow sheet number 5

FUEL ROD FABRICATION

STEP NO.	INPUT FLOW (KG. HEAVY METAL PER DAY) URANIUM	THORIUM	REMOVAL FLOW (IF NON-ZERO) (KG. HEAVY METAL PER DAY) URANIUM	THORIUM	PERCENT REMOVED
1	2.459	0.0			
2	2.459	0.0			
3	2.459	0.0			
4	2.459	29.506			
5	2.459	29.506	0.0025	0.0295	0.100
6	2.456	29.477			
7	2.456	29.477	0.0074	0.0884	0.300
8	2.449	29.388			
9	2.449	29.388			
10	2.449	29.388	0.0024	0.0294	0.100
11	2.447	29.359			
12	2.447	29.359	0.0007	0.0088	0.030
13	2.446	29.350			

PROCESS SUMMARY

URANIUM INPUT = 2.459 KGHM/DAY URANIUM OUTPUT = 2.446 KGHM/DAY TOTAL URANIUM REMOVED = 0.013 KGHM/DAY

THORIUM INPUT = 29.506 KGHM/DAY THORIUM OUTPUT = 29.350 KGHM/DAY TOTAL THORIUM REMOVED = 0.156 KGHM/DAY

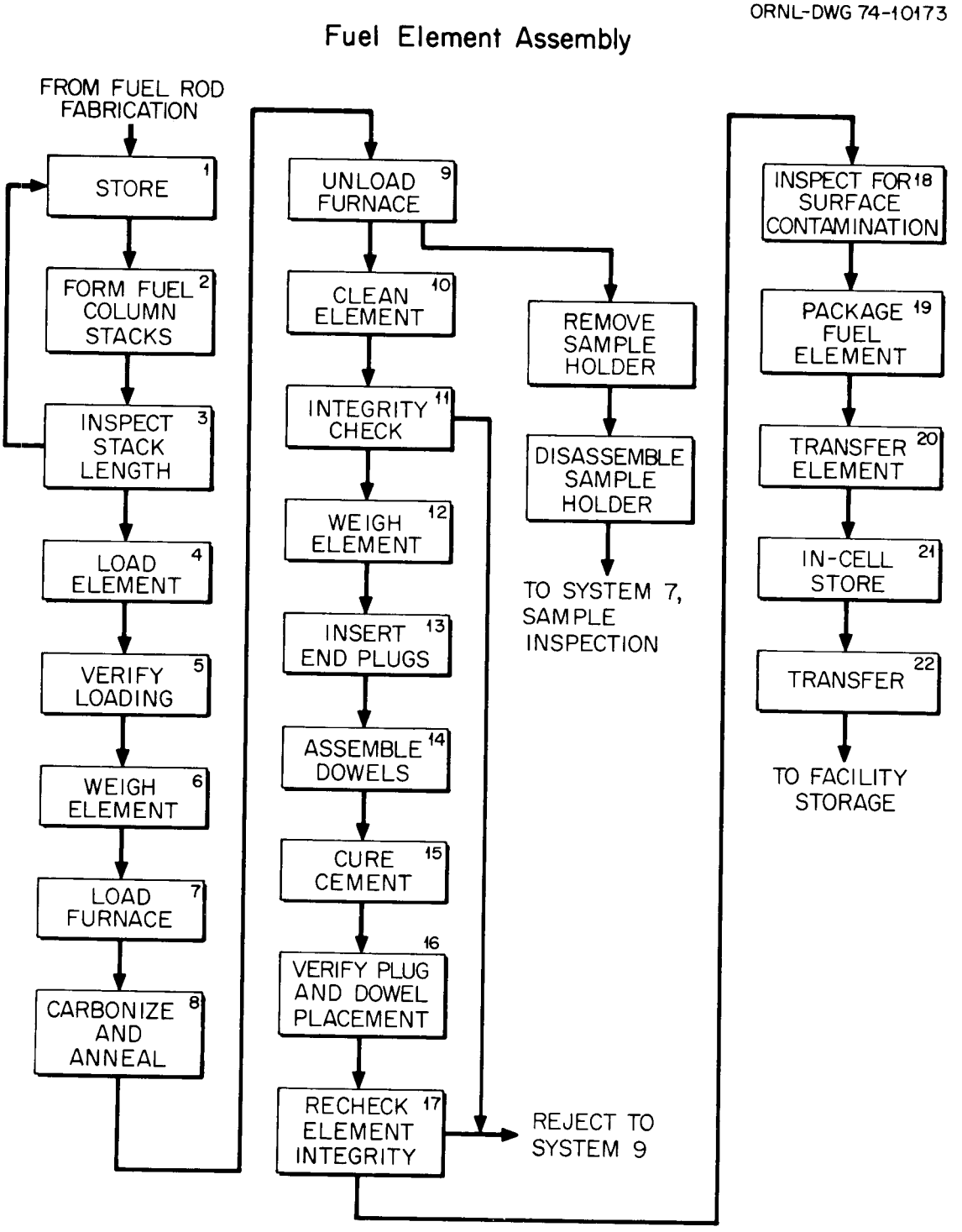

Fig. 2.8. Pilot plant material flowsheet number 6.

Table 2.7. Calculated material flow rates corresponding to flow sheet number 6

FUEL ELEMENT ASSEMBLY

STEP NO.	INPUT FLOW (KG. HEAVY METAL PER DAY) URANIUM	THORIUM	REMOVAL FLOW (IF NON-ZERO) (KG. HEAVY METAL PER DAY) URANIUM	THORIUM	PERCENT REMOVED
1	2.446	29.350			
2	2.446	29.350			
3	2.446	29.350			
4	2.446	29.350			
5	2.446	29.350			
6	2.446	29.350			
7	2.446	29.350			
8	2.446	29.350			
9	2.446	29.350	0.0108	0.1291	0.440
10	2.435	29.221			
11	2.435	29.221	0.0061	0.0731	0.250
12	2.429	29.148			
13	2.429	29.148			
14	2.429	29.148			
15	2.429	29.148			
16	2.429	29.148			
17	2.429	29.148	0.0061	0.0729	0.250
18	2.423	29.075			
19	2.423	29.075			
20	2.423	29.075			
21	2.423	29.075			
22	2.423	29.075			

PROCESS SUMMARY

URANIUM INPUT = 2.446 KGHM/DAY URANIUM OUTPUT = 2.423 KGHM/DAY TOTAL URANIUM REMOVED = 0.023 KGHM/DAY

THORIUM INPUT = 29.350 KGHM/DAY THORIUM OUTPUT = 29.075 KGHM/DAY TOTAL THORIUM REMOVED = 0.275 KGHM/DAY

Table 2.8. Summary of material flow rate calculations

	PROCESS NAME	INPUT (KGHM/DAY)		OUTPUT (KGHM/DAY)		TOTAL REMOVED (KGHM/DAY)	
		URANIUM	THORIUM	URANIUM	THORIUM	URANIUM	THORIUM
1	MATERIAL RECEIVING	3.480	0.0	3.480	0.0	0.0	0.0
2	ADUN PREP. RESIN LOADING	3.480	0.0	3.439	0.0	0.041	0.0
3	CARBONIZATION	3.439	0.0	3.000	0.0	0.440	0.0
4	CONVERSION AND COATING	3.000	0.0	2.459	0.0	0.541	0.0
5	FUEL ROD FABRICATION	2.459	29.506	2.446	29.350	0.013	0.156
6	FUEL ELEMENT ASSEMBLY	2.446	29.350	2.423	29.075	0.023	0.275

TOTAL AMOUNT OF URANIUN REMOVED FROM ALL PROCESSES = 1.057 KGHM/DAY

TOTAL AMOUNT OF THORIUM REMOVED FROM ALL PROCESSES = 0.431 KGHM/DAY

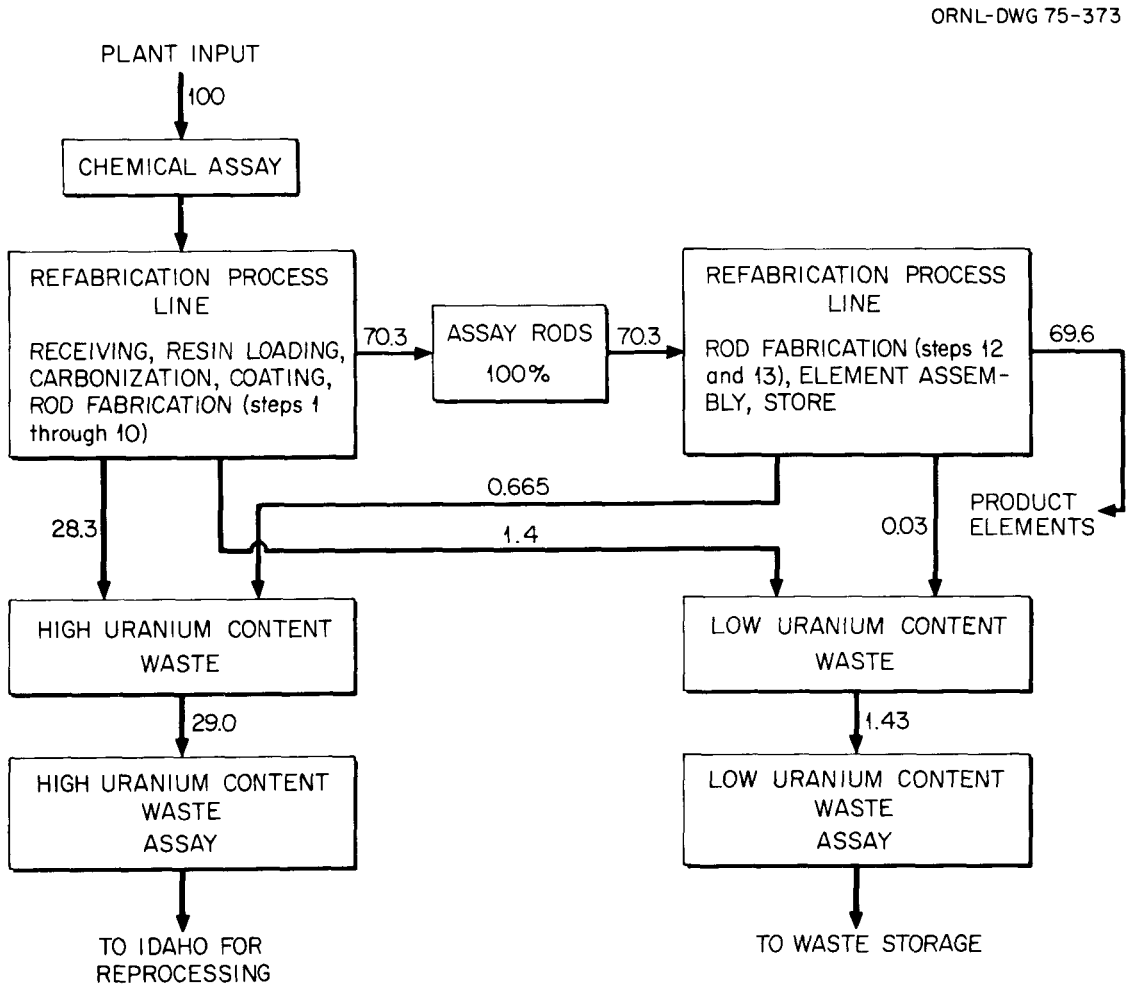

Fig. 2.9. Material flows through major assay points in the HTGR-FRPP.

In terms of material flows and relative errors in assay measurements, the absolute errors can be written as follows:

$$E_1 = P_1(100.0),$$

$$E_2 = P_2(70.3),$$

$$E_3 = P_3(29.0),$$

$$E_4 = P_4(1.43).$$

where

P_1 = relative error (95% confidence interval) on the input stream,

P_2 = relative error (95% confidence interval) on the product stream,

P_3 = relative error (95% confidence interval) on the high uranium content waste stream,

P_4 = relative error (95% confidence interval) on the low uranium content waste stream.

Substitution of the above into inequality (1) yields,

$$10{,}000\ P_1^2 + 4942\ P_2^2 + 841\ P_3^2 + 2.04\ P_4^2 \leqslant 0.25. \qquad (2)$$

Inequality (2) gives the relationship between the required assay precision at each point indicated on Fig. 2.9. Table 2.9 gives a number of solution sets that satisfy inequality (2). The first four sets give the maximum allowable error at each assay point, provided the others have no error.

2.3 SPECIAL FEATURES AFFECTING SAFEGUARDS

The special facilities and radiation shielding and containment required for the safe handling and processing of HTGR recycled fuel offer several advantages for safeguards.

The obvious special feature of this process is the almost total remote handling of the ^{233}U-bearing fuel. The remote nature of the process limits personnel access to the fissile material. Access to the material is not impossible, however, for two reasons. First, for material and equipment transfer, the processing cells are linked to other cells or to out-of-cell mechanisms. Second, some portions of the processing equipment may be maintained by having personnel enter the cells after appropriate source shielding or source removal. Thus some cells will be designed for personnel access. Although there is possible access,

Table 2.9. Maximum percent error of assay measurements on input and output streams to remain within ±0.5% LEMUF standard

Solution set	P_1 (Input stream)	P_2 (Product stream)	P_3 (High uranium content waste stream)	P_4 (Low uranium content waste stream)
1	0.500	0.0	0.0	0.0
2	0.0	0.711	0.0	0.0
3	0.0	0.0	1.72	0.0
4	0.0	0.0	0.0	35.0
5	0.100	0.500	1.13	7.00
6	0.100	0.300	1.49	7.00

all of the access points are controlled because of the requirement for alpha-activity containment. Health physics radiation monitors would provide an indication of breech of containment and of possible diversion. Because the ingress points from the cell are limited, portal monitors may also provide additional safeguards assurance.

It should be noted that although kilogram quantities of material represent high-radiation levels from the standpoint of occupational exposures, the levels of recently purified uranyl nitrate are low enough that direct handling of the material for several days would not result in noticeable health effects. Thus, diversion of unshielded material is not automatically precluded.

The remote nature of the refabrication process requires highly automated machinery for most of the fabrication. The elaborate control and monitoring instrumentation required for automatic operation and process control can provide additional data for material accountability and material balance consistency checks.

The planned computer-based management and monitoring program for the individual process systems provides real-time data suitable for adaption to a parallel real-time accountability system.

The remote nature of the process has the potential of substantially improving the safeguarding of the recycle fuel during refabrication. The extent of this improvement will depend on the specific facility design and on the degree to which the additional real-time process information can enhance the safeguards system.

REFERENCES FOR SECTION 2

1. *National HTGR Fuel Recycle Development Program Plan*, ORNL-4702, Rev. 1 (August 1973).

2. *Environmental Statement, HTGR Fuel Refabrication Pilot Plant*, WASH-1533 (August 1974).

3. *HTGR Fuel Refabrication Pilot Plant — Conceptual Design Report*, GCR:74-30 (November 1, 1974).

4. S. R. McNeany, *NOMUF — A Computer Code for Calculating Material Flows in the HTGR-FRPP*, GCR:74-23 (Sept. 9, 1974).

3. DESCRIPTION OF MATERIAL — NUCLEAR CHARACTERISTICS AFFECTING FISSILE MATERIAL ASSAY

3.1 INTRODUCTION

Certain nuclear properties of the fissile and fertile materials in the HTGR Fuel cycle are inherent through all phases of the process and exert a controlling influence on the selection and implementation of nondestructive assay techniques. Foremost among these is the high-gamma-radiation level associated with the ^{233}U due to the unavoidable inclusion of trace amounts of ^{232}U. This single factor vastly complicates the problem of performing all operations with the material, including nondestructive assay. For example, all operations must be performed remotely. This requirement imposes the physical complexities associated with automated operation and remote maintenance on the equipment design and increases by an order of magnitude the problems associated with construction, handling, and use of calibration standards. In addition, the high-gamma background excludes the application of certain proven techniques that have been developed for ^{235}U or clean ^{233}U systems and makes the implementation of others much more difficult.

Other nuclear characteristics that influence assay equipment selection and design include neutron response characteristics, delayed neutron yields, and (α,n) neutron production rates. All of these are discussed in detail below.

3.2 THORIUM-URANIUM LOADING RANGE AND URANIUM ISOTOPIC VARIATION

HTGR recycle fuel will contain fissile and fertile fuel particles. The fissile particles will be $\sim$670 μ in diameter and the fertile particles will be $\sim$820 μ in diameter. Uranium-233 in the form of UC_2 will be the prime heavy-metal constituent of the fissile particle, although other uranium isotopes will also be present. The fertile particle will contain thorium as ThO_2. These two types of particles are blended together in suitable proportions with a graphite "shim" material and are fabricated into fuel rods using a petroleum-based pitch mixed with graphite as a binder. The fuel rods to be fabricated in the pilot plant are of the Fort St. Vrain variety and are 1.94 in. long and 0.49 in. in diameter. These are loaded into holes in a hexagonal graphite block. Approximately 3130 rods are needed to fill a standard fuel element block. Fuel rods for commercial [1160 MW(e)] reactors that will be fabricated by a commercial facility will be similar in structure but longer and 5/8 in. in diameter.

The quantities of thorium and uranium that will be loaded into an element will vary considerably. This is due to the variety of functioning conditions that will exist in the operating reactors. Spatial-zoning factors and recycle-zoning factors will be changing from year-to-year during a transition period when the first quantities of recycle ^{233}U are introduced. Data on maximum and minimum loadings that are expected to be encountered have been supplied by General Atomic Company.[1] Table 3.1

gives the range of ^{233}U and thorium loadings that will occur during equilibrium. The values given are for the commercial HTGR, and the units are kilograms of heavy metal per fuel element block.

Table 3.1. Recycle fuel block loading ranges for the commercial HTGR

(Kilograms heavy metal per block)

Period	^{233}U	Thorium	Th/^{233}U ratio
Transition			
Maximum	0.72	12.1	16.8
Minimum	0.31	6.0	19.4
Equilibrium			
Maximum	0.72	11.6	16.1
Minimum	0.32	7.9	24.7

Table 3.2 gives the calculated uranium isotopic ratios for the beginning of recycle and at equilibrium recycle for the large commercial reactors.

From this information it is evident that nondestructive assay techniques developed for the HTGR fuel cycle must be able to accomodate a wide range of fissile loadings and uranium-to-thorium ratios. Conditions encountered in the pilot plant in processing Fort St. Vrain fuel will to a large extent cover the parameter ranges anticipated for a commercial facility.

3.3 Uranium-232 and Uranium-233 Daughters: Concentrations and Effects

All fuel material that contains ^{233}U also unavoidably contains small quantities of ^{232}U. This ^{232}U is formed through (n,2n) reactions in ^{233}U and (n,2n) reactions in ^{232}Th, followed by an (n,γ) reaction in ^{231}Pa. Most of the ^{232}U that is formed in thorium-bearing fuels results from the ^{232}Th(n,2n) reaction. In addition, for thorium ores containing appreciable quantities of ^{230}Th, significant amounts of ^{232}U may be formed from two sequential (n,γ) reactions on that isotope and its daughter, ^{231}Pa. These reactions, along with the natural radioactive decay chains of ^{232}U and ^{232}Th, are shown in Fig. 3.1.

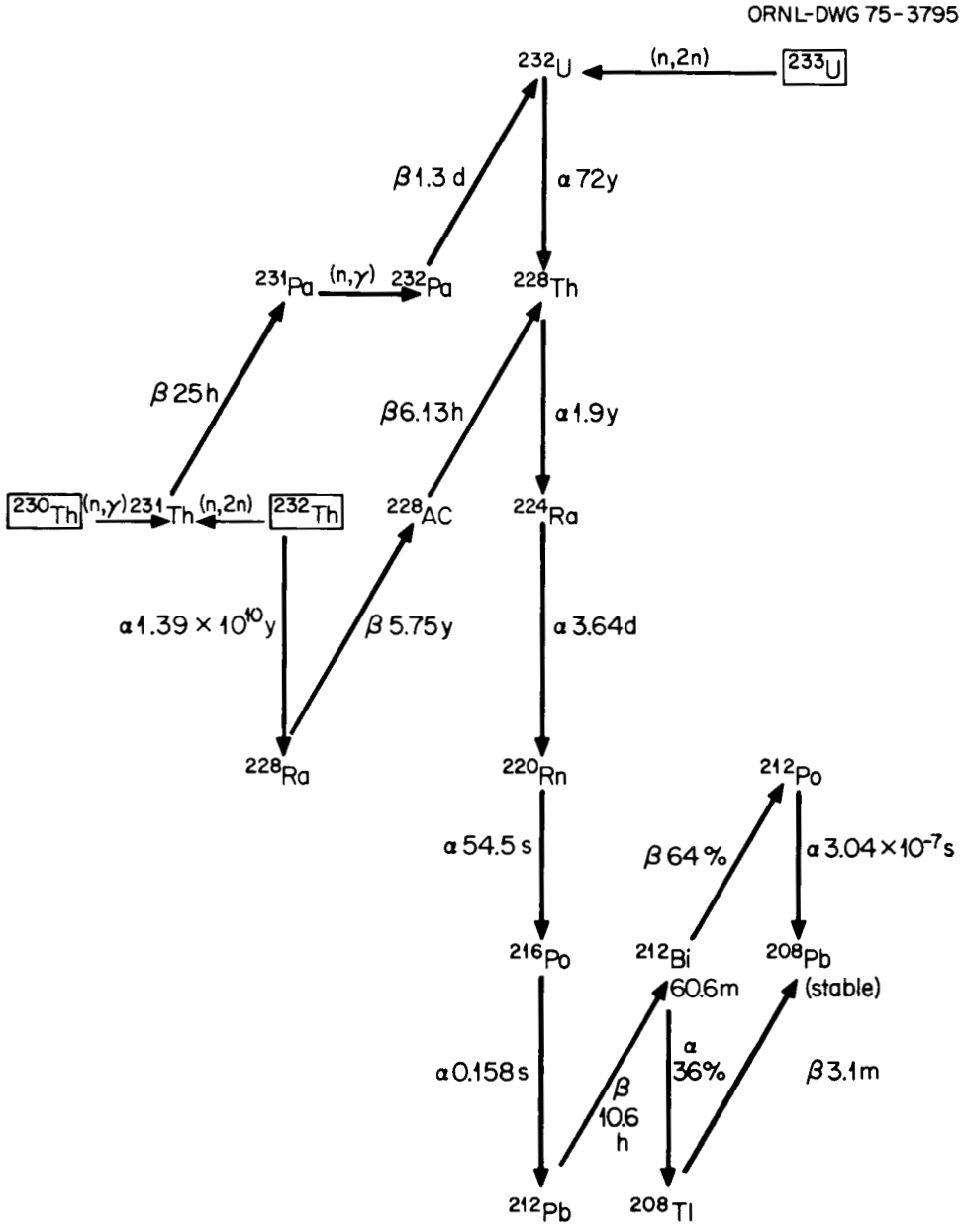

Fig. 3.1. Decay chains of ^{232}Th and ^{232}U.

Table 3.2. Uranium isotopic composition for commercial HTGR recycle fuel

Description	Isotope	Percent of total (atom density basis)
Beginning of recycle	^{233}U	92.1
	^{234}U	7.35
(Most reactive fuel)	^{235}U	0.568
	^{236}U	0.0245
	^{232}U	0.0126
Equilibrium recycle	^{233}U	61.4
	^{234}U	24.3
	^{235}U	8.02
	^{236}U	6.30
	^{232}U	0.0362

There is belief that the uranium which will be encountered in a refabrication facility can contain anywhere from 1500 ppm to less than 100 ppm ^{232}U. Hence, the design of an assay system must account for this large range in ^{232}U content.

Some of the daughter products in the natural decay chain of ^{232}U have high-energy gamma rays. This is particularly true of ^{208}Tl which beta decays to ^{208}Pb and in so doing causes the emission of a 2.61-MeV gamma ray during essentially 100% of the decays. Since the gamma activity of ^{232}U-bearing material increases with time, it becomes more difficult to handle from a radiation-exposure standpoint as it ages. In light of this, when uranium is received at the refabrication facility most of its daughter products will have been removed. After the separation process is complete, the daughters start to build back towards equilibrium with ^{232}U. Assuming complete removal of all daughters, their radioactivity will increase, as shown in Fig. 3.2.

The figure is based on the premise that at zero time 1.0 g of ^{232}U is the only material present. The ^{232}U activity is off scale on this figure, but has a constant value of 21.4 Ci over the 90-day time scale. About ten years would be required for all the daughters to come into a transient equilibrium with ^{232}U due to the 1.9-year half-life of ^{228}Th. At equilibrium, the ^{208}Tl activity will be 36% of the ^{232}U activity, and the ^{212}Po activity will be 64% of the ^{232}U activity because of the branching that occurs at ^{212}Bi.

Not all separation techniques will completely remove all the ^{232}U daughter products. For instance, an ion exchange system will remove the ^{228}Th but leave some of the ^{224}Ra, ^{220}Rn, and ^{212}Pb. Solvent extraction removes only part of the ^{228}Th but removes most of the other daughters. The effect on the ^{208}Tl activity of these two separation methods is shown in Fig. 3.3.[2] For periods less than 16 days after

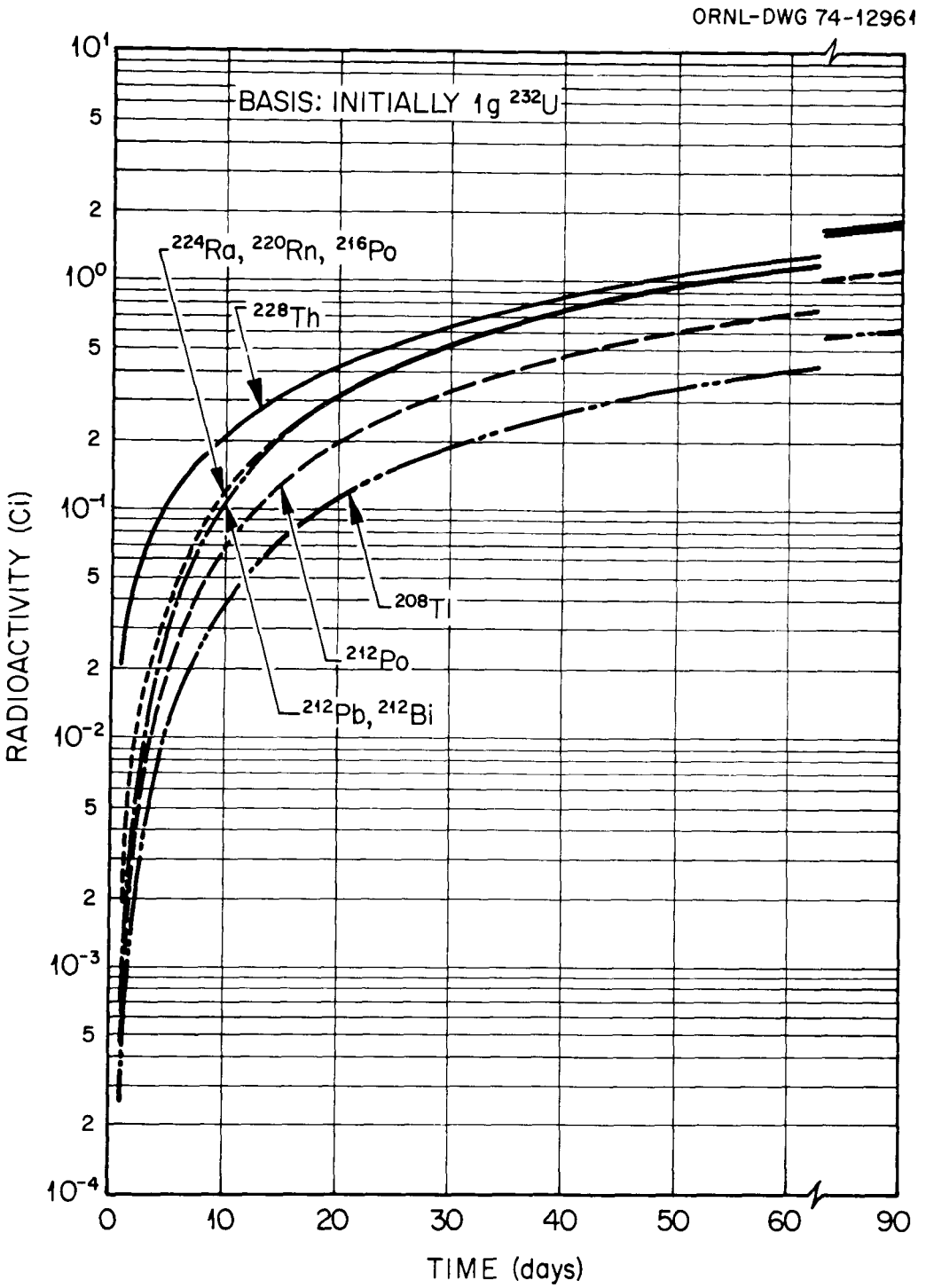

Fig. 3.2. Uranium-232 daughters radioactivity vs time for initially pure ^{232}U.

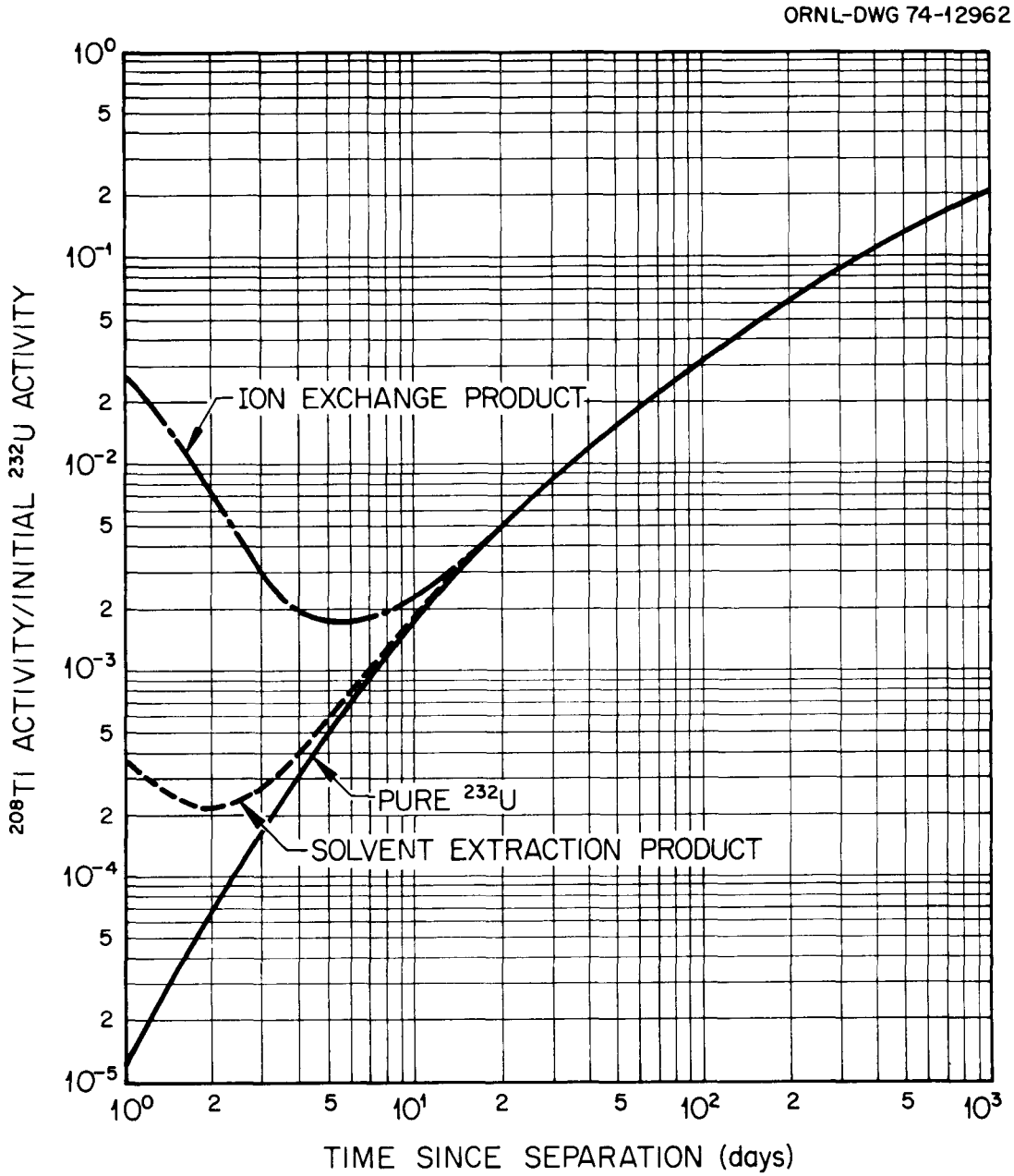

Fig. 3.3. Effect of postseparation time and type of separation on the radioactivity of ^{208}Tl per unit initial radioactivity of ^{232}U.

separation, the ^{208}Tl activity is dependent on the separation technique used. Thus, a determination of ^{232}U quantities using ^{208}Tl activity less than 16 days after separation requires detailed information on how the separation was made.

During HTGR fuel refabrication, the concentrations (or radioactivities) of the ^{232}U daughter products are not only a function of the time after 'cleanup' of the decay products, but also the concentrations are a function of the refabrication process. To illustrate this, consider the following situation.

At one point during refabrication, HTGR fuel particles are in the form of uncoated carbonized resins beads. These beads consist of UO_2 in a carbon matrix, having a density of $3.3 g/cm^3$ and a composition of 71% (by weight) uranium, 19% carbon, and 10% oxygen. At this point in the process the beads are heated up to 1800°C in a fluidized-bed furnace and held at that temperature for an, as yet, undetermined length of time. During this process the concentrations of ^{232}U daughters will be altered in the fuel particle.[3] For instance, ^{220}Rn which is a gas, diffuses out of the particles. In such cases, the approach to transient equilibrium (described above) will be affected. Two example cases of possible situations were studied, and their effects on ^{232}U daughter concentrations are presented in Figs. 3.4 and 3.5.

Figure 3.4 shows the effect on the ^{212}Pb number density of continuously removing various quantities of ^{220}Rn from an equilibrium concentration of daughter products. Figure 3.5 shows this same effect on the ^{208}Tl activity. One will note that as soon as the radon removal has ceased, the ^{212}Pb concentration begins to increase. This is because the ^{220}Rn has a very short half-life compared to the time scale used in Fig. 2.4 and returns to its equilibrium concentration very quickly. Along with this rapid return of ^{220}Rn to equilibrium, the formation rate of ^{212}Pb increases, which in turn increases the ^{212}Pb number density. A similar phenomena occurs with respect to the ^{208}Tl concentration. However, there is a time lag between the end of the radon removal and the beginning of ^{208}Tl number density increase, because the 10.6-hr half-life of ^{212}Pb is not short compared to the time scale presented.

Thus, the ^{232}U daughter product concentrations are naturally a function of time and can be affected by the process steps that occur in a refabrication facility. Any assay techniques that rely on these daughter activities as indicators must consider the possible variations in the material's history that could result in changes in their concentrations.

3.4 GAMMA SOURCES AND INTENSITIES

This section discusses the gamma rays that are emitted from the material that will be handled in the refabrication facility. The primary gamma emitting nuclides that will be present are ^{232}Th, ^{232}U, ^{233}U, and their associated daughter nuclides. Included in this section are a table of emitted gamma rays as compiled from reports on nuclear data[4,5] and a gamma-ray energy spectrum of some ^{233}U-loaded resin beads.

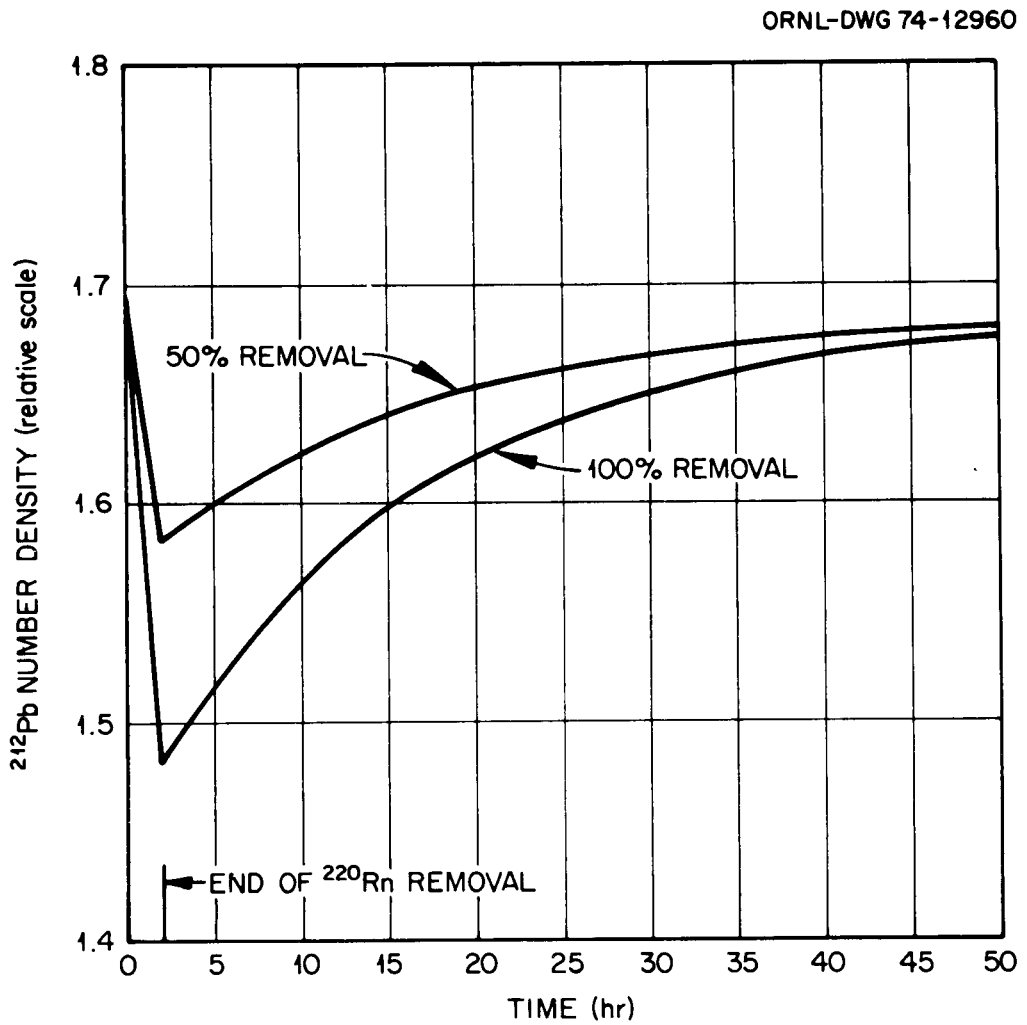

Fig. 3.4. Lead-212 number density vs time during and after 2-hr ^{220}Rn removal.

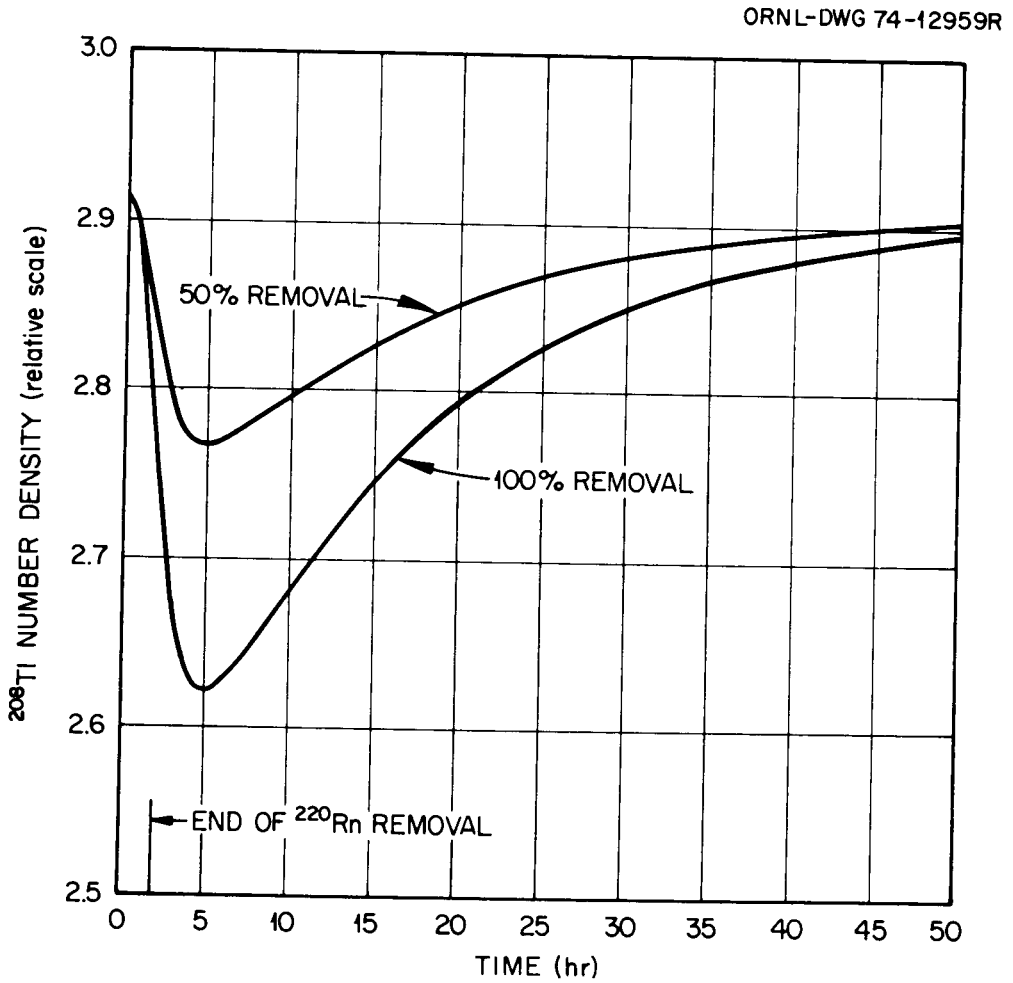

Fig. 3.5. Thallium-208 number density vs time during and after 2-hr ^{220}Rn removal.

The ^{232}Th and ^{232}U decay chains are given in Fig. 3.1. Both of these chains terminate at the stable nuclide ^{208}Pb and, in fact, are identical from the joining point at ^{228}Th through ^{208}Pb. It is important to be aware of this fact when attempting to assay for ^{232}U in the presence of ^{232}Th. To see the influence of the presence of ^{232}Th, consider the following two examples.

First, assume that a sample contains 90% thorium and 10% uranium and that the thorium was initially pure ^{232}Th and that it is ten years old. Further assume that the uranium was initially pure, that it contained only ^{233}U with 10 ppm ^{232}U, and that it is currently ten days old. In this case, 32% of the ^{208}Tl gamma rays would result from ^{232}Th decay and 68% from ^{232}U decay.

Now, assume the following conditions: sample composition, 90% thorium and 10% uranium; thorium initially pure ^{232}Th and three years old; uranium initially pure ^{233}U with 100-ppm ^{232}U and 90 days old. In this example, only 0.062% of the ^{208}Tl gamma rays would result from ^{232}Th decay while the rest would result from ^{232}U decay. Hence, it is seen that the influence of ^{232}Th on the activity of the daughter products can cover a wide range. In some cases, the presence of ^{232}Th will make only a very small addition to the ^{208}Tl activity, while in other cases ^{232}Th may be a prime source of the ^{208}Tl present.

Several high-energy gamma rays are emitted from the daughters of ^{232}Th and ^{232}U. Particularly, a 2.61-MeV gamma ray is emitted 100% of the time when ^{208}Tl beta decays to ^{208}Pb. A list of gamma rays from ^{232}Th and ^{232}U and the decay chain daughters is included in Table 3.3.

Column 1 of the table gives the parent nuclide whose decay initiates the gamma-ray emission. Column 2 gives the gamma-ray energy, and column 3 gives the average number of gammas that are emitted by the daughter per 100 decays of ^{232}Th or ^{232}U at equilibrium conditions. For example, on the average, 35.93 gamma rays with 2.61 MeV of energy each are emitted per 100 decays of ^{232}U or ^{232}Th in equilibrium with their daughters. There are uncertainties in the numbers given in the table that have not been included. These can be found in the referenced reports.

Figure 3.6 gives the decay chain of ^{233}U. Many low-intensity gamma rays are emitted as a result of ^{233}U decay itself. Table 3.3 also gives gamma rays emitted due to decay of ^{233}U.

A gamma-ray spectrum of some ^{233}U-loaded resin particles was measured with a 9% Ge(li) detector. The detector is true coaxial, with a total volume of 54 cm^3 and a measured resolution of 2.3 keV at 1332 keV. The uranium contained about 250-ppm ^{232}U and was about ten years old. The spectrum for this material is shown in Fig. 3.7. The labels near the peaks indicate the parent nuclide and the gamma-ray energy. All the major peaks in this spectrum are from gammas emitted during the decay of ^{232}U daughters, and there is no significant indication of any ^{233}U gamma lines. This indicates that the above detector would not be suitable to determine the ^{233}U

Table 3.3. Gamma rays, energies, and yields from ^{233}U, ^{232}U, and ^{232}Th and their daughters

PARENT NUCLIDE	GAMMA ENERGY (MEV)	INTENSITY AT EQUILIBRIUM GAMMAS PER 100 DECAYS OF CHAIN INITIATOR
U-233	0.029	0.0362
BI-212	0.040	1.060
U-233	0.042	0.1890
U-233	0.055	0.0414
AC-228	0.057	<0.1
U-232	0.058	0.2100
U-233	0.066	0.0021
U-233	0.068	0.0007
U-233	0.070	0.0016
U-233	0.072	0.0084
U-233	0.075	0.0044
U-233	0.076	0.0016
U-233	0.078	0.0009
AC-228	0.078	<0.1
U-233	0.083	0.0004
TH-228	0.084	1.2
U-233	0.091	0.0009
U-233	0.094	0.0059
U-233	0.097	0.0601
AC-228	0.098	<0.1
U-233	0.100	0.0001
U-233	0.102	0.0002
U-233	0.110	0.0010
U-233	0.112	0.0013
PB-212	0.115	0.57
U-233	0.117	0.0086
U-233	0.119	0.0108
U-233	0.121	0.0089
U-233	0.124	0.0021
U-233	0.125	0.0003
AC-228	0.128	1.6
U-232	0.129	0.0820
U-233	0.131	0.0002
TH-228	0.132	0.18
U-233	0.135	0.0064
U-233	0.140	0.0003
U-233	0.145	0.0052
U-233	0.146	0.0184
U-233	0.148	0.0010
U-233	0.150	0.0004
AC-228	0.151	0.8
U-233	0.153	0.0003
U-233	0.155	0.0005
U-233	0.156	0.0002
U-233	0.163	0.0004
U-233	0.165	0.0177
U-233	0.166	0.0014
TH-228	0.167	0.18
U-233	0.169	0.0003
U-233	0.171	0.0005
U-233	0.174	0.0009
PB-212	0.177	0.20

Table 3.3 (continued)

PARENT NUCLIDE	GAMMA ENERGY (MEV)	INTENSITY AT EQUILIBRIUM GAMMAS PER 100 DECAYS OF CHAIN INITIATOR
AC-228	0.179	<0.1
AC-228	0.184	1.6
U-233	0.188	0.0056
U-233	0.192	0.0003
U-233	0.206	0.0002
AC-228	0.208	2.7
U-233	0.208	0.0068
U-233	0.212	0.0003
TH-228	0.216	0.4
U-233	0.216	0.0026
U-233	0.217	0.0082
U-233	0.219	0.0005
U-233	0.223	0.0001
U-233	0.230	0.0003
TL-208	0.234	0.12
PB-212	0.239	40.0
U-233	0.240	0.0009
RA-224	0.241	4.1
U-233	0.245	0.0107
U-233	0.249	0.0043
TL-208	0.253	0.27
U-233	0.256	0.0002
U-233	0.260	0.0006
U-233	0.262	0.0009
U-233	0.269	0.0008
AC-228	0.270	4.0

PARENT NUCLIDE	GAMMA ENERGY (MEV)	INTENSITY AT EQUILIBRIUM GAMMAS PER 100 DECAYS OF CHAIN INITIATOR
U-232	0.271	0.0038
U-233	0.272	0.0003
U-233	0.275	0.0014
TL-208	0.277	2.4
U-233	0.278	0.0032
AC-228	0.282	0.3
U-233	0.288	0.0027
BI-212	0.288	0.45
U-233	0.291	0.0016
U-233	0.294	0.0004
PB-212	0.301	3.0
U-233	0.303	0.0003
U-233	0.310	0.0003
U-233	0.317	0.0231
U-233	0.321	0.0087
U-233	0.323	0.0025
AC-228	0.327	1.9
U-232	0.328	0.0034
BI-212	0.329	0.17
U-233	0.329	0.0003
U-233	0.337	0.0017
AC-228	0.337	11.0
U-233	0.354	0.0003
U-233	0.366	0.0025
U-233	0.384	0.0003
AC-228	0.409	1.6

Table 3.3 (continued)

PARENT NUCLIDE	GAMMA ENERGY (MEV)	INTENSITY AT EQUILIBRIUM GAMMAS PER 100 DECAYS OF CHAIN INITIATOR
BI-212	0.453	0.40
AC-228	0.461	2.7
TL-208	0.511	8.0
TL-208	0.583	30.0
U-233	0.609	0.0002
BI-212	0.727	7.1
TL-208	0.763	0.61
AC-228	0.780	1.4
BI-212	0.785	1.0
AC-228	0.793	3.5
AC-228	0.833	3.2
TL-208	0.860	4.4
BI-212	0.893	0.40
AC-228	0.909	30.
BI-212	0.953	0.11
AC-228	0.967	27.
BI-212	1.079	0.6
TL-208	1.094	0.15
AC-228	1.466	1.3
AC-228	1.500	2.1
BI-212	1.513	0.31
AC-228	1.595	5.6
BI-212	1.621	1.8
AC-228	1.636	3.2
BI-212	1.806	0.11
TL-208	2.615	35.93

ORNL-DWG 74-12958R

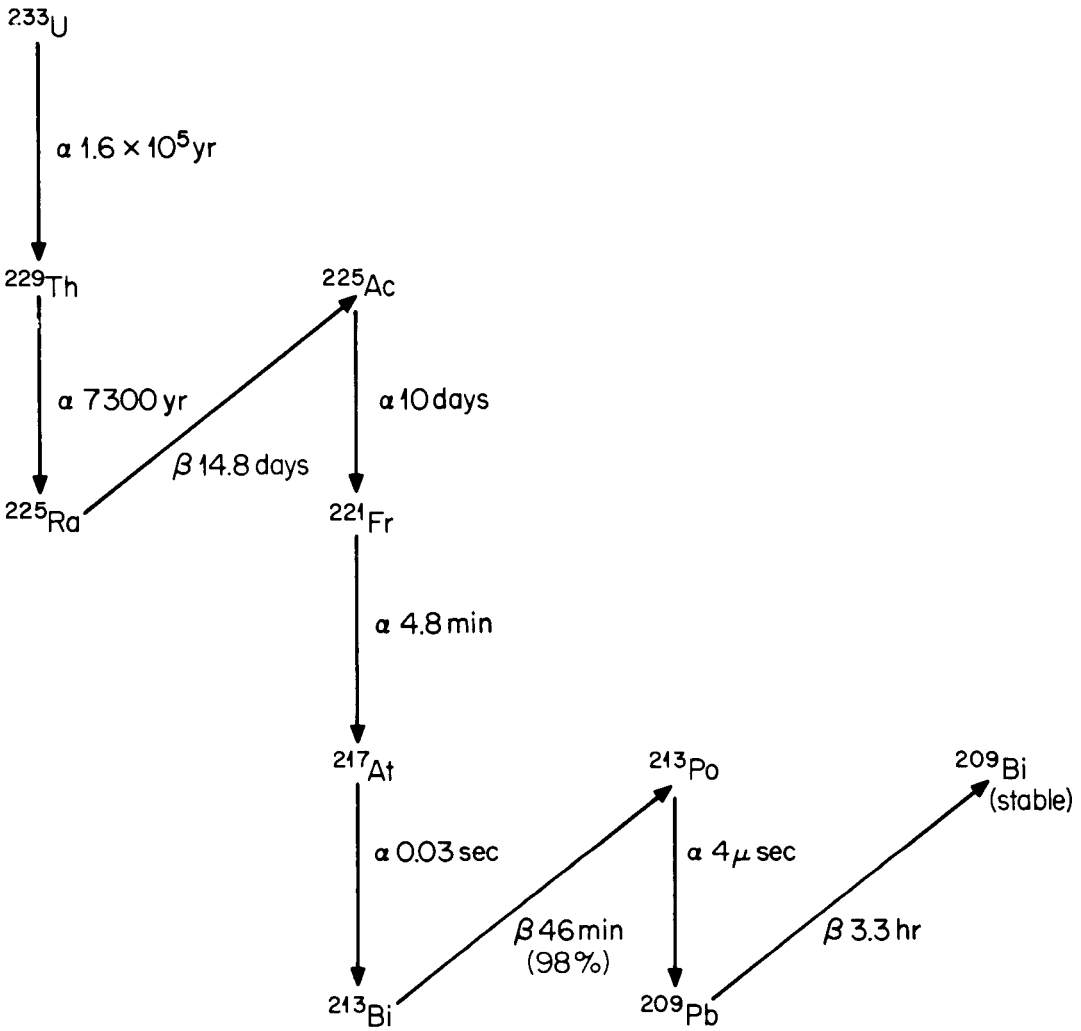

Fig. 3.6. Uranium-233 decay chain.

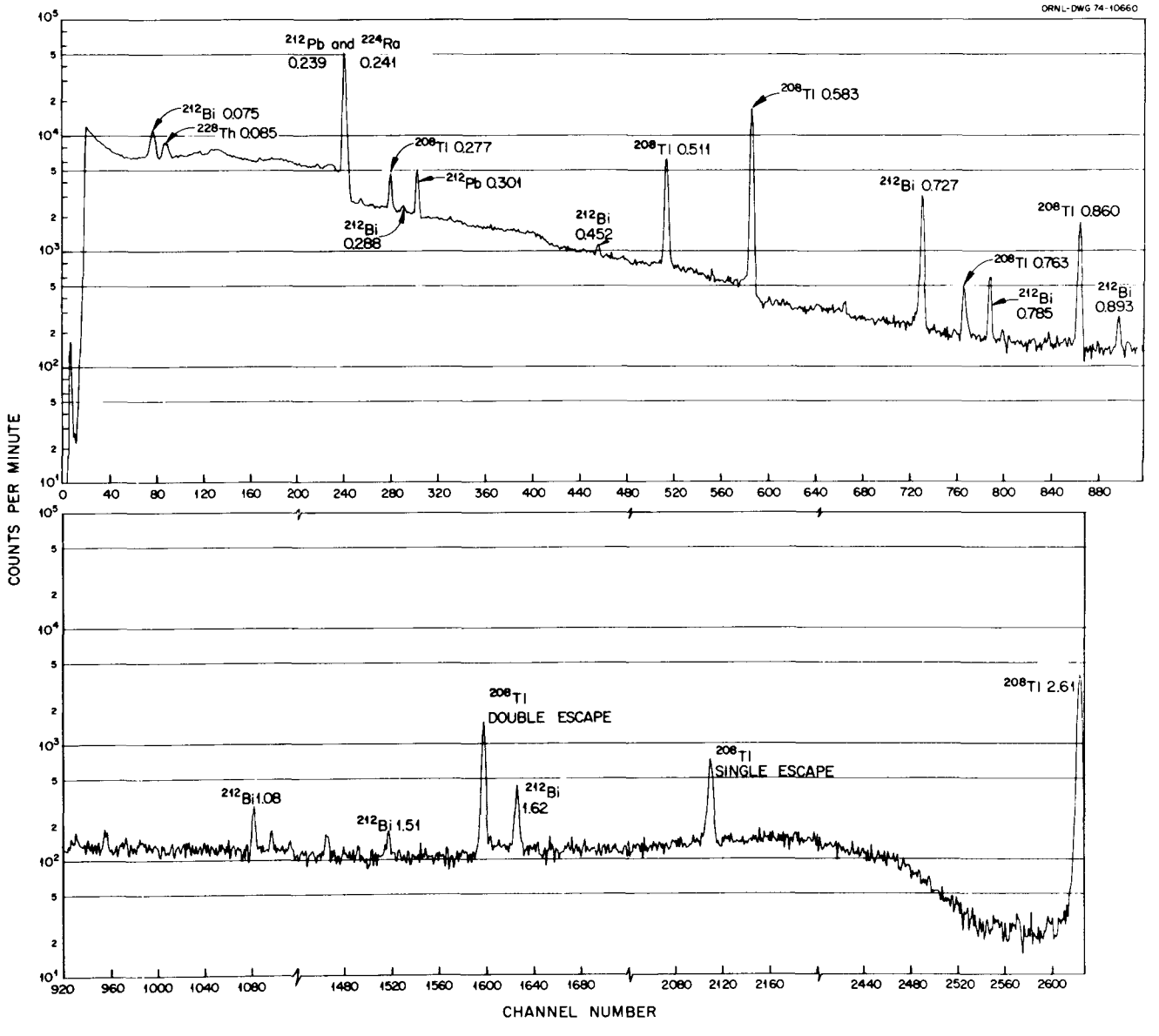

Fig. 3.7. Gamma-ray spectrum ^{233}U with high-ppm ^{232}U content.

content of this sample by direct detection of a ^{233}U gamma line. Ten-year-old 250-ppm ^{232}U material is equivalent to 90-day-old 2500-ppm ^{232}U material in terms of activity, and 90-day-old 1500-ppm ^{232}U material is expected to be encountered in a refabrication facility. Hence, more sensitive gamma assay equipment will be required to count ^{233}U directly in the presence of the expected ^{232}U background. An experiment is under way to measure this same material with a much smaller detector than the one described above. Use of a small detector should eliminate some of the low-energy Compton scattering background and may allow resolution of the low-energy ^{233}U peaks.

To obtain the relative intensities of gamma rays in material whose chains are not in equilibrium (similar to that which will be handled in the refabrication facility), the intensities in column 3 of Table 3.3 must be multiplied by the ratio of the activities of the parent nuclides to a selected nuclide in the decay chain. This information must be obtained from a separate calculation. For example, if a sample contains ^{233}U with 100-ppm ^{232}U and is 20 days old, the ^{228}Th activity is 1.34 times greater than the ^{224}Ra activity, the ^{232}U activity is 68.1 times greater than the ^{224}Ra activity, and the ^{233}U activity is 302 times greater than the ^{224}Ra activity. Therefore, to get the relative intensities of the ^{228}Th, ^{232}U, and ^{233}U, and ^{224}Ra gamma rays, the intensity in column 3 for ^{228}Th should be multiplied by 1.34, the intensity for ^{232}U should be multiplied by 58.1, the intensity for ^{233}U should be multiplied by 302, and the intensity for ^{224}Ra should be multiplied by 1.0.

It should be pointed out that when calculating relative intensities of the ^{208}Tl gamma rays, the numbers given in Table 3.3 include a 35.93% branching ratio at ^{212}Bi.

As mentioned in Sect. 3.2, daughter product concentrations are dependent on some of the refabrication process steps. Hence, the activities of these daughters are also process-history-dependent. This must be kept in mind when a determination is made of relative gamma intensities in a hypothetical sample. In a process-history-dependent case, to find the relative gamma ray intensities, it is necessary to find the relative concentrations of the daughter products. Usually this is very difficult if not impossible to accomplish. One alternative is to wait until any process-history-dependent transients have died away from the normal-time dependence of the daughter products. This was illustrated in Fig. 3.3, in which the separation-concentration dependence of two samples died away after 16 days.

Nichols et al. have measured the process dependence of ^{208}Tl activity associated with the operation of the ORNL Kilorod Facility for the fabrication of $^{233}UO_2$-ThO_2 fuel.[6] Although the process steps in the Kilorod operation are different from those that will be used in the HTGR-FRPP, there are enough similarities that the results can give an idea of how the ^{208}Tl activity may vary in the HTGR-FRPP. A description of their process is given below.

"This facility was used to prepare 900 Zircaloy-clad rods, 5/8-in. (1.6-cm) diam by 42-in. (106.7-cm) long, and 200 similar rods 19-in. (48.3-cm) long, containing 3% $^{233}UO_2$-97% ThO_2. The sol-gel process and the vibratory compaction technique were used. The sol-gel process was carried out in four steps: denitration of hydrated thorium nitrate and drying to obtain a reactive ThO_2; dispersion of this ThO_2 in dilute $^{233}UO_2(NO_3)_2$-HNO_3 solution in a blend tank to obtain a hydrosol; gelation by evaporation at 900°C in a shallow tray; and calcination at 1150°C in an alundum crucible within a remotely operated furnace to obtain particles of mixed oxide. The powder was then graded using a jaw-crusher, a ball mill and screen classifiers, all remotely operated. The oxide was compacted to a density of 8.8 to 9.0 g/cm^3 in the Zircaloy tubes using a pneumatic vibratory compactor. The filled tubes were then gamma scanned for density variation, sealed by welding, cleaned, and inspected. The ^{233}U feed in the Kilorod Facility contained 35-40 parts/10^6 of ^{232}U, which was approximately in transient equilbirium with its daughters. Prior to sol-gel processing the uranium was purified by one cycle of solvent extraction with di-sec-butyl-phenyl-phosphonate. This removed more than 99% of the longer-lived daughters of ^{232}U, with the exception of about 0.3% of the ^{212}Pb."

Their measured ^{208}Tl activity is compared to the ^{208}Tl activity calculated for an initially pure ^{232}U sample and presented in Fig. 3.8.

The rapid decrease in the activity between zero and 70 hr is due to the separation technique as described in Sect. 3.3. During the calcination step it was reported that most of the ^{220}Rn and about 50% of the ^{224}Ra were volatilized, thus the characteristic dip in the ^{208}Tl appeared. The increase that occurred during the gel preparation was due to the addition of ^{232}Th which contained some ^{208}Tl.

If enough detailed information was available on the history and age of a sample that had been passed through a process similar to the one given above, it could be possible to make approximate calculations on the ^{232}U content from ^{208}Tl. However, to get an accurate figure on the ^{232}U content of a sample by using ^{208}Tl activity, it might be necessary to wait until any process-dependent transients have died away, assuming also that self-shielding effects can be corrected for.

In addition to complicating the application of existing assay techniques to the ^{233}U-^{232}Th material, the presence of ^{232}U and its daughters also complicates the assay problem because of problems introduced due to personnel exposure considerations. Personnel shielding requirements are dictated by the presence of the highly penetrating 2.6-MeV gamma ray from ^{208}Tl decay.

Tables 3.4 and 3.5 list calculated dose rates from 1 g of ^{233}U containing 500-ppm ^{232}U at various times after purification. From this data it is evident that even small samples of this material will require substantial shielding. Any assay equipment located exterior to the main

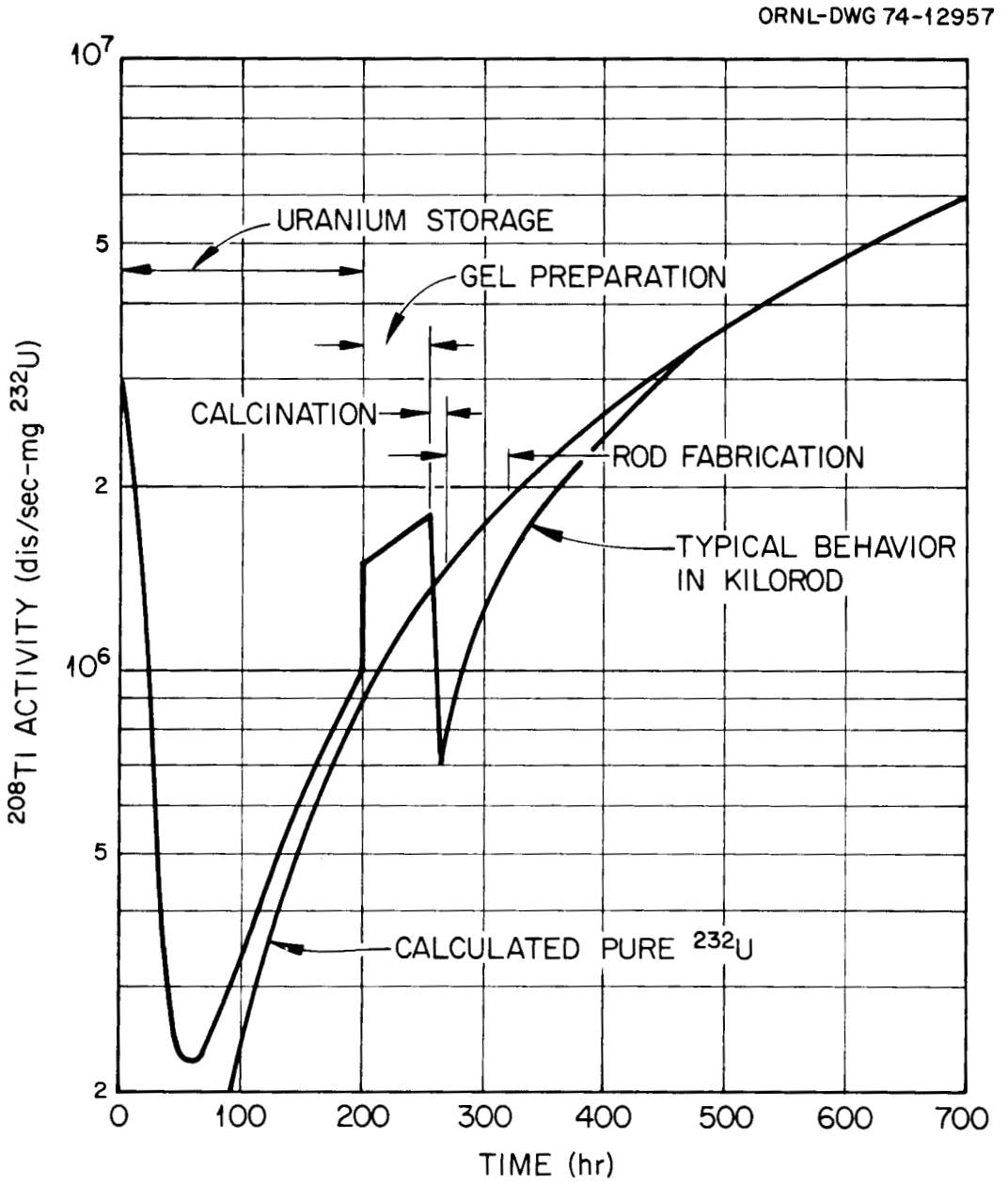

Fig. 3.8. Effect of postpurification time on the activity of ^{208}Tl for a typical sequence of operations in the Kilorod Facility.

processing cell must be designed for remote or semiremote operation. Table 3.6 shows the variation in ^{232}U content for a fixed sample size allowed under the stated shield and exposure assumptions for material of varying age. This information indicates that shielding requirements can be reduced if material can be processed through the plant within a fixed time after cleanup. Current assumptions for pilot plant operation call for a maximum 90 days aging for a given batch of material.

Table 3.4. Dose rates in millirem per hour for a 1-g source of ^{233}U with 500-ppm ^{232}U (without shielding)

Distance from source point to dose point (cm)	Decay period (days)			
	30	60	90	180
1	2,203	4,444	7,407	14,605
2	551	1,112	1,854	3,655
5	88.3	178	297	585
10	22.1	44.5	74.2	146
20	5.52	11.1	18.6	26.6
35	1.80	3.64	6.06	12.0
50	0.88	1.78	2.97	5.86
100	0.22	0.45	0.74	1.47

Table 3.5. Dose rates in millirem per hour for a 1-g source of ^{233}U with 500-ppm ^{232}U (with 5-cm lead shield)

Distance from source point to dose point (cm)	Decay period (days)			
	30	60	90	180
5.2	7.41	14.9	24.9	49.1
10.0	2.00	4.04	6.73	13.3
20.0	0.50	1.01	1.68	3.32
35.0	0.164	0.33	0.55	1.08
50.0	0.080	0.162	0.27	0.53

Table 3.6. Time windows for handling ^{233}U-^{232}U fuels in a sample inspection laboratory

Criteria: Sample size, 0.5 g uranium
Shield thickness, 2 in. lead
Gamma dose rate at operator location, 0.25 mR/hr

Time window (Days after separation of daughter nuclides)	Maximum ^{232}U concentrations of samples (ppm ^{232}U in uranium)
20	2750
30	1650
40	1200
60	760
90	500
120	375
150	300
180	250
365	130
10 year (equilibrium)	45

3.5 NEUTRON SOURCES AND INTENSITIES

The HTGR recycle fuel is a source of spontaneous-fission neutrons and (α,n) reaction neutrons that have potential effects on the methods selected for nondestructive assay. This section describes the neutron source intensities expected from each of these reactions.

3.5.1 Spontaneous fission

The specific spontaneous fission activities and neutron-emission rates of the nuclides of interest in the HTGR recycle fuel are listed in Table 3.7. The neutron emission rates are relatively low for all nuclides except ^{232}U; however, the ^{232}U concentration in recycle ^{233}U is expected to be in the range of 100 to 1500 ppm so that the spontaneous-fission neutron yield of equilibrium recycle fuel (61.4 at. % ^{233}U, 24.3 at. % ^{234}U, 8 at. % ^{235}U, 6 at. % ^{236}U, and 0.12 at. % ^{232}U is only 4 neutrons sec^{-1} kg^{-1}. This low neutron-emission rate excludes the use of spontaneous-fission neutrons as a fissionable material signature.

In addition, the low neutron yield from spontaneous fission should not interfere with other nondestructive assay (NDA) methods employing neutrons as the interrogating or signature radiation.

Table 3.7. Specific activities and neutron-emission rates for spontaneous fission[8]

Nuclide	Spontaneous fission half-life (years)	Specific activity for spontaneous fission (dis sec^{-1} g^{-1})	Neutron emission (νsp = 2) (neutrons sec^{-1} g^{-1}
^{230}Th	$>1.5 \times 10^{20}$	$<3.8 \times 10^{-7}$	$<7.6 \times 10^{-7}$
^{232}Th	$>10^{21}$	$<5.7 \times 10^{-8}$	1.1×10^{-7}
^{232}U	8×10^{13}	7.1×10^{-1}	1.4
^{233}U	1.25×10^{17}	4.55×10^{-4}	9.1×10^{-4}
^{234}U	2×10^{16}	2.8×10^{-3}	5.6×10^{-3}
^{235}U	1.9×10^{17}	3.0×10^{-4}	6.0×10^{-4}
^{236}U	2×10^{16}	2.8×10^{-3}	5.6×10^{-3}
^{238}U	7.19×10^{15}	7.73×10^{-3}	1.5×10^{-2}

3.5.2 (α,n) neutrons

Neutron production by alpha bombardment of light elements is a second source of neutrons from HTGR recycle fuels. The alpha activities of ^{233}U, ^{232}U, and the decay daughters of ^{232}U provide the time-dependent alpha source. The principal light nuclides of interest are ^{13}C and ^{18}O.

The "thick target" neutron yields for the elements carbon and oxygen are 0.11 neutrons/10^6 alphas and 0.07 neutrons/10^6 alphas, respectively, for an alpha particle energy of 5.305 MeV.[7] The relationship between the neutron yield and the alpha-particle energy has been determined from the calculations of Van Tuyl.[9] The energy-dependent thick target yields of carbon and oxygen can be written as

$$\text{Neutron yield from carbon} = 4.89 \times 10^{-11}\ E_\alpha^{4.65}\ n/\alpha \qquad (3.1)$$

$$\text{Neutron yield from oxygen} = 2.18 \times 10^{-11}\ E_\alpha^{4.84}\ n/\alpha \qquad (3.2)$$

where E_α is the alpha-particle energy.

For compounds containing oxygen, carbon, and heavy elements, the total neutron yield is determined by the expression of Matlack and Metz.[10]

$$Y = \frac{\Sigma m_i\ S_i\ Y_i}{\Sigma m_i\ S_i}\ , \qquad (3.3)$$

where Y is the total neutron yield, m_i is the mole fraction of the ith element, S_i is the stopping power of the ith element, and Y_i is the thick target yield. The stopping power S is proportional to $Z(Z + 7)^{-1/2}$, where Z is the atomic number.[10]

The calculational method based in Eq. (3.3) provides only an approximation of the neutron yield. For a more precise calculation of the (α,n) yield on oxygen, the methods of Taherzadeh[11] and Taherzadeh and Gingo[12] should be utilized. To the authors' knowledge there have been no reported measurements of the (α,n) yield of ^{233}U-^{232}U carbide or oxide. Such measurements are needed to verify the calculated yields, particularly in the case of carbide fuel.

The (α,n) reaction yields calculated with Eqs. (3.1 through 3.3) are listed in Table 3.8 for the three solid fuel compounds that occur in the fuel refabrication process. Table 3.8 presents the (α,n) yields of each compound for 1 kg of beginning-recycle uranium and 1 kg of equilibrium-recycle uranium at two aging times. The uranium ages of 10 days and 90 days, respectively, represent practical minimum and maximum aging times for the refabrication of HTGR fuel.

Table 3.8. Calculated yields of (α,n) neutrons from HTGR recycle fuel

Uranium age (days)	Uranium type	Fuel compounds in refabrication		
		Loaded resin ($UC_{15}O_5H_{15}$)[a]	Carbonized resin ($U_2C_9O_4$)[a]	Fuel kernel (U_2C_7O)[a]
		x 10^4 neutrons sec^{-1} kg^{-1} of uranium		
10	Beginning recycle[b]	4.5	3.5	2.7
	Equiblbirum recycle[c]	4.2	3.3	2.5
90	Beginning recycle[b]	7.6	5.8	4.5
	Equilibrium recycle[c]	7.5	5.8	4.4

[a]Chemical formula indicates element ratios only, does not imply chemical form.

[b]Atom percent of beginning-recycle uranium (^{232}U, 0.05%; ^{233}U, 92.1%; ^{234}U, 7.35%; ^{235}U, 0.57; ^{236}U, 0.025%).

[c]Atom percent of equilibrium-recycle uranium (^{232}U, 0.05%, ^{233}U, 61.4%; ^{234}U, 24.3%; ^{235}U, 8.02%; ^{236}U, 6.30%).

The neutron yields of the HTGR recycle fuel are comparable to the (α,n) yields of $^{239}PuO_2$ (ref. 13). In addition, the neutron yield is time dependent and possibly process-history-dependent because selected daughter nuclides (radium and radon) may evolve from the fuel during the refabrication process. The (α,n) yields from the fuel compounds can be used as a qualitative indication of fissile materils content; however, the dependence of the neutron yield on age and process variables as well as the possibility of limited (α,n) production from fuel impurities

render any (α,n)-based methods impractical for accurate quantitative nondestructive assay. The (α,n) yield may affect other assay methods that rely on neutron detection methods. These effects will be documented in later sections describing specific nondestructive-assay techniques.

3.6 THERMAL EMISSIONS

Spontaneous alpha decay of fissile ^{233}U and its companion ^{232}U and the accompanying release of thermal energy are of interest as a potential source of information for nondestructive assay by calorimetric techniques. While the spontaneous decay heat from ^{233}U is small relative to the plutonium isotopes (270 μW/g of ^{233}U vs 1929 μW/g for ^{239}Pu), it is sufficient to allow assay of concentrated samples by passive calorimetry. The presence of the ^{232}U contaminant introduces problems, however, both by virtue of its own spontaneous decay and by the additional time-dependent heat production of its daughter products. On a gram for gram basis ^{232}U produces approximately 2500 times as much heat as does ^{233}U.[14] Hence, in ^{233}U containing 400 ppm clean ^{232}U, half of the decay heat is attributable to the contaminant. At the end of ten years, the same material will be producing an additional amount of heat equal to 5.8 times that attributable to ^{233}U, due to the build in of ^{232}U daughter products.

The controlling time constant in the ^{232}U daughter chain is the decay constant of its first member, ^{228}Th. Approximately ten days after uranium cleanup the remaining daughters have reached dynamic equilibrium with the ^{228}Th, and from that point on (barring physical removal of any of its members) the entire chain follows the growth curve of the 1.9-year half-life of ^{228}Th. Over the first 100 days, the period of interest for HTGR fuel refabrication, the increase is almost linear and, at the end of that period, the daughter activities have reached approximately one-tenth of their final equilibrium values.

The fissile ^{233}U also has an extensive family of alpha-active daughters. However, the 7340-year half-life of ^{229}Th, the first member of that chain, acts as an effective throttling valve on the growth of the following members. At 100 days after uranium cleanup the ^{233}U daughters contribute less than 0.02% of the heat generated by the parent nuclide and can, for most purposes, be ignored.

The decay chain for ^{232}U is shown in Fig. 3.1. Table 3.9 gives the Q values for each reaction and the average energy in each decay, which is attributable to gamma-ray emission and recoil plus particle emission.[14] The rationale for this breakdown is that while all of the recoil and particle energy from radioactive decay will remain within a calorimeter, the gamma energy may be only partially absorbed. The fraction absorbed will depend on the sample and calorimeter size and composition. It is evident from Table 3.9 that the heat generation components of ^{233}U and ^{232}U are only slightly sensitive to this effect. The energy released by the ^{232}U daughters, however, is 4.4% gamma. In any calorimetric measurement where ^{232}U daughter activity is a significant contributor to total heat output, account will have to be taken of the partial escape of the emitted gamma energy.

Table 3.9. Energy release of U-233, U-232, and U-232 daughters from radioactive decay

Component of decay heat	Reaction	Reaction Q value (MeV)	Recoil plus particle energy per decay, MeV (av)	Gamma energy per decay, MeV (av)
U-233 decay	U-233 $\xrightarrow{\alpha}$ Th-229	4.909	4.901	0.0081
U-233 daughters	Th-229 $\xrightarrow{\alpha}$ Ra-225	Negligible (see text)		
	⋮			
U-232 decay	M-232 $\xrightarrow{\alpha}$ Th-228	5.414	5.395	0.019
			Recoil plus particle energy per Th-228 decay at chain equilibrium, MeV (av)	Gamma energy per Th-228 decay at chain equilibrium, MeV (av)
U-232 daughters	Th-228 $\xrightarrow{\alpha}$ Ra-224	5.521	5.496	0.0251
	Ra-224 $\xrightarrow{\alpha}$ Rn-220	5.787	5.774	0.0134
	Rn-220 $\xrightarrow{\alpha}$ Po-216	6.405	6.405	0.0004
	Po-216 $\xrightarrow{\alpha}$ Pb-212	6.906	6.906	0.00002
	Pb-212 $\xrightarrow{b}$ Bi-212	0.580	0.366	0.214
	Bi-212 $\xrightarrow{b,\ 64\%}$ Po-212	2.246	1.330	0.107
	Bi-212 $\xrightarrow{36\%}$ Tl-208	6.206	2.220	0.0143
	Po-212 $\xrightarrow{\alpha}$ Pb-208	8.954	5.731	0.0
	Tl-208 $\xrightarrow{b}$ Pb-208	4.994	0.568	1.229
U-232 daughter chain — total at chain equilibrium			34.796	1.603

Figure 3.9 shows the magnitudes of the heat generation components in 1 g of ^{233}U containing 400, 800, and 1200 ppm ^{232}U as a function of time after uranium cleanup. From the figure it is evident that measurement of the ^{233}U content in a sample requires accurate knowledge of both the ^{232}U contamination ratio and the material's age. In addition, some assurance must be obtained that the daughters of ^{232}U are in dynamic equilibrium with ^{228}Th. It can be seen also that increasing ^{232}U content places correspondingly increasing accuracy requirements on the overall heat generation measurement needed to maintain a fixed accuracy in the ^{233}U content determination.

3.7 NEUTRON RESPONSE CHARACTERISTICS

An important nuclear characteristic of the HTGR recycle fuel is its response to neutron interrogation. This section enumerates the fission cross sections and the yields of prompt and delayed neutrons from fission. The use of prompt and delayed gamma rays from neutron-induced fission are also discussed as a potential nondestructive-assay technique for HTGR fuel. Response characteristics of neutron radiative capture have not been evaluated.

3.7.1 Neutron cross sections and fission thresholds

The fission cross sections of the fissile nuclides ^{233}U and ^{235}U are shown in Fig. 3.10. The thermal-neutron cross sections and resonance integrals of the fissile and fertile nuclides of interest are listed in Table 3.10. The fission cross sections of the fertile nuclides[15] are shown in Fig. 3.11. Two important features that affect the nondestructive assay of this fuel are the low magnitude of the ^{232}Th fission cross section and the relatively high cross section and low threshold for the fission of ^{234}U, which will comprise 25% of the equilibrium-recycle uranium.

3.7.1.1 Prompt neutron yields

The prompt fission neutron yields at thermal energies are listed in Table 3.11. The ^{233}U and ^{235}U yields are similar, and the $\nu\sigma_f$ values of each of these isotopes are also similar for thermal fission.

3.7.1.2 Delayed neutron yields

The absolute delayed-neutron yields are enumerated in Table 3.12 for fission induced by thermal, 3.1-MeV, and 14.9-MeV neutrons. It should be noted that the ratio of the delayed-neutron yields of ^{235}U to ^{233}U is 2.4. This difference could be used as the basis of an isotope discrimination technique.

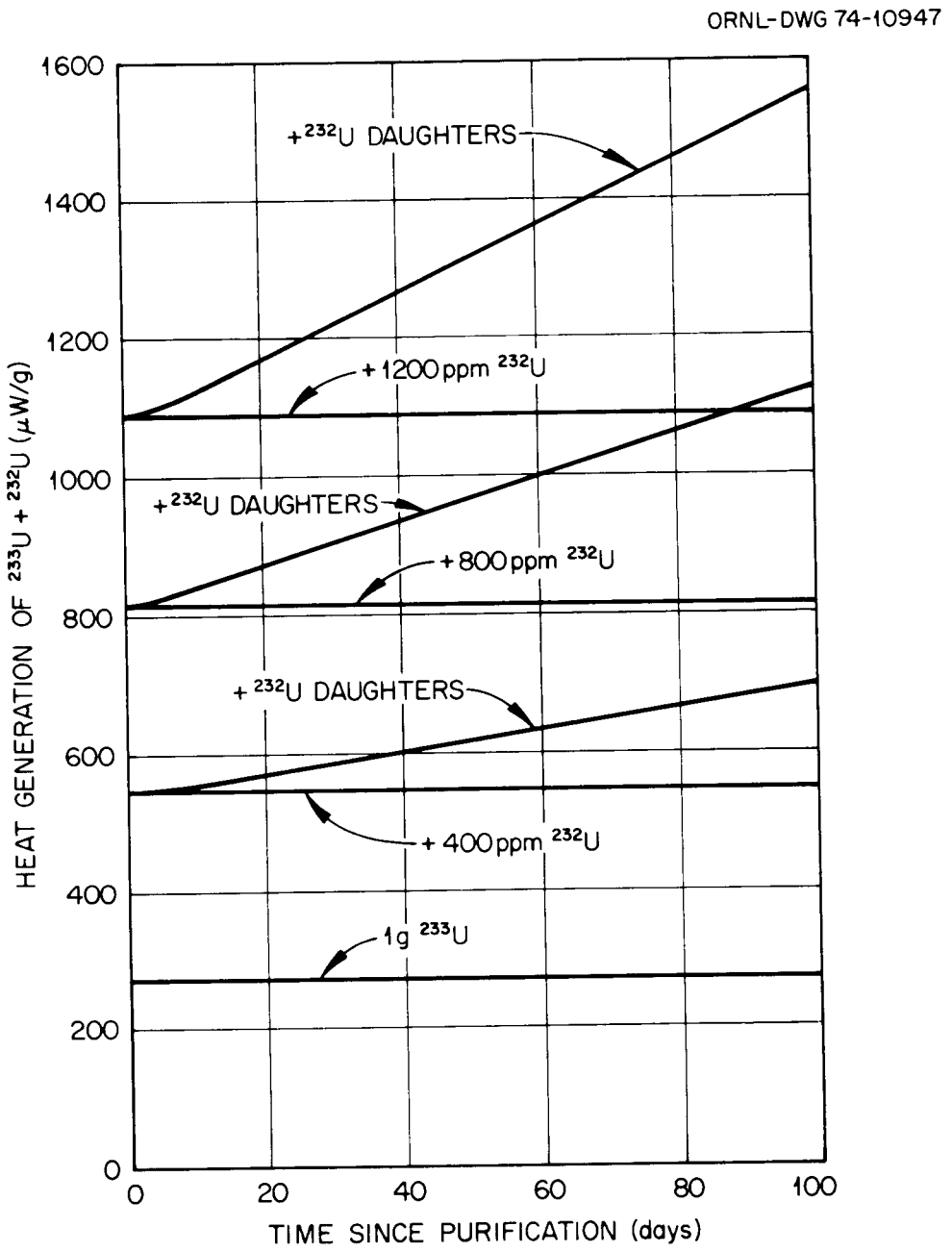

Fig. 3.9. Heat generation of 1 g of ^{233}U containing 400, 800, and 1200 ppm ^{232}U as a function of time after uranium cleanup.

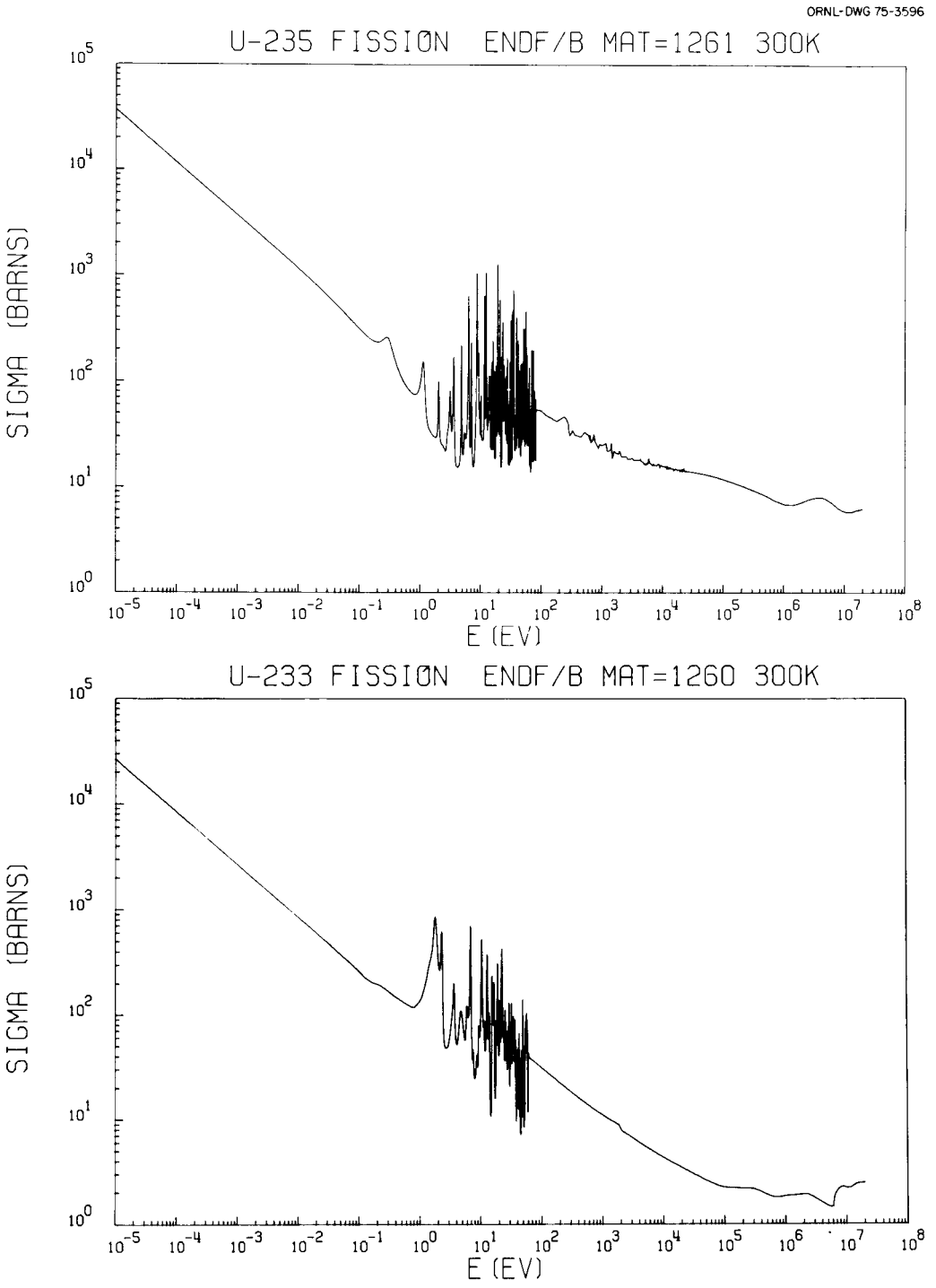

Fig. 3.10. Fission cross sections of the fissile nuclides ^{233}U and ^{235}U.

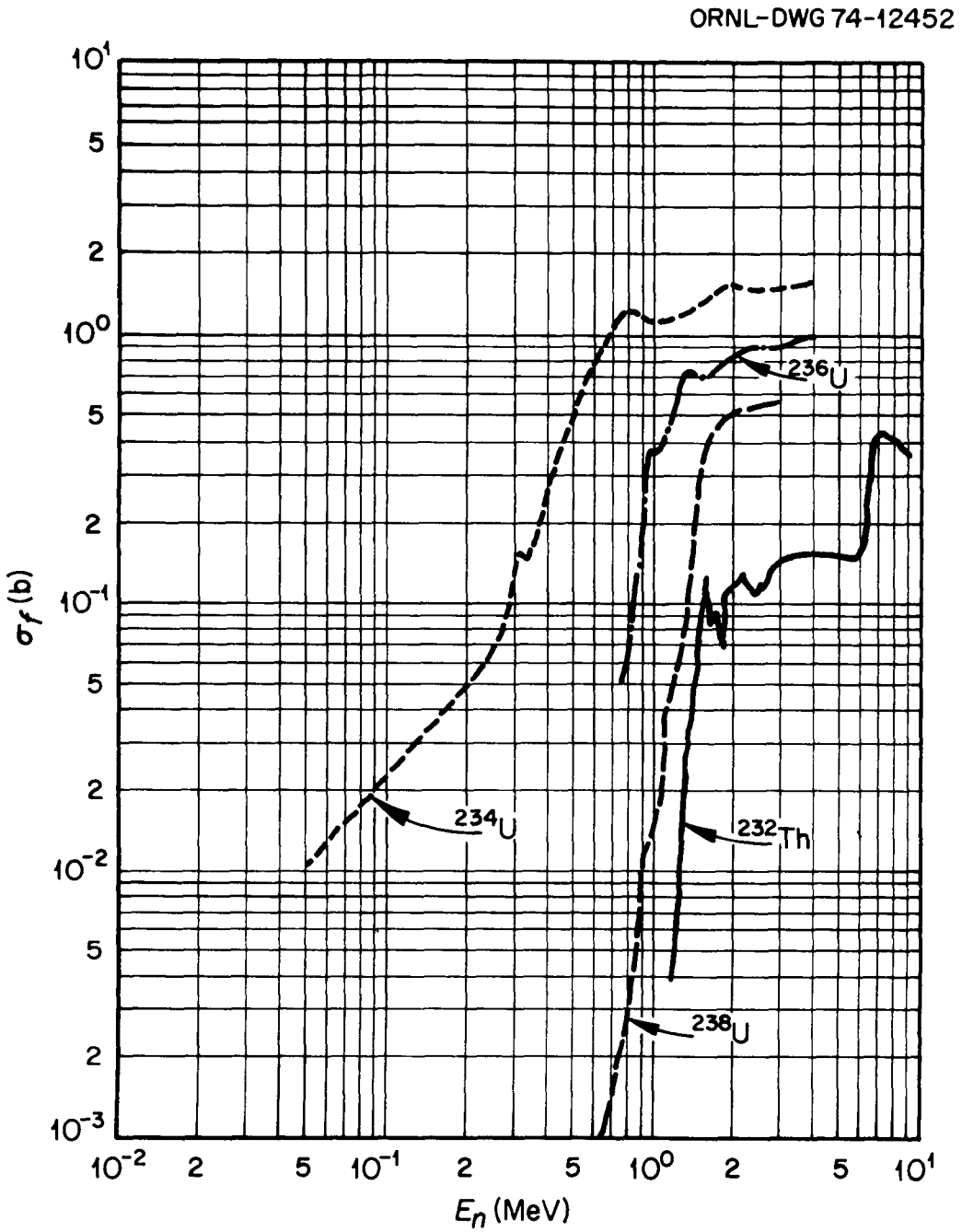

Fig. 3.11. Fission cross sections for the fertile nuclides.

Table 3.10. Thermal cross sections (barns) and resonance integrals for the uranium and thorium nuclides[15]

	U-232	U-233	U-234	U-235	U-236	U-238	Th-232
σ_γ	73.1	47.7	100.2	98.6	5.2	2.70	7.40
σ_f	75.2	531.1	<0.65	582.2			4×10^{-10}
σ_a	148.3	578.8	100	680.8		2.70	7.4
$\bar{\sigma}_s$	14.7	8.2	12	13.8		8.90	12.67
σ_t	163.0	587.0	112	694.6		11.60	20.07
I_f	320	764		275			
I_γ	280	140	630	144	365	2.75	85

Table 3.11. Prompt fission neutron yields for thermal fission[16,17]

Fission nuclide	ν_p
U-232	3.13
U-233	2.485
U-235	2.402

Table 3.12. Delayed neutron yields for thermal and fast fission

Fission nuclide	Neutron energy inducing fission		
	Thermal[17]	3.1 MeV[18]	14.9 MeV[18]
Th-232		0.060 ± 0.006	0.031 ± 0.003
U-233	0.0066 ± 0.003	0.0077 ± 0.0008	0.0043 ± 0.0004
U-234		?	?
U-235	0.0158 ± 0.0005	0.018 ± 0.002	0.0095 ± 0.0008
U-236		?	?
U-238		0.049 ± 0.005	0.0286 ± 0.0025

3.7.2 Gamma yield

The prompt and delayed gamma yields have not been investigated in detail because it can be demonstrated that the gamma signal rates from the prompt and delayed gammas are substantially lower than the background rate from the ^{232}U daughter nuclides in the recycle fuel. Menlove has reported results of his pin and pellet assay system (PAPAS) on PWR-type fuel pins.[19] Using his data, we have estimated that the ratio of net signal to background would be 0.15 for the assay of HTGR recycle fuel rods containing ^{233}U, with 100 ppm ^{232}U and 20 days aging. The very-low net signal-to-background ratio obtained with 400 μg of ^{252}Cf in PAPAS could be improved by increasing the ^{252}Cf source from 1 to 2 mg; however, the design basis of the plant requires that the assay system handle uranium with 1200 ppm ^{232}U at a 90-day age. The background activity of this fuel is about 50 times higher than the radiation from 100 ppm ^{232}U, 20-day uranium.

On this basis and as a result of communications with Dr. Howard Menlove of Los Alamos Scientific Laboratory's Nuclear Analysis Research Group A-1, it is concluded that neutron-induced gamma-ray signals cannot be utilized in nondestructive-assay (NDA) techniques for HTGR recycle fuel.

This conclusion has a strong impact on the research and development program associated with NDA for recycle HTGR fuel because assay methods using neutron-induced gamma-ray signals have been the most widely used and accepted active NDA techniques for light-water reactor fuels.

REFERENCES FOR SECTION 2

1. Letter, Colin A Heath to A. L. Lotts, "Design Information for Reload Fuel Elements for Fort St. Vrain and Large HTGR Systems; Thorium Utilization Program, P.S. 53" (Aug. 10, 1974).

2. V. A. DeCarlo, *Design of a System for the Nondestructive Assay of ^{233}U in Waste Drums*, ORNL-TM-4249 (August 1973).

3. P. B. Jackson, H. H. Ficke, S. A. Reber, C. I. Teich, *Determination of ^{232}U Daughter Release Rates from HTGR Fuel During Refabrication*, ORNL-MIT-206 (Dec. 17, 1974).

4. *Nucl. Data. Sect. A*, Vol. 8, Nos. 1 and 2, p. 137, Academic, New York, 1970.

5. J. E. Cline, "Gamma Rays Emitted by the Fissionable Nuclides and Associated Isotopes," prepared for USAEC Idaho Operations Office under Contract No. AT(10-1)-1230, p. 9.

6. J. P. Nichols, R. E. Brooksbank, and D. E. Ferguson, "Radiation Exposures in Fabricating ^{233}U-Th Fuels," *Nucl. Appl.* 1(2): 176 (April 1965).

7. G. V. Gorshkov, V. A. Zyabkin, and O. S. Tsvetkov, "Neutron Yield from the Reaction (α,n) in Be, B, C, B, F, Mg, Al, Si, and Granite Irradiated with Polonium Alpha Particles," *Sov. J. At. Energy* 13: 654 (1963).

8. W. Schirmer and N. Wächter, "Table of Specific Activities of the Nuclides with Z = 88 to Z = 104," *Actinides Rev.* 1: 125-34 (1968).

9. *Fuel Recycle Quarterly Report, Hanford Engineering Development Laboratory*, HEDL-TME-71-55 (1971).

10. G. M. Matlack and C. F. Metz, *Radiation Characteristics of Plutonium-238*, LA-3696 (1967).

11. Mojtaba Taherzadeh, "Neutron Yield from the (α,n) Reaction in the Isotope Oxygen-18," *Nucl. Sci. Eng.* 44: 190-93 (1971).

12. Mojtaba Taherzadeh and P. Gingo, "Neutron Radiation Characteristics of Plutonium Dioxide Fuel," *Nucl. Technol.* 15: 396 (1972).

13. R. H. Augstson and T. D. Reilly, *Fundamentals of Passive Nondestructive Assay of Fissionable Material*, LA-5651-M (September 1974).

14. C. M. Lederer, J. M. Hollander, and I. Perlman, *Table of Isotopes*, 6th ed., Wiley, New York, 1967.

15. J. B. Marion and J. L. Fowler, *Fast Neutron Physics*, vol. I, p. 467, Interscience Publishers Inc., 1960.

16. S. F. Mughabghab and D. I. Garber, *Neutron Cross Sections, Vol. I Resonance Parameters*, BNL-325 (ed ed., Vol. I) (1973).

17. G. R. Keepin, *The Physics of Nuclear Kinetics*, Addison-Wesley, 1965.

18. C. F. Masters, M. M. Thorpe, and D. B. Smith, "The Measurement of Absolute Delayed-Neutron Yields from 3.1- and 14.9-MeV Fission," *Nucl. Sci. Eng.* 36: 202-208 (1969).

19. R. A. Forester, H. M. Forehand, and H. O. Menlove, *Nuclear Analysis Research and Development, Program Status Report*, LA-5091-PR, p. 11 (1972).

4. PHYSICAL CHARACTERISTICS OF MATERIALS THAT AFFECT HEAVY-METAL ASSAY

4.1 INTRODUCTION

The chemical composition and physical form of the special nuclear material changes drastically while passing through the refabrication plant, from liquid uranyl nitrate solution on entrance to finished HTGR fuel blocks on exit. At intermediate stages in the process, the product material can be found in the form of loaded resin particles, coated particles, or green and carbonized rods. In addition, heavy metal will appear in various waste streams in both homogeneous samplable forms, in highly heterogeneous mixtures, and as contamination on other material and equipment that will have to be removed from the hot cell.

The requirement for accountability of in-process material and the demand for an accurate assay of the effluent waste streams to achieve an overall plant material balance necessitates the development and implementation of techniques and equipment capable of determining the fissile content of each of these varied materials. This section describes those physical characteristics of the materials that influence the selection of specific assay techniques and the design of the assay equipment. Physical characteristics of interest include, for example, whether the material is in a form from which representative samples can be drawn, the hydrogen content of the material and its variability, the size and fissile loading of a unit element of the material, and the fissile element density in the material and its blackness to thermal-neutron interrogation.

4.2 SOLUTIONS

Fissile material will enter the fuel refabrication facility in the form of clean uranyl nitrate solution containing ∿125 g/liter of uranium. In this form the fissile material is amenable to sampling and assay by standard chemical techniques. No nondestructive-assay techniques are contemplated for the uranium feed solutions.

Small amounts of uranium containing liquids will be produced during the fuel fabrication process. The current operating philosophy is to solidify these liquids by absorption on vermiculate or by distillation and then transfer the solid components to the solid waste disposal facilities (see Sect. 4.7), or to accumulate the solutions in a common liquid waste tank for chemical recovery or other disposition. Low-uranium-content aqueous wastes from decontamination washdowns, etc., will be sent to the ORNL low-level liquid waste storage facility. In these latter cases, assay will be by sampling and chemical analysis.

4.3 LOADED RESIN

Recycle fuel particles for the HTGR first start to take form when the uranyl ion in the uranyl nitrate solution is loaded onto weak acid resin. Before loading, the resin is in the form of tiny beads about 700 μ in diameter. After loading and drying, the diameter of the beads decreases to about 550 μ. The loading of the resin is accomplished through an ion exchange process that takes place when the resin and the uranyl nitrate solution are contacted in a loading column. When loaded, the resin particles consist of uranyl ions in a $C_6O_2H_6$ matrix. At this point, uranium makes up about 47% of the particle by weight.

Figure 4.1 is a composite photograph showing the particles in their early stages of refabrication (the carbonized particles are discussed in Sect. 4.4). Examination of the figure reveals that a high degree of uniformity exists among the particles. Hence, a representative sample can be taken by running the material through a splitter. Occasionally, a batch of loaded resin may appear with many defects in the particles. One such particle defect is seen in the figure near the bottom of the center photograph. Here two small "satellites" are attached to a larger particle. Another defect may be a large range of particle sizes in a loaded batch. The effect of defects on sample selection by a splitter is currently being evaluated.

The nominal density of dried loaded resin beads is 1.7 g/cm^3 with a uranium content of 47% by weight, with expected variations from these average values of 1.6 to 1.8 in density and 43 to 49% in uranium content. This range in composition corresponds to a range in the hydrogen-to-uranium atom ratio of 11 to 15.

Table 4.1 lists some of the properties of the loaded resin beads, while Table 4.2 gives the atom number densities and element density for each constituent in a loaded bead.

4.4 BARE AND COATED PARTICLES

After resin beads are loaded and dried, they are carbonized by placing them in a fluidized-bed furnace and slowly increasing their temperature to 800°C. This treatment decomposes the resin leaving a product mixture of UO_2 and carbon. Figure 4.1 contains a photograph of some carbonized beads.

The carbonized beads are heated to 1700°C to form "converted kernels," which form the core of a coated HTGR fuel particle. The product of this high-temperature process is a mixture of UC_2, UO_2, and carbon. Four coatings are applied to the kernels in fluidized-bed furnaces. The first is a low-density carbon layer called a buffer coating. Next, a high-density isotropic carbon coating is applied. This is followed by an SiC coating and another high-density isotropic carbon coating. Since the particles are coated with three different

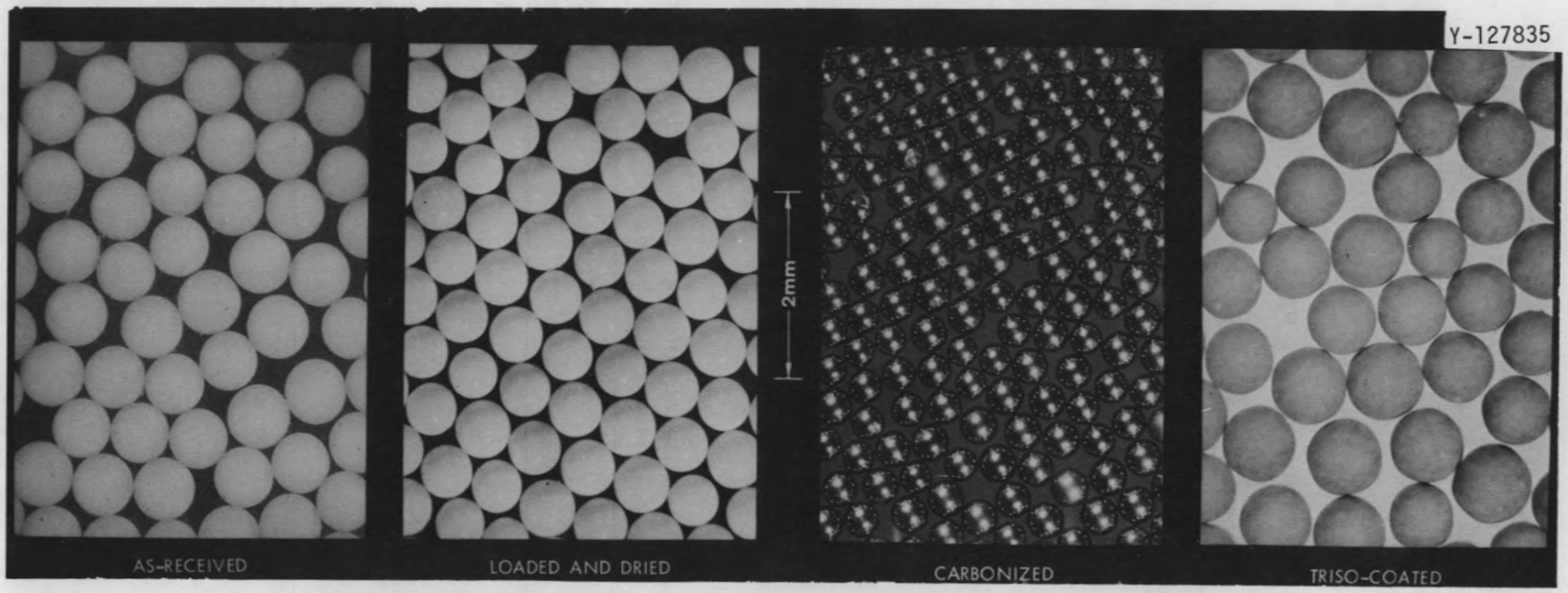

Fig. 4.1. Preparation of fuel particles from weak-acid resins.

Table 4.1. Dry loaded resin beads (average physical parameter values)

Diameter, μm	550
Particle density, g/cm^3	1.7
Uranium content, wt. %	47
Uranium mass, μg/bead	70

Table 4.2. Calculated average composition of dry loaded resin beads

Element	Percent	Density (g/cm^3	Number density (atom/b-cm)
Uranium	47	0.799	2.065×10^{-3}
Carbon	34.6	0.589	2.598×10^{-2}
Oxygen	15.5	0.263	1.279×10^{-2}
Hydrogen	2.91	0.0494	2.598×10^{-2}

materials, namely, low-density carbon, high-density carbon, and SiC, they are called TRISO particles.

Figure 4.2 is a photomicrograph of a sectioned TRISO particle. The kernel of this particular particle is composed of ThO_2 (formed by a sol-gel process) rather than the uranium kernel described above; however, the coatings are the same as those previously described. Tables 4.3 through 4.6 list some average values of particle parameters. The number densities in Table 4.5 indicate that the probability of absorption of a thermal neutron entering a TRISO particle is about 9%.

As in the case of the loaded resin beads, representative samples can be selected from a large batch of particles by running the batch through a splitter. Here again the effects of defective particles on the sample selection process are being studied.

4.5 GREEN AND CARBONIZED RODS

4.5.1 Description of green and carbonized fuel rods

The coated fissile and fertile fuel particles are blended with graphite shim particles and dispensed into a rod mold. The interstitial volume of the rod is saturated with a heated matrix material which consists of coal-tar pitch and graphite flake. The matrix solidifies around the particles and the green fuel rod is ejected from the mold. The rod is referred to as a green fuel rod because it is uncarbonized, that is, the particles are bound together by a hydrocarbon filler rather than by a carbon lattice. The green fuel rods for the fuel elements of the Fort St. Vrain Reactor (FSVR) have a diameter of 1.245 cm and a length of 4.93 cm. The fuel rods for the commercial HTGRs have a diameter of 1.576 cm and a length of 6.19 cm. The green rods are inserted into the graphite fuel blocks and carbonized in place; therefore, the green rod is the primary fuel rod type in the process. For quality control and quality assurance purposes, a small number of rods will be carbonized and then examined in the Sample Inspection Laboratory.

4.5.2 Physical aspects affecting assay

4.5.2.1 Elemental and isotopic composition of green fuel rods

The elemental and isotopic composition of the green fuel rod is dependent on the uranium and thorium loadings, the particle sizes, the packing fraction, and the matrix composition. Table 4.7 lists the elemental composition and Table 4.8 lists the nuclear number densities for two uranium and thorium loadings and for two isotopic compositions of uranium. The uranium and thorium loadings correspond to the maximum and minimum loadings contemplated for commercial HTGR recycled fuel (Table 3.1). There are large variations in the uranium content of the fuel rods. For nondestructive assay this means that the technique must

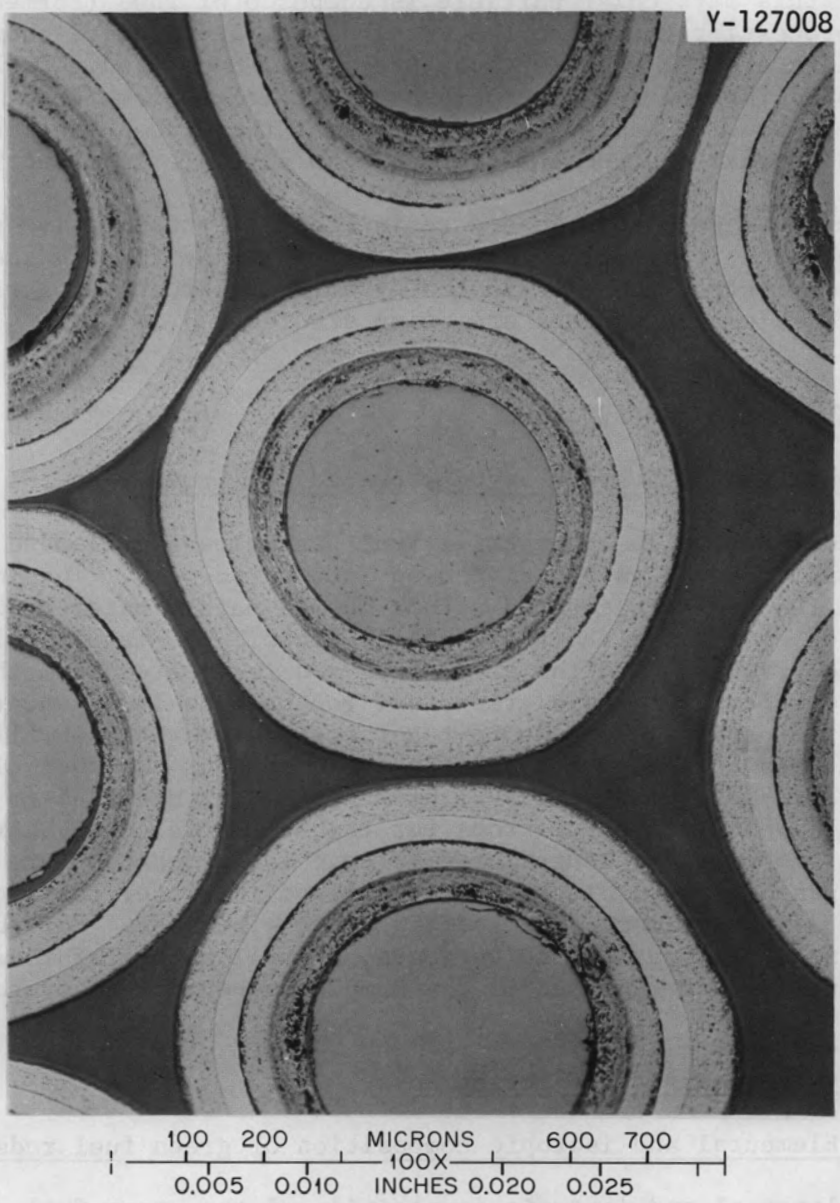

Fig. 4.2. Photomicrograph of sectioned TRISO particle.

Table 4.3. Carbonized resin beads (average physical parameter values)

Diameter, μm	385
Particle density, g/cm^3	3.3
Uranium content, wt %	71.4
Carbon content, wt %	18.8
Oxygen content, wt %	9.8

Table 4.4. Calculated average composition of carbonized resin beads

Element	Density (g/cm^3)	Number density (atom/b-cm)
Uranium	2.3.56	6.089×10^{-3}
Carbon	0.620	3.114×10^{-2}
Oxygen	0.323	1.217×10^{-2}
Hydrogen	0	0

Table 4.5. TRISO-coated particles (average physical parameter values)

Kernel diameter, μm	370
Kernel density, g/cm^3	3.2
Kernel composition, wt %	
Uranium	82.0
Carbon	15.2
Oxygen	2.8
Buffer coating thickness, μm	50
ILTI[a] coating thickness, μm	35
SiC coating thickness, μm	30
OLTI[b] coating thickness, μm	35
Buffer coating density, g/cm^3	1.1
ILTI[a] coating density, g/cm^3	1.95
SiC coating density, g/cm^3	3.2
OLTI[b] coating density, g/cm^3	1.95

[a]ILTI is the abbreviation for Inner Low Temperature Isotropic and is used when referring to the inner high-density isotropic carbon coating.

[b]OLTI is the abbreviation for Outer Low Temperature Isotropic and is used when referring to the outer high-density isotropic carbon coating.

Table 4.6. Calculated average atom densities of TRISO-coated particles

Element	Average particle Weight %	Average particle Density (g/cm^3)	Coating No. density (atom/b-cm)	Particle No. density (atom/b-cm)
		Converted kernel		
Uranium	82	2.62	0	6.781×10^{-3}
Carbon	15.2	0.486	0	2.441×10^{-2}
Oxygen	2.8	0.0896	0	3.373×10^{-3}
		Buffer coating		
Uranium	60.3	1.28	0	3.308×10^{-3}
Oxygen	2.0	0.0437	0	1.645×10^{-3}
Carbon	37.7	0.801	5.521×10^{-2}	4.018×10^{-2}
		Inner LTI[a] coating		
Uranium	40.9	0.844	0	2.181×10^{-3}
Oxygen	1.4	0.0288	0	1.085×10^{-3}
Carbon	57.7	1.19	9.787×10^{-2}	5.983×10^{-2}
		Silicon carbide coating		
Uranium	25.9	0.615	0	1.590×10^{-3}
Oxygen	0.886	0.0210	0	7.909×10^{-4}
Carbon	47.6	1.13	4.821×10^{-2}	5.668×10^{-2}
Silicon	25.6	0.607	4.821×10^{-2}	1.306×10^{-2}
		Outer LTI coating		
Uranium	19.6	0.442	0	1.142×10^{-3}
Oxygen	0.67	0.0151	0	5.680×10^{-4}
Silicon	19.3	0.436	0	9.382×10^{-3}
Carbon	60.4	1.36	9.787×10^{-2}	6.829×10^{-2}

[a]Low temperature isotropic.

Table 4.7. Elemental composition of green fuel rods, wt %

Element	Beginning of U-233 recycle		Equilibrium U-233 recycle	
	Minimum U+Th	Maximum U+Th	Minimum U+Th	Maximum U+Th
Hydrogen	0.95	0.80	0.90	0.80
Carbon	79.20	65.16	74.11	64.58
Oxygen	2.28	3.81	2.81	3.70
Silicon	0.86	1.67	1.24	2.51
Thorium	15.81	26.83	19.65	25.81
Uranium	0.90	1.73	1.29	2.60

Table 4.8. Nuclear number densities of green fuel rods, atom/b-cm

Nuclide	Beginning of U-233 recycle		Equilibrium U-233 recycle	
	Minimum U+Th	Maximum U+Th	Minimum U+Th	Maximum U+Th
Hydrogen	1.14×10^{-2}	1.14×10^{-2}	1.14×10^{-2}	1.14×10^{-2}
Carbon	7.97×10^{-2}	7.80×10^{-2}	7.91×10^{-2}	7.70×10^{-2}
Oxygen	1.72×10^{-3}	3.42×10^{-3}	2.25×10^{-3}	3.31×10^{-3}
Silicon	3.73×10^{-4}	8.55×10^{-4}	5.70×10^{-4}	1.28×10^{-3}
Th-232	8.24×10^{-4}	1.66×10^{-3}	1.08×10^{-3}	1.59×10^{-3}
U-233	4.27×10^{-5}	9.81×10^{-5}	4.35×10^{-5}	9.79×10^{-5}
U-234	3.41×10^{-6}	7.83×10^{-6}	1.72×10^{-6}	3.87×10^{-5}
U-235	2.72×10^{-7}	6.24×10^{-7}	5.68×10^{-6}	1.28×10^{-5}
U-236	1.14×10^{-8}	2.61×10^{-8}	4.46×10^{-6}	1.00×10^{-5}

be capable of operating over a wide range of rod loadings, with particular emphasis on those rod loadings that would lead to poor signal-to-background characteristics. Table 4.8 indicates a constant hydrogen content in all cases. This data is somewhat misleading in that a constant-particle packing fraction (0.62) was assumed. The different sizes of fertile, fissile, and shim particles would cause some variation in the hydrogen content of the rod. The hydrogen content of the rod and the hydrogen variability are important factors in the selection of a nondestructive-assay technique for green fuel rods.

4.5.2.2 Dimensional stability of green rods

The green fuel rods are formed in a molding operation, and consequently the radial dimensions of individual fuel rods are extremely precise. Diameters are uniform to ±0.001 cm, and the lengths of individual rods are within ±0.02 cm. The small variations in the diameter eliminate one source of uncertainty, dimensional variations, common to most nondestructive assay methods. The only dimensional uncertainty is due to small variations around the bottom edges of the rod where the removal of matrix flashing may have caused small (∿0.05 cm) pitting.

4.5.2.3 Material uniformity and particulate structure of green rods

The distribution of uranium within the fuel rod is not only an important factor in determining the fuel performance but may also be a critical factor in the ability to achieve precise uranium assay. The development of nondestructive-assay techniques for LWR fuel has produced methods for handling variations in total fuel rod loadings insofar as the uranium is uniformly dispersed within each rod. For HTGR fuel rods, the particulate nature of the fuel rod components and the fact that the fissile particles are only a fraction of the total number of particles per rod can cause the uranium to be nonuniformly dispersed in the rod. Because the fuel specifications impose uniformity requirements, the assumption is that the assay of green fuel rods can be based upon the assay of rods with uniformly dispersed fissile particles. Methods selected for nondestructive assay should, however, be insensitive to small nonuniformities in fissile loadings.

Even with fuel rods that are uniform on a macroscopic scale, the rods are still quite heterogeneous on the scale of a particle diameter. The fissile material is concentrated in the particle kernels rather than being dispersed uniformly throughout the medium. This heterogeneity can pose significant problems for some nondestructive assay methods because an individual particle can exhibit significant neutron self-shielding at low neutron energies.

In support of the neutron physics design of the HTGR, methods have been developed to compute the energy-dependent neutron self-shielding factor for fuel particles, which is defined as the ratio of the spatially

averaged neutron flux in the kernel to the average neutron flux in the moderator (matrix plus coatings). The technique of Wälti[1] has been used to calculate the kernel self-shielding factors at a neutron energy of 0.025 eV for fissile kernels of varying diameter and density. The sensitivity of the self-shielding factor to ^{233}U loading of a fuel rod is illustrated in Fig. 4.3. The self-shielding factor for each individual particle is dependent upon the number of fissile particles within the rod, because the shadowing effect of each particle tends to decrease the particle self-shielding. Figure 4.4 illustrates the sensitivity of the self-shielding factor to kernel diameter for three density values, and Fig. 4.5 indicates the relationship between density and self-shielding for four kernel diameters. Other calculations of the Wälti self-shielding factors indicated no dependence on the variations in thorium loading of the fuel rod. The relative insensitivity of the particle self-shielding factor to changes in uranium and thorium loadings of the rod implies that effects due to particle-to-particle self-shielding can be effectively separated from effects due to intraparticle self-shielding. The application of assay methods with high-energy interrogating neutrons would lessen the intraparticle self-shielding, but the hydrogen content of the matrix would lead to thermalization within the rod. Thus, variations in hydrogen content might cause more serious effects on assay precision and accuracy than the intraparticle self-shielding effects for resin-derived kernels.

4.6 LOADED FUEL BLOCKS

4.6.1 Introduction

As described in Sect. 4.5, the green fuel rods are loaded into graphite fuel blocks and the rods are carbonized in place. The standard fuel elements for the Fort St. Vrain Reactor (FSVR) and the commercial size HTGR are shown in Figs. 4.6 and 4.7. The primary difference between the two elements is the diameter of the fuel rod and the number of fuel rod and coolant channels per element.

4.6.2 Physical characteristics affecting assay

The loaded fuel blocks contain in the range of 0.3 to 0.9 kg of $^{233}U + ^{235}U$, 6 to 12 kg of thorium, and 110 kg of carbon, with small quantities of silicon carbide (from the SiC coating) and oxygen (from the ThO_2 fraction of the kernel). The physical size of the fuel element and the dispersed nature of the fissile content make nondestructive assay of these elements difficult. Development work at LASL has been reported recently on the whole-block assay of fresh (^{235}U loaded) HTGR fuel blocks.[2-4] The LASL research utilized a 14-MeV neutron generator to induce fissions in the fissile and fertile material in the fuel element. Delayed neutrons were then detected to measure the amount of ^{235}U and thorium within the element. Discrimination between the ^{235}U and thorium was accomplished by modifying the energy of the interrogating

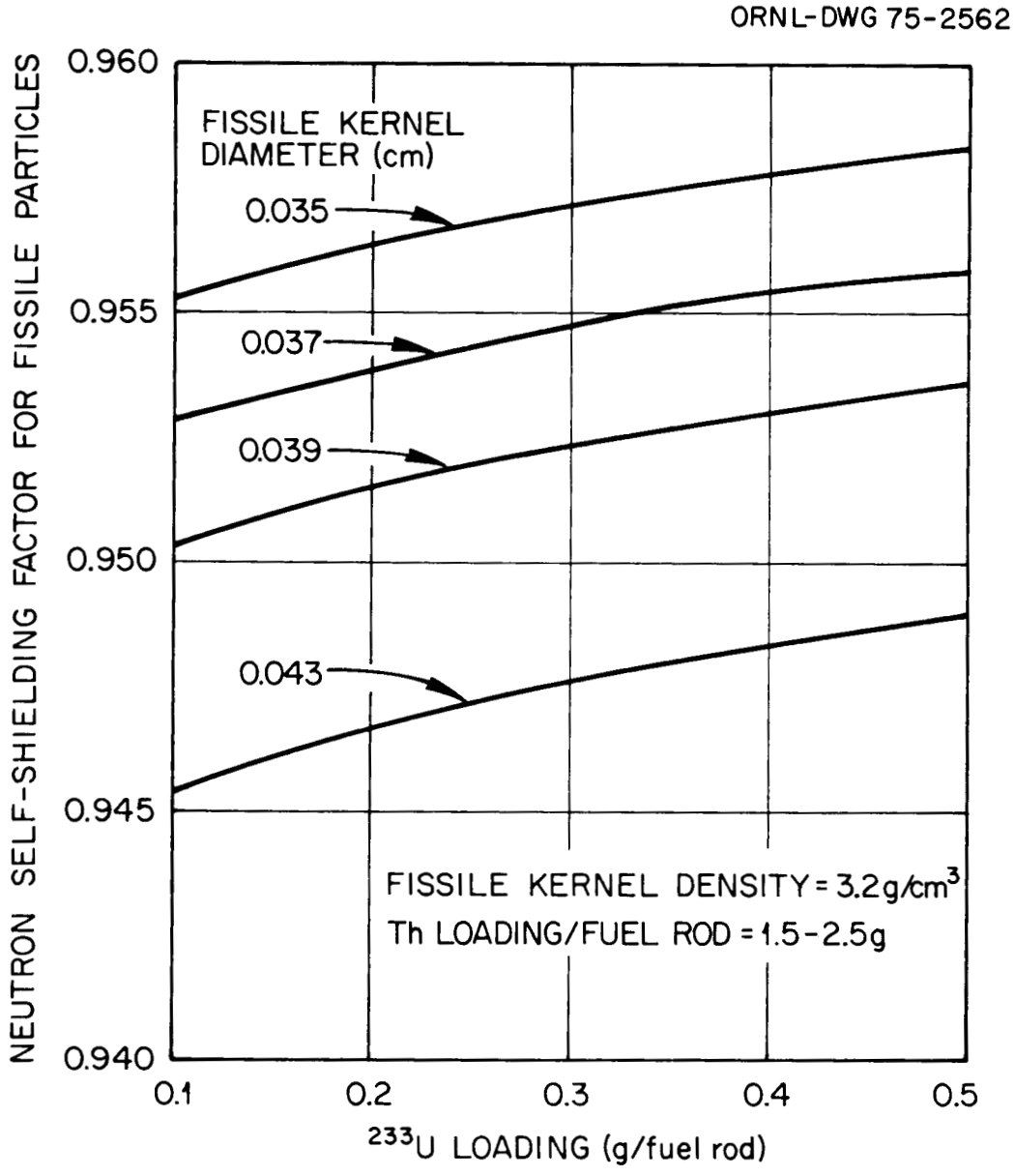

Fig. 4.3. Neutron self-shielding factors for weak-acid resin-derived ^{233}U kernels as a function of ^{233}U fuel rod loading for four diameters.

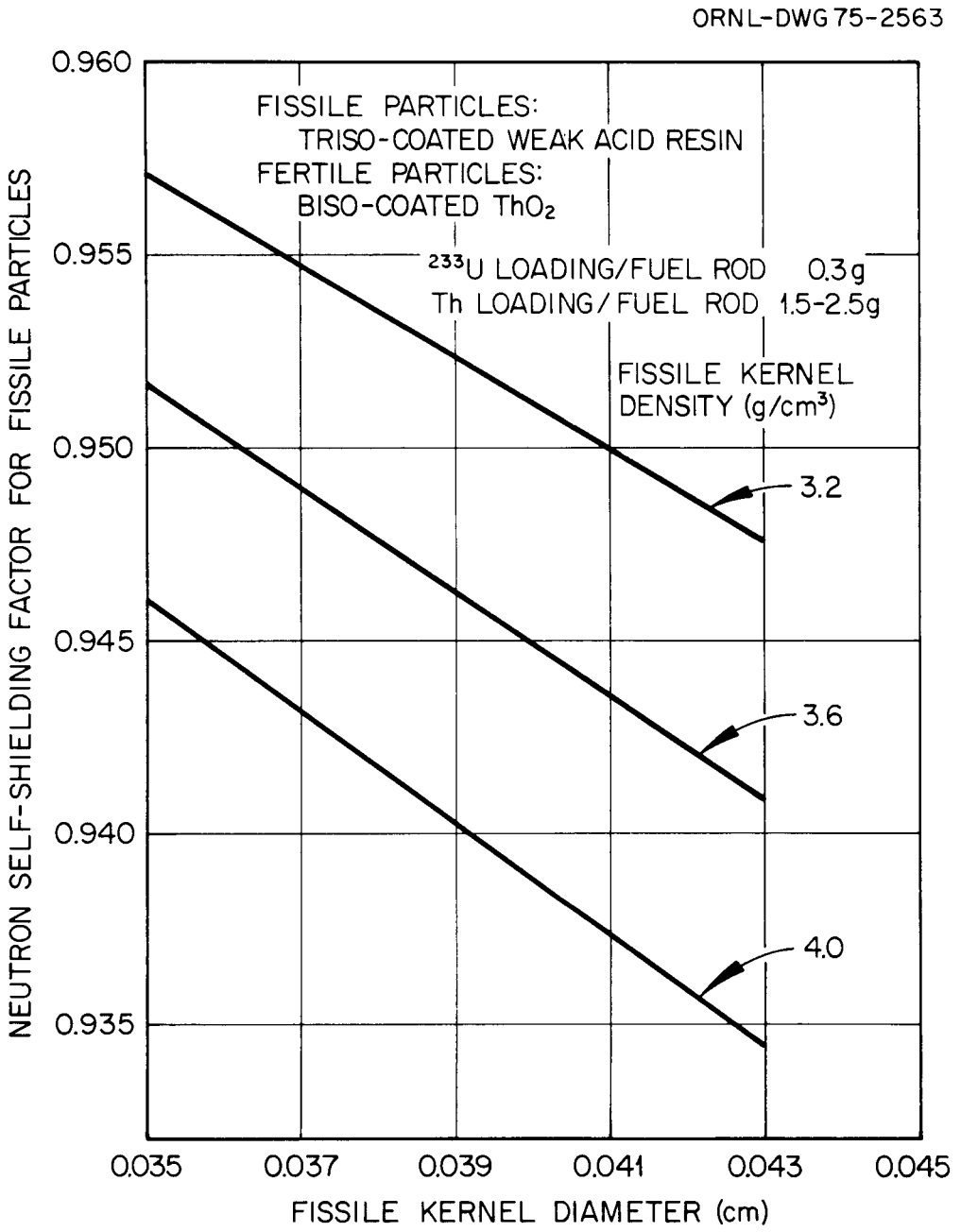

Fig. 4.4. Neutron self-shielding factors for weak-acid resin-derived ^{233}U kernels as a function of fissile kernel diameter for three kernel densities.

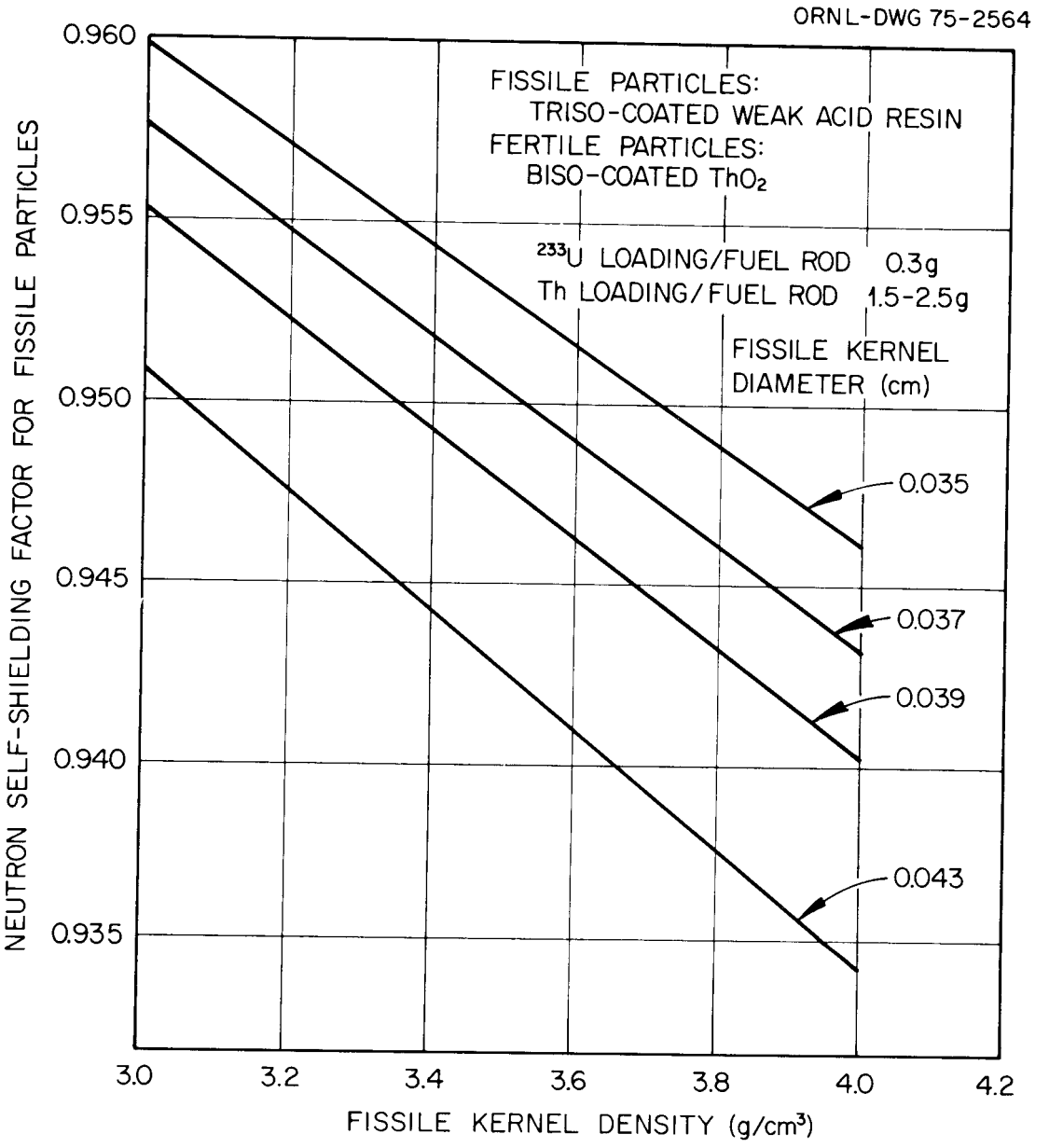

Fig. 4.5. Neutron self-shielding factors for weak-acid resin-derived ^{233}U kernels as a function of fissile kernel density for four kernel diameters.

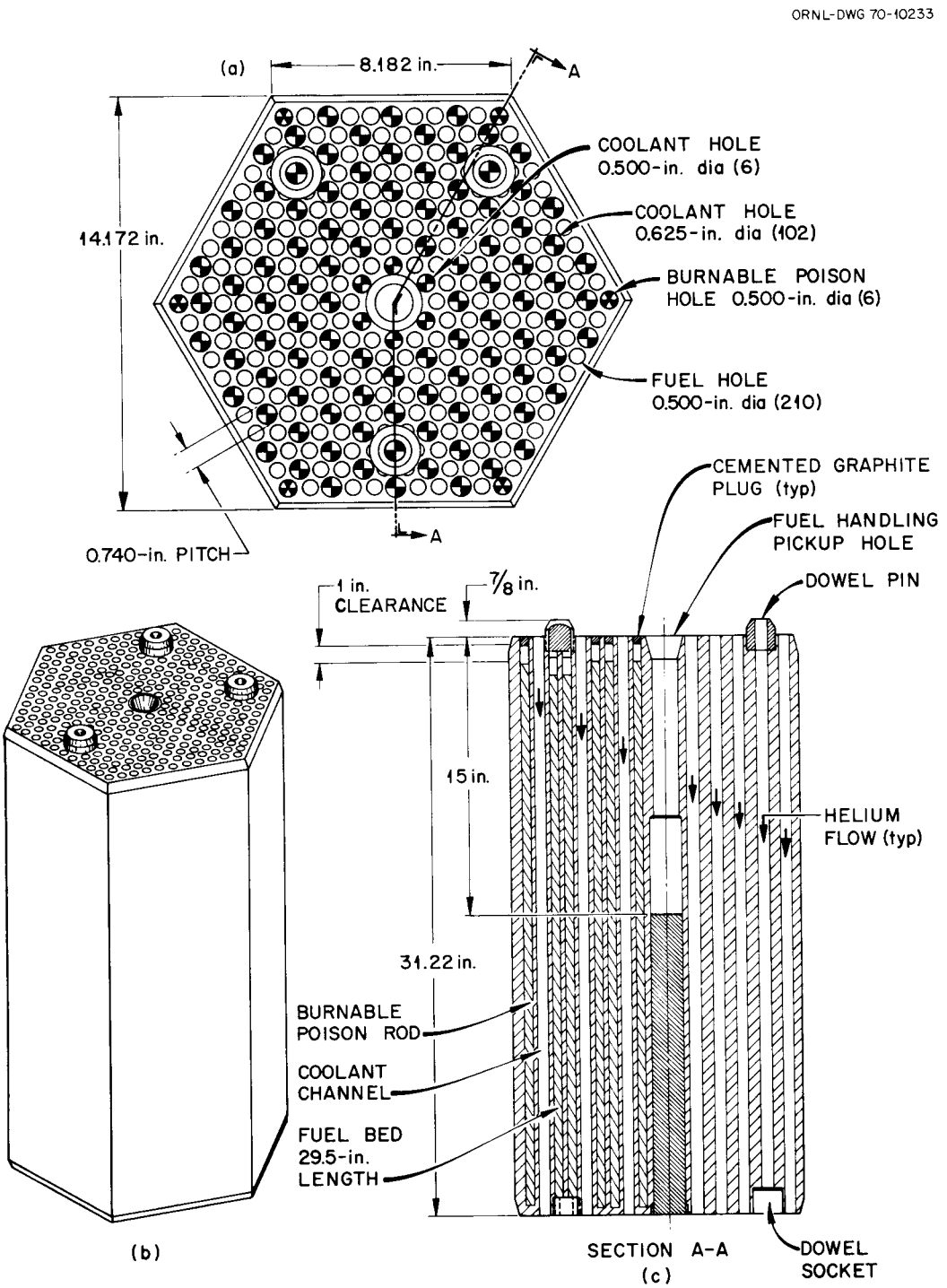

Fig. 4.6. Fort St. Vrain reactor fuel element.

ORNL-DWG 75-1570

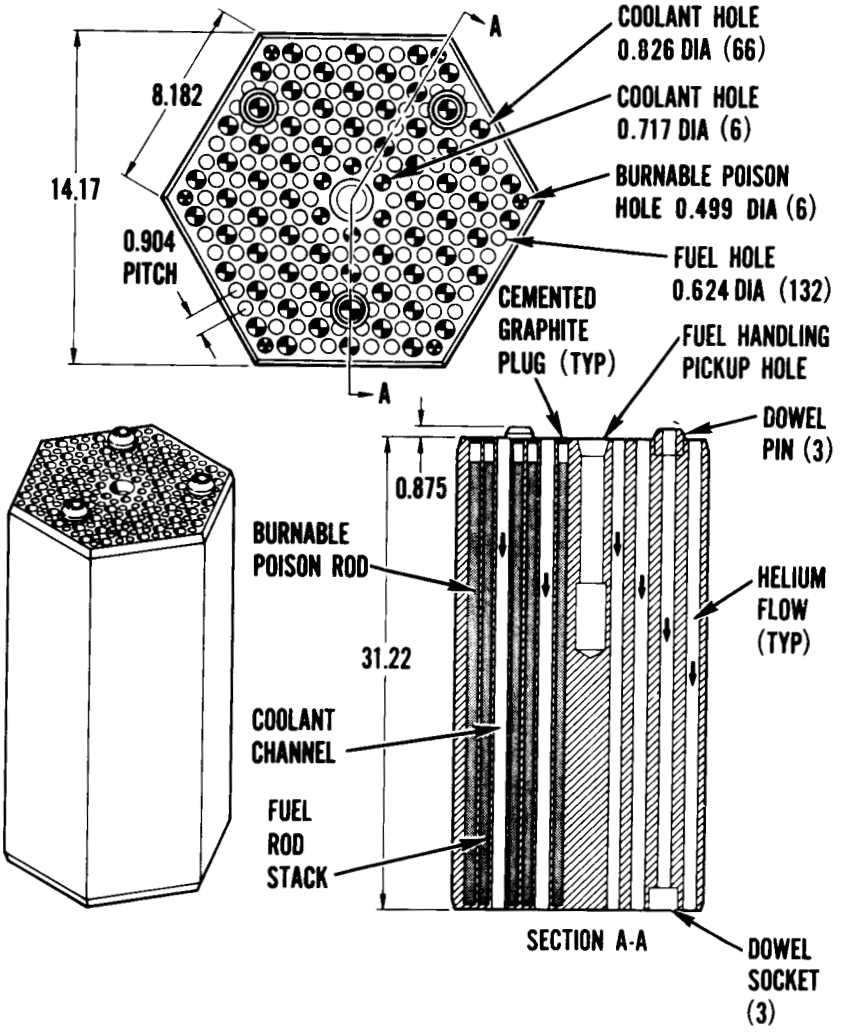

Fig. 4.7. Typical 1160-MW(e) HTGR fuel element.

neutrons. The results of the initial tests indicated that the method was promising; however, accuracies of 5 to 7% were quoted for the ^{235}U content. The accuracy required for safeguards purposes is at least a factor of 10 better than the current performance.

For the fuel refabrication pilot plant (FRPP) we have tentatively decided not to incorporate whole-element assay in the facility nor to develop a method for this purpose. The LASL technique, if developed to achieve the requisite accuracy, should be applicable to recycled elements because the method uses neutron detection methods which can be made insensitive to the gamma radiations of ^{232}U and its daughters. One possible problem for the extension of this method to recycled fuel is the large difference in the delayed neutron yields of ^{233}U and ^{235}U. Because both ^{233}U and ^{235}U are present in the recycled uranium, the ^{233}U to ^{235}U isotopic ratio for each fuel block must be known to achieve accurate assay results. The preparation of fuel element standards for any ^{233}U whole-block assay system would also be a difficult, time consuming, and expensive operation.

The assay approach for the fuel product adopted for the pilot plant is a method that can be transferred to a commercial operation. The basic accountability system for the fuel product consists of 100% assay of QC-accepted green fuel rods in combination with a rigid material control program to record the ^{233}U and ^{235}U contents of individual fuel blocks during the block-loading operation. In the FRPP the fuel rod assay machine will feed a rod storage system which serves as surge storage between the fuel rod forming machine and the element loader. One option for the commercial facility would be to incorporate a rod assay system in the element loading operation. This configuration would prevent diversion or substitution between fuel rod assay and block loading in addition to yielding a precise fissile content for each element. Such a method would be a logical extension of the FRPP fuel rod assay concept (described in Sect. 5.3.1). The key to using fuel rod assay as a final product assay is the ability to design a system that eliminates the possibility of rod substitution or diversion between the assay point and the point in the process at which the elements are packaged for shipment.

The gamma activity of the fuel element cannot be employed for accurate nondestructive assay because of the time dependence of the gamma radiation. It should be possible, however, to utilize the radiation characteristic of the fuel as a semiquantitative verification of uranium content. A gamma scan of the element using miniature detectors that could be translated through the coolant holes would yield an independent check on uranium content. The value of such a semiquantitative check would depend on the goals and criteria of the overall safeguards and accountability program.

4.7 WASTE STREAMS

During operation of the HTGR refabrication pilot plant, substantial quantities of solid radioactive waste products will be generated. The bulk of the material (from the standpoint of grams of ^{233}U) will be in the form of reject product material. In addition, alpha active fissile material will be present in process waste streams and will appear as contamination on combustible and noncombustible material removed from the cell.

Our current thinking is that the alpha-contaminated waste from TURF can be segregated into two categories: high-uranium-content material consisting primarily of reject product and quality control samples and low-level waste material whose total gamma activity per cubic foot is less than that of 10 g of ^{233}U containing 500 ppm ^{232}U 90 days old.

Table 4.9 lists the average daily quantities of high-uranium-concentration reject material anticipated from the TURF product line based on our most recent calculations.[5] The bulk of this material is amenable to sampling, and it is anticipated that this technique can be used for in-plant inventory control. Any given batch of reject particles, resin, or rods will differ only slightly from acceptable product material and, from a nondestructive assay point of view, will conform to the descriptions given in Sects. 4.2 and 4.5. Hence, it is anticipated that individual batches of reject material can be sampled and assayed by the same techniques used to determine product material fissile content.

However, after sampling and possible processing to render the reject material compatible with the head-end processing equipment for reclamation purposes, the high-uranium-content material will be loaded, with no attempt for segregation into waste cans, for shipment to the Allied Chemical Corporation facilities in Idaho. These cans, a conceptual design of which is shown in Fig. 4.8, must be reassayed to confirm the total fissile content before shipment from the facility.

Since no segregation of material is anticipated prior to shipment, the cans will contain a polygenetic mixture of microspheres in various stages of processing, reject fuel rods (carbonized to make them compatible with the head-end processing facilities), and, perhaps, coating furnace liner scrapings containing a high proportion of graphite. It is anticipated that each 3-in.-diam by 9-in.-long can will contain from 50 to 1000 g of fissile material, and, for those cans containing reject rods, an appreciable amount of ^{232}Th.

The more heavily loaded cans will be opaque to thermal neutrons. In addition, there will be substantial self-absorption of internally produced gammas. Calculations indicate that for a homogeneously loaded can containing 150 g of ^{233}U and no ^{232}Th, 35% of the ^{208}Tl gamma rays

Table 4.9. Estimated average daily production of high-uranium-content solid-waste material

Material form	Uranium (g/day)	Source
Loaded and dried resin	247	Resin loading reject and samples
Carbonized resin[a]	161	Resin carbonization reject and samples
Converted resin[a]	12	Resin conversion reject and samples
Coated particles	530	Particle coating reject and samples
Green rods	13	Reject rods, samples, and assay calibration standards
Carbonized rods	11	Quality assurance samples
Reject blocks[a]	12	Reject blocks
Coated particles and carbon	18	Coating chamber scrapings and fritts
Epoxy impregnated rods	0.15	Metallographic mounts
U_3O_8 ash	3	Sample inspection station

[a]Routine production of this type of waste is not anticipated. Numbers represent daily average, but, in fact, an occasional infrequent large batch will have to be handled.

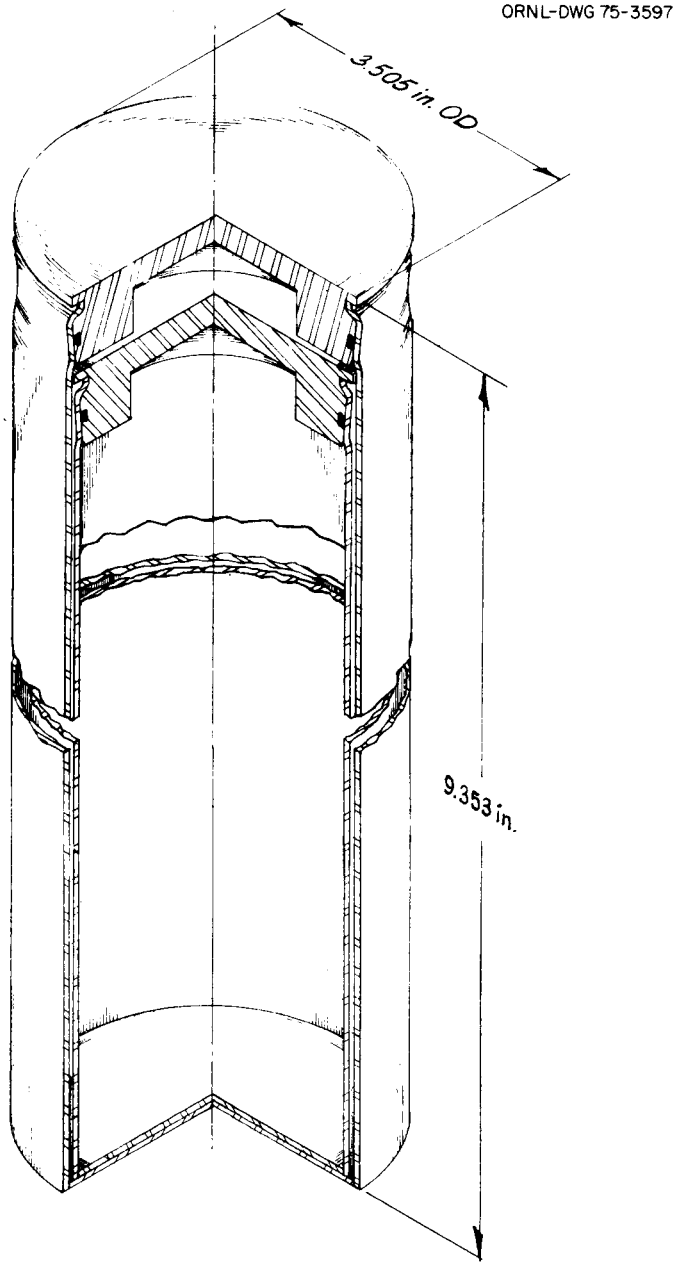

Fig. 4.8. HTGR-FRPP system 9 reject fissile and fertile material storage can conceptual design.

generated are absorbed or degraded in energy within the can. The self-absorption has also been shown to be extremely sensitive to arrangement of the fissile material within the can. Thorium, present in the waste material, will also contribute to absorption of internally generated gammas.

The high-uranium-content waste cans will also produce significant numbers of (α,n) neutrons. This source will be a function of both the age of the material that determines the concentration of alpha-emitting ^{232}U daughters present and the type of material that determines the concentration of light target atoms for the (α,n) source.

It is anticipated that the remainder of the contaminated solid waste will consist of material containing sufficiently low concentrations of uranium and other alpha-active isotopes to allow it all to be lumped in a single low-level waste category. This material will be further segregated into combustible and noncombustible categories before canning in 30-gal drums for disposition in retrievable storage.

The low-level combustible wastes include material generated during normal hot cell operation (e.g., manipulator boots, cloth wipes, etc.) and process-related material peculiar to the fuel fabrication process. This latter material will consist of low-level carbon-uranium mixtures that will be generated as a result of the replacement of graphite furnace internals and the clean out and solidification of the furnace off-gas scrubber solvent recovery system. No attempt will be made to segregate these various types of combustible low-level wastes in the TURF facility. It is noted, however, that in a commercial integrated reprocessing and refabrication plant, the low-level combustible waste would most probably be processed in a common low-level waste incinerator.

Additional development data are necessary before all quantities and forms of the low-level waste can be completely specified. For example, the amount of material lost due to furnace blowover during the carbonization process is unknown, as is the eventual form that this material assumes after contact with the scrubber solution. Thus, construction and operation of prototype development equipment is necessary before the fissile content of the solidified waste from the off-gas scrubber traps can be quantified. Also, additional information is needed on the quantities of material adhering to coating-furnace fritts and liners.

Table 4.10 indicates the currently estimated quantities of the various types of low-level waste materials that will be generated daily during TURF operation. Neither ORNL nor ACC has facilities for the recovery of fissile material from combustible low-level waste in the quantities anticipated. Accordingly, plans are to contain both this and the noncombustible material appropriately for disposition in a retrievable storage facility.

This material must be assayed for fissile content prior to storage. The high degree of heterogeneity of the material and its low fissile

content makes neutron interrogation techniques inapplicable. Gamma scanning is a possible solution (see Sect. 5.3.4) if the uranium content can be maintained at a low enough level to avoid the need for high-accuracy measurements.

Some small amounts of uranium will be present in various liquid waste streams within the facility. These amounts should be small and assayable by sampling and chemical analysis techniques.

Table 4.10. Estimated daily production of combustible and noncombustible low-level waste

Material form	Quantity (ft^3/day)
Manipulator boots	1.0
Miscellaneous combustible	9.0
Soot from solvent reclamation	0.6
Broken equipment, tools, etc. (noncombustible)	1.0

REFERENCES FOR SECTION 4

1. P. Walti, "Evaluation of Grain Shielding Factors for Coated Fuel Particles," *Nucl. Sci. Eng.* 45: 321 (1971).

2. J. L. Macdonald, D. B. Smith, R. A. Foster, R. H. Augustson, and G. D. Turner, *Nuclear Analysis Research and Development Program Status Report, May-August 1973,* LA-5431-PR (November 1973) pp. 6-8.

3. R. H. Augustson and J. J. Malanify, *Nuclear Analysis Research and Development Program Status Report, January-April 1973,* LA-5291-PR (May 1973) pp. 1-4.

4. R. H. Augustson and J. J. Malanify, *Nuclear Analysis Research and Development Program Status Report, January-April 1974,* LA-5675-PR (August 1974) pp. 9-10.

5. S. R. McNeany, *NOMUF — A Computer Code for Calculating Material Flows in the HTGR-FRPP,* GCR: 74-23 (Sept. 9, 1974).

5. ASSAY SYSTEM DESCRIPTION

5.1 ASSAY PHILOSOPHY

The conceptual design of the assay and accountability system for the HTGR refabrication pilot plant is directed toward the objectives of providing a system to generate material balance and accountability information on a real-time basis. This system (which includes both hardware and software for interpretation of process data), must be applicable and transferable to a larger commercial fuel refabrication facility. The requirement of commercial applicability is one which necessitates frequent reiteration in order to avoid the pitfall of adopting too myopic a view and solving only the smaller scale problems peculiar to pilot plant operation.

The system is predicated on the ability to determine fissile content of batches of material in process throughout the plant by the measurement of small representative samples coupled with the ability to maintain continuous surveillance of the mass of material in each batch and its progress from one processing station to another. This information will be available through the use of continuous readout scales and a dispatch—receive signal system that is continuously monitored and updated by a central plant data management system. (See Sect. 6 of this report for a description of data flow and data handling.)

Two qualifications are necessary. The system is not "real time" in the sense that continuous verification of the entire fissile inventory will not be available. Because one major input to the system comes from in-line weighers, the assumption must be accepted that substitution of inert material has not been made in the intervals between sampling and assaying points. However, in view of the fact that all of the material with the exception of quality assurance, quality control, and assay samples will be contained within the hot cells, the fact that samples are extracted for fissile content verification at almost every process step and hence at frequent intervals, and the fact that the high specific activity of the material will render it extremely visible to area radiation monitors and portal monitors, this assumption becomes plausible.

In addition, continuous verification of the fissile content of certain of the waste streams will not be possible. Particular problem areas arise in monitoring losses due to particle and fines blowover from the carbonization and coating furnaces and the loss of material due to its adherence to the walls of furnaces and gas distributors. It is anticipated that reasonable limits can be set for losses through these channels and, by monitoring the difference between input and output of these processes, a continuous waste stream inventory can be maintained by difference. Routine cleanout of the off-gas scrubber solvent recovery system and direct measurement of its fissile content, together with the assay of spent furnace liners and the scrapings from their walls, will provide a periodic verification of this running total. At any point in

the process, if losses exceed some preset limits, this would signal the need for a nonroutine shutdown for inventory verification. Such a shutdown would also be required for process control and criticality safety considerations.

At one point in the process, a 100% product stream inventory is included. This 100% assay takes place downstream of the green rod fabrication step and is included for quality assurance as well as accountability purposes. While the green rods are amenable to inventory by sampling, handling problems associated with extracting a relatively large number of samples, coupled with the personnel exposure problems such a sample load would place on sample inspection station operations, were expected to be equivalent to designing an in-cell on-line assay device. The deciding factor, therefore, is the reassurance provided by a complete accounting of the material at the final accessible point in the fabrication process. This concept is not directly transferable to a larger commercial facility and 100% assay of the product stream in a commercial facility at this point may not be economically feasible because of the much larger throughput and the time required to accumulate significant statistical information (see Sect. 5.3.1). In such a facility, the on-line machine could be relegated to the role of a side stream sample assay device, and the task of 100% screening of the green rods could be assumed by multiple gamma-scanning units similar to those described in Sect. 5.3.2.

5.2 ASSAY SYSTEM DESCRIPTION

The conceptual design of the assay and accountability system for the refabrication pilot plant includes destructive chemical analysis capabilities both on and off site, three major nondestructive assay components, assorted process control instruments including on-line scales, hopper-fill measuring devices and material transfer indicators, and a data management system for the integration of data from all of these sources to provide meaningful and current material accountability information.

This section describes in detail the nondestructive assay components of the system which consists of the sample inspection assay equipment, the on-line assay devices, and the waste assay devices.

The presence of the remaining equipment and the destructive chemical analysis capabilities are, however, an integral part of the overall accountability system. In addition, the presence of an on-line data management system with automatic communication links to the various system sensors is vital to the effective functioning of the system. Data flow and processing by this data management system is described in Sect. 6.

Figure 5.1 is a schematic of the overall plant showing principal material flows and the location of the nondestructive assay devices in these flow paths. For material accountability purposes the main fabrication facilities located in the cells is considered a closed balance area, and the sample inspection station is a separate balance area. This separation is indicated schematically in the figure. Note that all material flowing into and out of the plant must pass through one of the several assay devices for inventory verification.

5.3 SPECIFIC CONCEPTUAL DESIGN SOLUTIONS

5.3.1 On-line assay machine

5.3.1.1 Function and operating requirements

The on-line assay machine measures the fissile material content of 100% of the green fuel rods produced by the pilot plant. This device provides real-time verification of the ^{233}U plus ^{235}U flow and, with appropriate material management of the fuel rods, can provide a direct measurement of the fissile content for each fuel assembly. The assay device must provide the total ^{233}U plus ^{235}U content of green fuel rods in groups of 1000 to 10,000 rods. The precision of the assay on 1000 rods must be better than 0.3% at the 95% confidence interval. The machine must assay at the rate of 10 rods per minute. This throughput represents approximately 5 to 10% of the total fuel rod output of a commercial facility. The on-line assay machine is located between the fuel rod molding machine and the fuel rod magazine storage subsystem. The fuel rods will have been gamma scanned prior to being assayed, and rods with uranium loadings differing by more than 10% from the mean loading will have been rejected from the line and, hence, will not be assayed by this machine. (The gamma scanner is described in Sect. 5.3.2.)

5.3.1.2 Assay technique and rationale for selection

The assay technique selected for the on-line green fuel rod assay machine employs active thermal-neutron interrogation with prompt-fission neutron counting. This technique has been developed by LASL for the assay of LWR fuel rods.[1,2]

In the review of nondestructive assay methods surveyed for this application, first priority was given to methods being developed or in use for HTGR fresh fuel. These methods are delayed neutron activation analysis,[3] the fission multiplicity method of the isotopic source assay system (ISAS),[4] the random driver,[5] the Sb-Be active assay system,[6] and the two-energy gamma-ray transmission method.[7] Of these methods only the delayed neutron and Sb-Be assay systems could be applied to the determination of ^{233}U and ^{235}U in green fuel rods. ISAS and the random driver will not function in the high gamma field associated with recycle

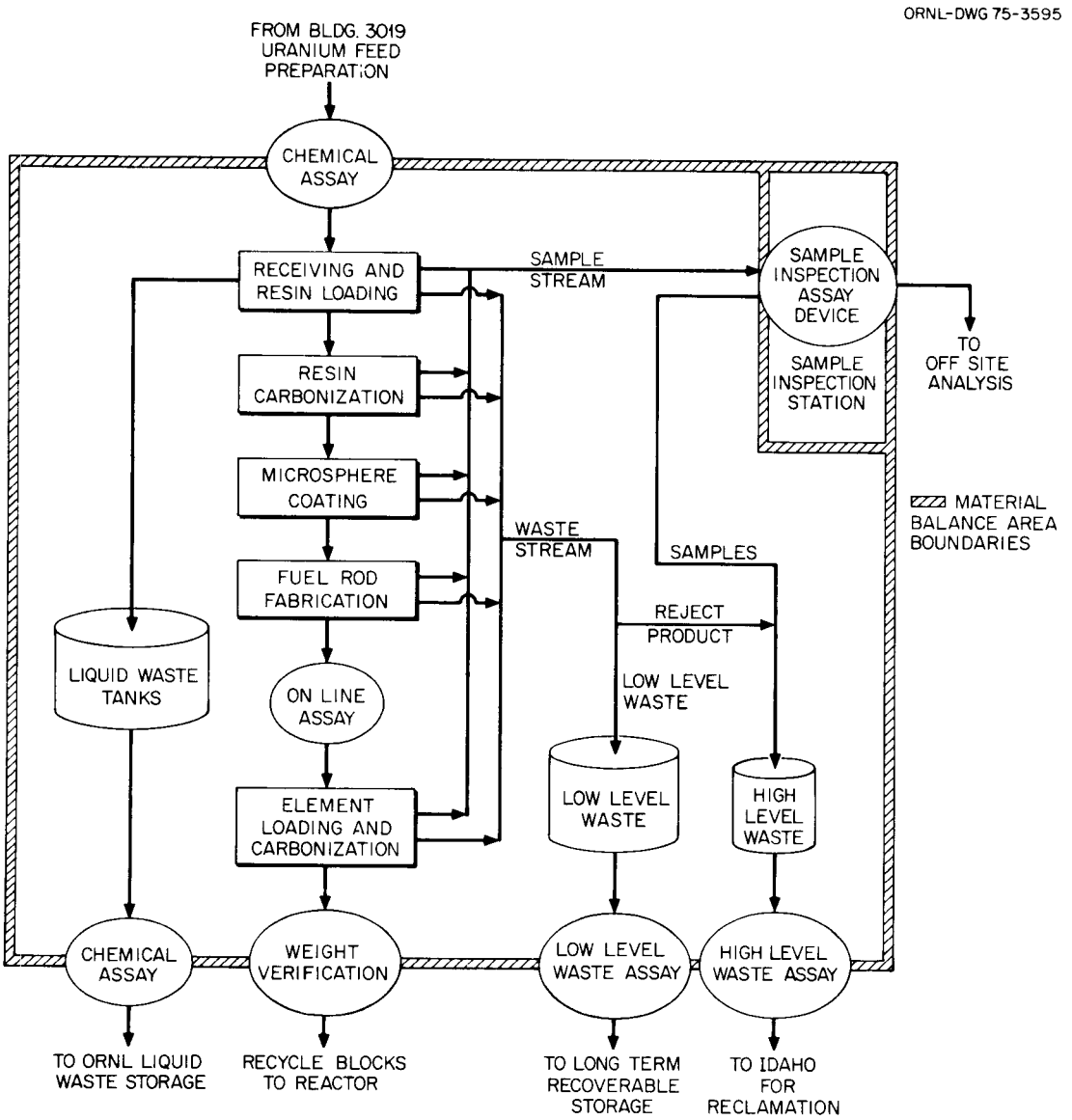

Fig. 5.1. Overall plant material flow and assay points.

fuel. The two-energy gamma-ray transmission method determines only the total heavy metal content. The delayed neutron method described in Ref. 3 used a TRIGA reactor as the interrogating source, and, consequently, is a method for assaying samples only. A delayed neutron method based on a ^{252}Cf neutron source is a potential method for a high-throughput green fuel rod assay machine. The Sb-Be system could also be applied to green fuel rods; however, to achieve required throughput rates, an antimony source that is 10 to 100 times more intense than present Sb-Be systems would be necessary. We have eliminated the Sb-Be system for this application because of the difficulty in handling the 100- to 1000-Ci antimony sources on a trimonthly or semiannual basis.

Other techniques considered that have not previously been applied to green fuel rods are neutron-generator-based active assay techniques and thermal neutron irradiation methods with prompt or delayed neutron counting. Techniques using thermal or epithermal irradiation and delayed gamma ray counting are not applicable to HTGR recycle fuel because of the high gamma radiation levels (see Sect. 3.7.3).

Several characteristics of the fuel material and the refabrication process determine the nondestructive assay method selected. The first characteristic is the hydrogen content of the green fuel rods. This characteristic makes fast irradiation techniques difficult for the assay of single rods or a single column of rods and almost unworkable for bulk samples of rods. The hydrogen moderates the interrogating neutrons, and the fast irradiation becomes a partially thermal irradiation technique. Second, the fissile content per unit volume is relatively low in HTGR rods. A single Fort St. Vrain fuel rod (2 in. x 0.5 in. in diameter) contains from 0.1 to 0.3 g of fissile material. This fissile concentration is a factor of 5 below average fissile concentration in LWR fuel. Third, the process produces rods at high rates, and unless a sampling method is used, the assay machine must operate at a comparable throughput. The throughput rate of an assay machine is determined by the precision required, the source strength, the detector efficiency, the fission probability per source neutron, and the number of rods assayed simultaneously. Fourth, the assay machine must be operated and maintained remotely. This last condition implies high reliability, and neutron generator techniques have not been considered in detail for this reason. There are still considerable questions in the industry about the reliability of neutron generators, sealed tube or otherwise. For reasons of cost and complexity, photofission-based techniques have not been studied.

With these characteristics as the basis, the ^{252}Cf thermal neutron irradiation, prompt neutron counting method was selected as the method with the highest probability of meeting the performance requirements. LASL experience with this technique was an additional reason for its selection. Delayed neutron counting after thermal or epithermal irradiation was also investigated, but the analysis indicated lower overall efficiency for this method compared to the prompt fission neutron detection system.

The thermal irradiation system has a high fission probability per source neutron, reasonable gamma discrimination, and the ability to assay a number of rods or columns of rods simultaneously. The thermal irradiation method has one potential disadvantage for HTGR fuel. The particulate nature of the fuel results in a double self-shielding effect within the material. Individual fuel kernels exhibit some self-shielding, and particle-to-particle self-shielding is also possible. The fuel kernel self-shielding is thought to be the more serious problem because the extent of the self-shielding is a function of the kernel diameter and density. These two variables, kernel diameter and density, may affect the assay results independent of the fissile content. The extent of this problem for the recycle fuel is not precisely known at this time, and consultations with LASL are under way to determine the effects of these variables on assay precision. The approximate magnitude of the particle self-shielding effect is in the range of 5 to 15%.[8,9] The reference fissile particle exhibits an approximate 5% self-shielding effect, as discussed in Sect. 4.4.

A series of calculations have been completed to size the moderator assembly for the ^{252}Cf irradiator. Figure 5.2 presents the ^{233}U and ^{232}Th count rates and count rate ratios as a function of position for a D_2O tank 60 cm in diameter. The fuel rod would be located in the polyethylene just outside the D_2O region.

5.3.1.3 System description and performance characteristics

The conceptual design of the on-line fuel rod assay machine is described in this section. The device can be operated in two modes. The first mode enables assay of individual fuel rods at the rate of 10 rods per minute, and the second method assays for fissile uranium in a large number of rods (>100) without providing information on individual rods. Both techniques utilize a circular fuel rod carriage to move green rods through a thermal neutron interrogation, prompt-fission neutron detection assay system. An early design of this system is illustrated in Fig. 5.3.

The HTGR fuel rod assay system is patterned after the LASL LWR fuel rod scanner.[1,2] The neutron source is 1 mg of ^{252}Cf; neutron moderation is provided by the D_2O-filled tank that surrounds the source. The tungsten sleeve around the californium reduces the gamma-ray background at the detector position and enhances neutron moderation through inelastic scattering in the tungsten. The neutron detectors shown in Fig. 5.3 are ZnS-lucite scintillators. These were initially selected because of their neutron efficiency, compared to the ^{4}He detectors used in the LASL device. The gamma-ray discrimination ability of the ZnS compared to ^{4}He and the better geometric coupling possible with ^{4}He may make ^{4}He detectors more suitable for this application.

Two significant differences between the LASL design and the ORNL design are the increased size of the D_2O region and the unique rod-handling

ORNL-DWG 74-4509R

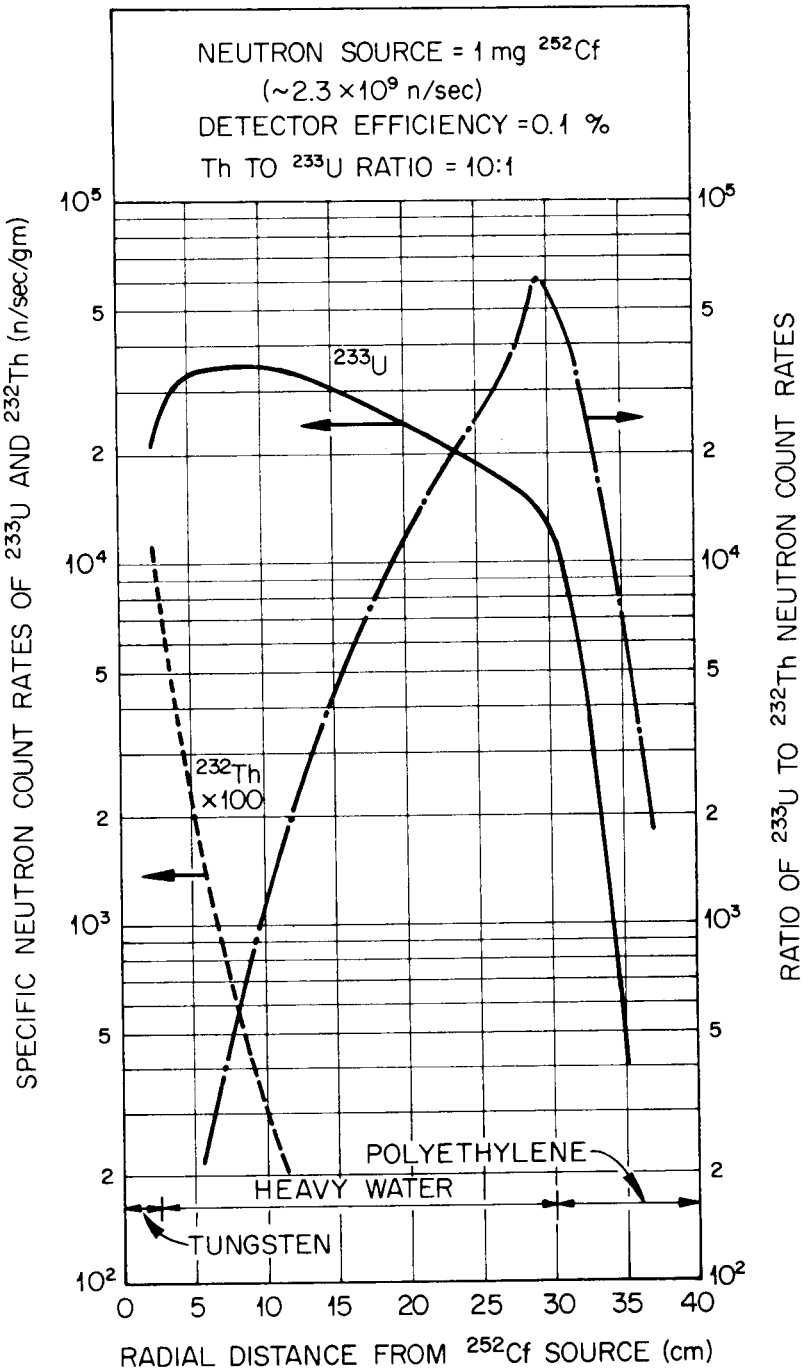

Fig. 5.2. Specific neutron count rates and count rate ratios of ^{233}U and ^{232}Th irradiated in the ^{252}Cf assay device.

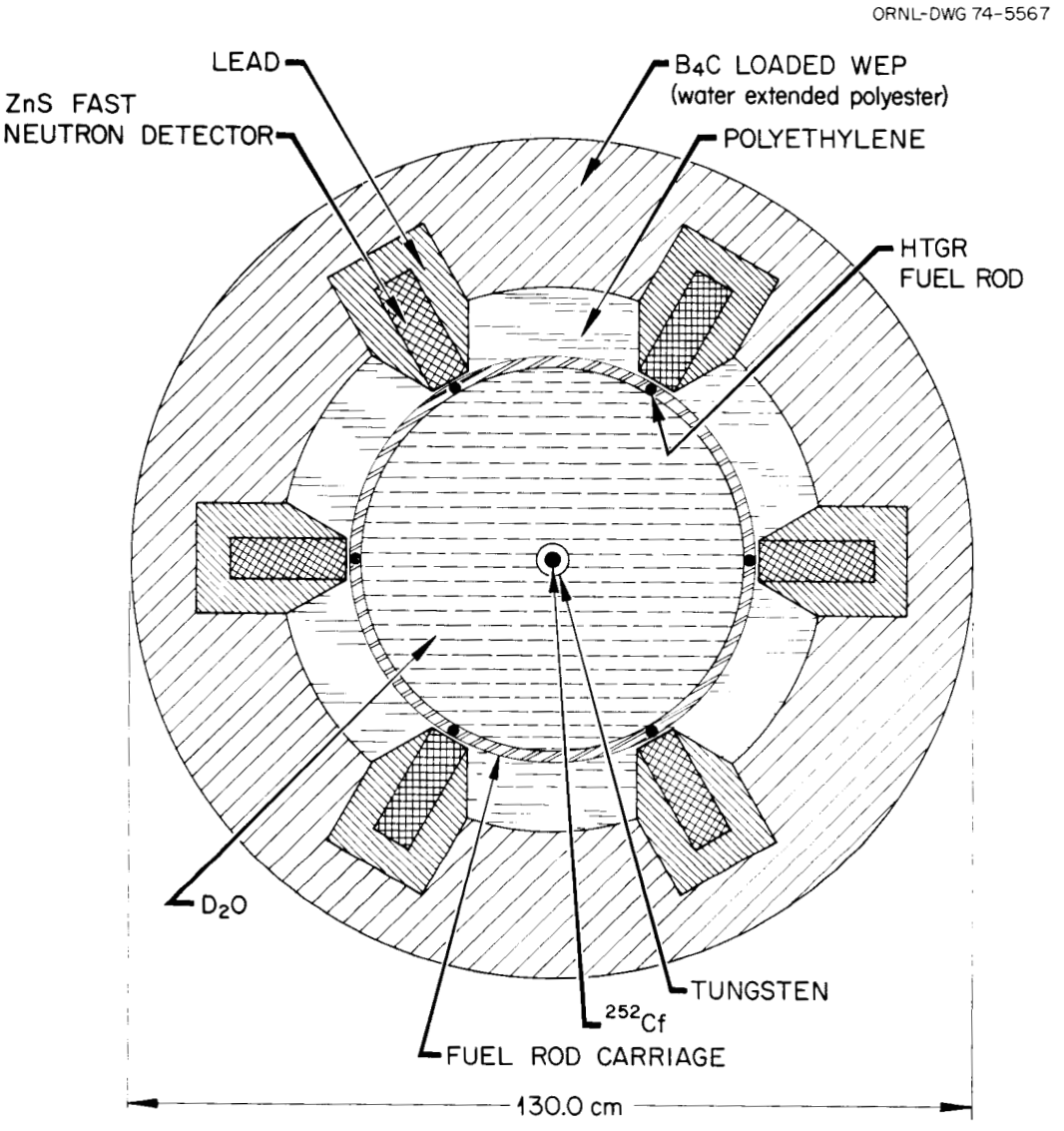

Fig. 5.3. HTGR fuel rod assay system.

mechanism. The thickness of the D_2O region between the source and sample was increased from 20 to 25 cm to increase the signal-to-background ratio. This size increase was necessary because the HTGR rods have lower fissile loadings per unit length than LWR rods.

The rod-handling system was designed primarily to limit the space requirements of the assay machine. Rather than moving individual rods or columns of rods through the irradiation position, as was done in the LWR assays, the rods are loaded individually on a circular carriage that revolves in a stepwise manner around the circumference of the D_2O tank. The latest design has ten fuel rod positions equally spaced around the carriage. Eight of these positions have detectors; one position is the loading position and one position is the unloading position. A rod is loaded and another unloaded from the carriage while assay counts are taken on the other eight rods in the carriage. After the count, the carriage is indexed to the next position and the procedure is repeated. The cycle time is 6 sec; thus each rod is counted one time by each of the detectors as the rod travels in the carriage. Each rod is, therefore, counted for a total of about 30 sec. By keeping a record of the individual detector counts, a total count can be assigned to each fuel rod. Calculations based on the count rate information in Fig. 5.2, and a fuel rod containing 0.25 g of ^{233}U, indicate that a 30-sec count would yield a net count of 60,000 counts/rod. This technique has several advantages. First, each rod passes through the same irradiation positions and past the same detectors; therefore, there can be no channel-to-channel variations as in the case where six channels are operated independently. Second, calibration of the device requires fewer standards because the rods are moved individually through the machine. Third, the loading and unloading operations occur simultaneously with the assay and do not require any additional space at the ends of the device for rod feeders or trays. Fourth, the assay machine provides rod-to-rod measurements of fissile content. The prime disadvantage of this method compared to the LASL design is that the neutron detector, which must be longer than the sample to reduce any spatial sensitivity, is used inefficiently and consequently leads to a lower signal-to-background ratio.

The above description of the rod assay machine has concentrated on the first mode of operation in which individual rods are assayed. By increasing the number of carriage positions and detectors, for example, to 22 carriage positions and 20 detectors, the throughput rate of the machine may be increased. In this mode, however, the proximity of samples and detectors will cause substantial cross talk.[2] Thus, the detectors are not operated independently in this mode and the count data from all detectors is accumulated to yield a total count for the total lot of fuel rods assayed. Because both modes of operation use the same irradiator and similar rod handling mechanisms, a demonstration of the first mode of operation in the pilot plant would allow this assay concept to be scaled up in a commercial plant by using the second mode with its higher throughput rate.

5.3.1.4 Development program

The development program consists of three major steps: (1) design, construction, and testing with ^{235}U samples of a laboratory model of the ^{252}Cf irradiator; (2) design, construction, and testing of an optimized, prototypic ^{252}Cf irradiator with rod handling equipment; and (3) evaluation of the prototypical machine with ^{233}U-^{235}U loaded rods under simulated operating conditions. The first step of this development is in progress.

5.3.2 On-line gamma-scan machine

5.3.2.1 Function and operating requirements

The on-line gamma-scan machine performs a total or segmented gamma count on each of the green fuel rods produced in the FRPP to utilize the gamma activity of the fuel rods as a measure of their relative uranium loadings and the axial homogeneity of uranium loadings. This device is primarily intended as a quality control device, but it simultaneously provides information for accountability and verification of special nuclear material flow. The gamma-scan machine must have a throughput rate of at least 10 sticks/min and have uncomplicated construction and relatively low cost so that multiple units could be utilized in a commercial facility.

The precision and accuracy requirements for the gamma scanner depend upon the fuel specifications and the extent to which the gamma activity is used for safeguards purposes. The actual design limits for accuracy remain to be determined.

5.3.2.2 Assay technique and rationale for selection

The on-line gamma-scan machine can provide a test bed for a rather simple passive technique that can provide verification of fissile material flows at several process steps in a commercial refabrication facility. The method hinges on being able to relate the gamma activity of the green fuel rod to the fissile content of the rod.

The gamma activity can be related to the fissile content by analyzing samples of a rod batch for fissile uranium content after these rods have been gamma scanned. The ratio of the gamma activity to uranium content for the rod samples can then be applied to the entire batch of rods.

This method is affected by several factors that determine the gamma activity of the rods.

The gamma activity of the fuel rods is a function of (1) ^{232}U and ^{232}Th content of the fuel rod, (2) the span of time since the purification of the ^{232}U and thorium, (3) the degree of purification, (4) the process

history that may affect daughter nuclide concentrations, and (5) the residual fission-product activity. For the ^{232}U levels expected in recycled fuel, the contribution to the gamma activity from thorium is negligible compared with the gamma activity associated with ^{232}U and its daughters. The level of residual fission-product activity will also be small compared with the ^{232}U-related activity. The primary variables affecting the gamma activity are the ^{232}U content, the time since separation of the uranium from its daughters, and the degree of separation achieved. As demonstrated in Sect. 2.4, the degree of daughter-nuclide separation is important only for aging times of less than ten days.

It is important to note that the gamma activity is not dependent (in a significant way) on the ^{233}U or ^{235}U content of the fuel rod. To utilize the gamma activity as a signature for fissile uranium, a method of relating the gamma activity and fissile content is required. The variation in age, the uncertainty in the exact age of a given batch of uranium, and the dependency of the gamma activity on process variables indicate that a precise general relationship between gamma activity and ^{233}U-^{235}U content is not possible. Despite this, this batch operating mode of the FRPP and the commercial plant may still enable the gamma activity to be used as an indication of fissile content. The uranium movement through the process will be on a batch basis. By measuring the ratio of gamma activity to the fissile uranium content of samples of fuel rods from a batch and by knowing the approximate age of the uranium, the gamma activity can become a signature of the fissile content for that batch of material. The gamma activity, corrected for age-dependent changes, can then be used at later process steps to verify that the correct fuel rods are loaded into an element and/or to verify that an element contains its book value of uranium. The above concept has not been tested; however, the success of this technique could lead to a straightforward nondestructive-assay method of verifying fissile material flow in a commercial refabrication facility.

5.3.2.3 System description and performance characteristics

The on-line gamma-scan system is conceived as a pair of shielded NaI detectors with collimators designed to view the entire rod or possibly segments of the rod. Each fuel rod will be counted individually, with the rod held in a fixed position during the count. Two methods of analyzing the detector signals are being considered. The first technique is a standard pulse-shaping and pulse-analysis system. This technique permits energy discrimination which can be used to reduce self-absorption effects. Stabilization of the electronic circuitry can also be accomplished with this technique. The second method will employ a current integrator to digitize the anode signal from the photo-multiplier tube. This method has advantages for high counting rates, but no gamma-energy discrimination is possible. Selected absorbers between the sample and the detector may enable limited energy discrimination. One of the interesting design problems for this device is that it will be operated

in a hot cell environment in a fluctuating radiation background of 1 to 20 R/hr. The shielding required to isolate the detectors from this radiation environment will be part of the machine design.

5.3.2.4 Development program

The development program centers about the construction of a prototypic gamma scanner that will be tested in the TURF facility. Early testing will be with thorium-loaded rods to simulate the gamma spectrum from ^{232}U and its daughters. The primary development functions will be to select and test the optimum method of signal analysis from the NaI detector.

5.3.3 High-uranium-content waste assay system

5.3.3.1 Function and operating requirements

Substantial quantities of high-uranium-content radioactive waste material will be generated during the operation of the HTGR fuel refabrication pilot plant. A description of the waste material, along with anticipated production rates, was given in Sect. 2.2 and 4.7. According to plans set down by the National HTGR Fuel Recycle Development Program,[10] significant quantities of waste are to be recycled for reclamation of usable quantities of fissile material. The current design for the refabrication facility does not include equipment to effect recycle of waste material. However, it is proposed[11] that the recycle waste be placed in small waste cans (3 in. in diameter, 9 in. high) and shipped to the head-end reprocessing plant in Idaho. Before shipment, the waste cans will be assayed for ^{233}U content.

The problem of assaying a number of high-fissile-content waste cans is not necessarily peculiar to the pilot plant. In an integrated HTGR reprocessing and refabrication facility, the bulk of the reject material (off-spec particle batches, etc.) would be amenable to sampling and would probably be recycled directly to the head end within the facility without canning. However, some nonsamplable and nonroutine high-concentration wastes will be generated. To maintain the material balance for such a facility and for the pilot plant operation, a high-uranium-content waste assay is required.

The quantities of waste that are being considered represent a relatively large portion of the plant throughput. It has been estimated that the high-uranium-content waste assay system will be handling up to 40% of all material that passes through the plant. This high percentage requires that the assay system must have an accuracy of about ±1.0% for the total accountability system to meet the federal regulations on limits of error for material unaccounted for (LEMUF).[12]

5.3.3.2 Assay technique and rationale for selection

Two concepts are being considered for the assay of high-uranium-content waste. One is a device developed by LASL called a ^{252}Cf "shuffler."[13] The technique employs a fast-neutron irradiation of a sample followed by removal of the neutron source and detection of delayed neutrons emanating from the sample. A number of irradiations of the sample are required to obtain good counting statistics.

The other technique being considered employs a high-precision calorimeter to measure the heat generation of the sample followed by a gamma-ray scan of the sample. The heat generation in the sample depends not only on the ^{233}U content but also on the presence of ^{232}U and its associated daughter products. The gamma-ray scan determines the relative quantities of ^{232}U daughter products that are present. Information from the gamma scan and an earlier calorimetric measurement on fresh, zero-age feed material (to determine ^{232}U content) will be used to determine the ^{233}U heat generation in the sample. The ^{233}U content of the can will be directly inferred from its heat generation.

A decision on which technique to use awaits further evaluation of the two concepts.

5.3.3.3 System description and performance characteristics

A diagram of the ^{252}Cf shuffler device is given in Fig. 5.4.[13] The ^{252}Cf source is repetitively moved from an interrogation position near the sample to a shielded position. When the source is in the shielded position ^{3}He detectors count induced delayed neutrons. The source is moved by a motor-driven cable that requires about 0.6 sec to move the source over the 1.32-m transfer distance. The fissile material content of a sample is determined by comparison of the number of delayed neutron counts from the sample with the number of counts from an identical irradiation of a known standard.

Preliminary measurements on ^{235}U indicated that a sensitivity of a few milligrams is possible using thermal-neutron interrogation. The present application of the device will require a fast-neutron irradiation to overcome self-shielding effects that would occur during a thermal irradiation of the 3-in.-diam waste cans. In this fast-neutron interrogation mode, count rates of 10 cps/g have been obtained with ^{235}U.[14] The lower delayed-neutron yield of ^{233}U and the requirement for additional gamma-ray shielding will reduce the count rates for ^{233}U from 3 to 5 cps/g. Since it is anticipated that the reject material waste cans will contain from 100 to 1000 g of ^{233}U, these count rates are sufficient to achieve reasonable statistics in the absence of any significant background. (Two or three of these cans would be produced per day in the pilot plant.) However, (α,n) reactions in the waste material will produce a significant neutron background of as much as five times the induced signal (see Sect. 2.7). This background may be sufficient

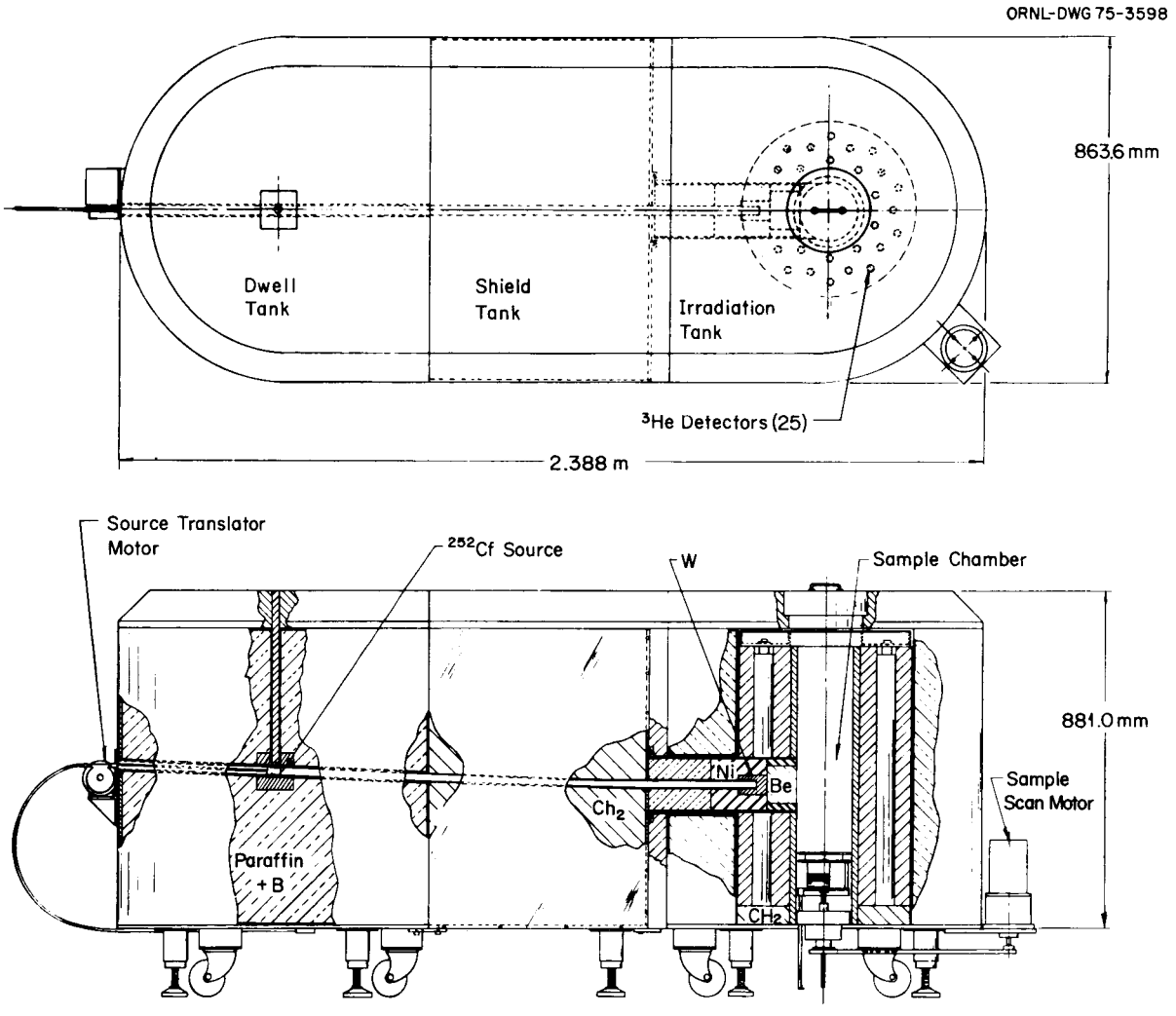

Fig. 5.4. Californium-252 shuffler.

to require counting times beyond practical limits. Additional development work to determine the magnitude of the (α,n) sources in typical high-concentration waste materials will be needed before this technique can be fully evaluated.

An alternative technique to the ^{252}Cf shuffler interrogation device is the utilization of a calorimeter coupled with a gamma-activity determination to correct for the heat production of nonfissile isotopes. The use of calorimeters for heavy-metal accountability purposes is well established,[15,16] and the heat generation rates of ^{233}U make it amenable to measurement by this method (see Sect. 3.6). Twin-bridge calorimeters of the size required to assay a 3-in.-diam by 9-in.-long waste can have been constructed and are operated routinely at the Mound Laboratory. Devices of this size are capable of sensitivities of approximately 100 μW, which corresponds to approximately one-third gram of ^{233}U. Since the high-uranium-concentration waste cans are expected to contain from 100 to 1000 g of fissile material, such sensitivities would be adequate to meet the accountability requirements, provided the other heat sources in the material can be quantified with sufficient accuracy. The presence of substantial quantities of ^{235}U in the refabricated fuel introduces complications in the method, since that isotope generates relatively low quantities of heat and would not be visible to a passive calorimeter.

The gamma-scan device is still in the early stages of design. Currently, it is proposed that the device will consist of one or more Ge(Li) detectors to count gammas being emitted by ^{232}U daughter products. The device will be used to determine concentrations of ^{232}U daughter products relative to the concentration of ^{232}U that is present.

Since the waste material will be contained in 3-in.-diam cans, self-shielding factors will influence the observed gamma flux outside the can. These must be studied and their effects must be considered in the design of the system. The degree of self-shielding will be dependent on the amount of bulk material in the can, its absorption properties, and its distribution in the can. In light of these self-shielding factors, corrections must be applied to the observed flux outside the can in order to make accurate determinations of daughter-product concentrations in the can. The success of the method hinges on the ability to generate these gamma attenuation correction factors to sufficient accuracy.

5.3.3.4 Development program

Much development remains to be accomplished on the high-uranium-content waste assay system. Calculations are being performed to determine the optimum performance of the combination calorimeter-gamma-scan device. Upon completion of these calculations, an evaluation of the precision of the "shuffler" against the precision of calorimeter-gamma-scan device will be made, and one will be selected as best. Experimental mockups of this system will be built to perfect and test the technique in an operating environment.

5.3.4 Low-level waste assay system

5.3.4.1 Function and operating requirements

In addition to the high-uranium-content waste discussed in Sect. 5.3.3, other contaminated material will be generated in the refabrication facility. The estimated quantities of these types of material which will be generated daily during plant operation have been presented in Table 4.9. This material will be placed in 30-gal drums and assayed for ^{233}U content. The description of the waste material indicates that the low-level waste assay system will be measuring small quantities of uranium spread over a relatively large volume. Since this system will be handling much smaller quantities of uranium than other systems, it will not be necessary for this assay to be as highly accurate as others for the total safeguards system to meet the requirements of the limit of error for material unaccounted for (LEMUF).

5.3.4.2 Assay technique and rationale for selection

The assay technique selected is one that is currently in use at ORNL. The technique is to determine ^{233}U content by comparison of the activity of the 2.61-MeV gamma ray between a standard of known ^{233}U content and the waste drum. A standard which is representative of the material in the can must be used for this procedure. In order for the technique to be accurate, the standard should be made from the same batch of uranium as the material in the waste. Corrections must be made for self-shielding effects, and sufficient time must pass to allow any process-dependent transients in the ^{208}Tl activity to die out. A more complete description of the device is given in Sect. 5.3.4.3.

The rationale behind the selection of this device is threefold. First, it is a tried and proven technique. Second, its accuracy is about the same as that needed in our application; however, a few modifications to the present technique and data analysis will be made to improve its accuracy. Finally, it has been developed at ORNL and is currently in operation here, making it quite accessible for testing and also as a source of experience.

5.3.4.3 System description and performance characteristics

The following description contains a summary of the report by V. A. DeCarlo[17] on the design of the present assay system in operation at ORNL. Two NaI scintillation detectors are positioned such that one 'sees' the top half of the waste drum and the other 'sees' the bottom of the drum. The drum is placed on the center of a table that rotates at 1 rpm. The detectors are mounted in a housing that can be moved towards or away from the center of the can. Counts by the detectors are stored in a multichannel analyzer equipped with an integrator. The steps required in making a measurement are as follows:

1. A waste drum is placed on the rotating table and a counting rate for the 2.61-MeV gamma ray is determined. The drum is rotated to average out the effect of distance between the material and the detectors. Before the count is made, sufficient time must pass to allow process-dependent transients in the counting rate to die out.

2. Another drum filled with glass foam with blind holes at its center and at other radial positions is placed on the rotating table. The function of the glass foam is to simulate the absorbing characteristics of the waste drum. A standard of known ^{233}U content is placed at a certain depth in one of the blind holes. The results are best if the standard is placed in a location that corresponds to the center of mass of the uranium in the waste drum. Also, the standard must be composed of material of the same age as the material in the waste drum. The drum is rotated and the counting rate is determined.

3. In order to account for differences in the absorption of the two drums, a transmission experiment is performed on each drum. A fixed source, emitting 2.6-MeV gamma rays, is placed behind and in front of each drum. A background-corrected counting rate is determined for the source at each location. A comparison is made between the attenuation of the source for each drum and a correction factor is obtained to account for any difference in the absorbing properties of the drums.

4. The ^{233}U content of the waste drum is then determined by a direct ratio of the counting rates of the standard and the sample with a knowledge of the ^{233}U content of the standard. The self-shielding correction factor measured in step 3 above is included in this calculation.

Results obtained for actual waste drum analyses indicate that the described technique is accurate to within 7% for a 95% confidence interval.

5.3.4.4 Development program

The development program for this device revolves around efforts to improve the accuracy of the technique. Specific areas of interest are an improved technique of correcting for self-shielding and the possibility of detecting heterogeneities in the waste can by counting different energy gamma rays emitted by ^{208}Tl.

5.3.5 Sample inspection station radioassay unit

5.3.5.1 Function and operating requirements

The nondestructive assay device to be installed in the sample inspection station will be required to fulfill several functions. Initially, the sample inspection station is to be maintained as a separate material balance area. The assay device, together with chemical analyses, will therefore serve as the primary means for determining material flows into and out of the sample inspection station and will provide the material balance information for that facility. In addition, the device will function as one of the quality control instruments and will, in conjunction with other analytical equipment, provide information on product acceptability and assist in process control. Finally, the device will serve as a standards calibration facility and will provide a means for supplying calibrated green rods to the in-cell on-line assay machine.

Table 5.1 lists the anticipated daily sample load to the sample inspection station radioassay unit.[18] In addition, in its function as a secondary standard calibration device, batches of perhaps 20 green rods extracted from the product line will have to be assayed to fractional percent accuracy and returned to the cell to serve as secondary calibration standards for the in-cell assay device (see Sect. 5.3.1). The frequency with which this calibration function will have to be performed has not yet been determined, but certainly new secondary standards will be calibrated whenever the rod fissile loading is changed or when a fresh lot of material for a new campaign is introduced into the system. This latter requirement is to ensure that the in-cell calibration rods are constructed of the same age material as the product rods in order to bias out any effects that the rod's gamma activity might have on the in-cell assay machine's detectors. Since the maximum campaign lot size consists of 50 kg of ^{233}U, this sets a lower limit on the calibration sample load to the sample inspection station radioassay unit of one batch at the start of each campaign. It is anticipated, however, that wear and tear on the calibration samples due to repeated cycling through the in-cell assay device will require more frequent replacement of these standards, perhaps as often as once a day.

One additional load on the radioassay unit is the need for continuing calibration of the device using a fixed set of calibration samples. Estimates are that ten calibration readings per day will be required.

Summing up the samples from Table 5.1 and making the conservative assumption that an additional 30 readings will be needed for standards calibration and machine calibration, the probable maximum load on the radioassay device is seen to be approximately 90 readings per day or one every 13-1/3 min in a 20-hr duty cycle.

Table 5.1 also shows that the device will be required to accommodate a variety of material forms from every phase of the fabrication process, including hydrogenous dried resin particles, green rods, nonhydrogenous

Table 5.1. Estimated daily nondestructive assay sample load during pilot plant operation

Subsystem		Nature of sample	Origin of sample	Sample obtained via	Sample frequency	Sample size	Inspection			Sample disposition
Number	Name						Desired attribute	Nominal value	Precision required	
3	Radioassay	Loaded, dried resin microspheres from loading batch	System 3, resin carbonization	System 7, subsystem 4, particle size	3/day	1 g	Fissile uranium content	TBD[a]	±0.3% TBV[b]	~0.5 g uranium per sample to waste as loaded dried microspheres
		Loaded, dried resin microspheres from loading lot	System 3, resin carbonization	System 7, subsystem 4, particle size	1/day	1 g	Fissile uranium content	TBD	±0.3% TBV	System 7, subsystem 2, particle sample subdivision
		Converted microspheres from coating batch	System 4, microsphere coating	System 7, subsystem 4, particle size	6/day	1 g	Fissile uranium content	TBD	±0.3% TBV	System 7, subsystem 2, particle sample subdivision
		OLTI coated microspheres from coating lot	System 4, microsphere coating	System 7, subsystem 4, particle size	1/day	1 g	Fissile uranium content	TBD	±0.3% TBV	System 7, subsystem 7, surface contamination
		Unfired fired rods	System 5, fuel rod fabrication	Cell D, fuel rod assay subsystem	3/day	1 rod	Fissile uranium content	0.16-0.41 g TBV	±0.3% TBV	System 7, subsystem 8, matrix filler dispersion
		Fired fuel rods	System 6, fuel element assembly	Cell D, fuel rod assay subsystem	44/day	1 rod	Fissile uranium content	0.16-0.41 g TBV	±0.3% TBV	System 7, subsystem 15, dimensional

[a]To be determined.

[b]To be verified.

coated microspheres, and carbonized rods. Sample sizes will range from approximately 0.5 g of ^{233}U (in the uncoated carbonized particle samples) to a minimum of approximately 0.13 g of ^{233}U in the green and carbonized rods.

Accuracy and precision demands on the device will be high. With an overall design objective to maintain the LEMUF for the pilot plant below 0.5%,[12] the sample inspection station radioassay device, in its function of calibrating secondary standards, should be capable of accuracy in the ±0.3% range for a single measurement.

5.3.5.2 Assay technique and rationale for its selection

The conceptual design solution for the sample inspection station radioassay unit envisions a californium-source-driven, active thermal-neutron interrogation device. Two options are currently under consideration. The first is a californium-source D_2O-moderated device which would function by counting prompt-fission neutrons generated in the sample during irradiation. Its physics design is essentially similar to the on-line assay device described in Sect. 5.3.1. This device would operate in the same fashion but would not require the rotating sample-holder ring, automatic feed mechanisms, and multiple detectors incorporated in the on-line device. The second option envisions a californium-source-driven flux multiplier device which would function by irradiating the sample in a thermal flux trap region and subsequently removing the sample to a detector facility for delayed neutron counting. Inclusion of an active fission-heat twin-bridge calorimeter for very precise sample assay is under consideration for both devices. The detailed characteristics of these devices are discussed in Sect. 5.3.5.3.

Alternatives that were considered for the sample inspection station radioassay unit during the initial planning stages included a neutron-generator-driven device and a photoneutron (^{124}Sb-Be) intermediate-neutron-energy interrogation device. Passive techniques were not a serious contender because of the problems introduced by the strong inherent gamma background of the material (see Sect. 3.4).

The neutron generator was ruled out for this system for essentially the same reasons as described in Sect. 5.3.1.2. While accessibility and maintenance problems would not be as severe for this system as for the on-line assay device, the additional complexity introduced by the inclusion of a complicated electronic neutron source did not seem warranted.

A ^{124}Sb-Be photoneutron device similar to that described in Ref. 6 is attractive in that the kilovolt interrogating neutrons are not subject to strong attenuation through the small HTGR samples. Thus the need for self-shielding corrections, necessary in the thermal interrogation system, is reduced. The system is, however, sensitive to the hydrogen content of the sample, and variations in hydrogen content between green rods or batches of dried resin particles could introduce errors.

Principal reasons for relegating this concept to secondary status are, first, the low count rates generated from the sample with a reasonable-sized antimony source precludes achieving the desired throughput and statistical precision, and second, the short half-life (60.2 days) of the ^{124}Sb introduces the complication of continual source regeneration by reactor irradiation and the attendant problems associated with routine source replacement. At least an order of magnitude increase in ^{124}Sb source strength over that used in the LASL machine[6] would be necessary to overcome the first obstacle. This increase in source strength would make the second problem of handling and source activation more difficult. Currently, the Sb-Be device is considered a backup in the event that unanticipated problems arise in the application of the thermal-neutron interrogators.

5.3.5.3 System description and performance characteristics

A schematic of the first option, the californium-source device, is shown in Fig. 5.5. Its physics design, operation, and performance characteristics are essentially identical to those of the in-cell assay device described in Sect. 5.3.1. Principal differences are that samples are transferred to and from the device in rabbits via pneumatic lines which connect to a sample preparation and loading glove box; an additional penetration is included to accommodate an active calorimeter for performing a very precise assay of the individual fuel rods, and a provision for source withdrawal (to turn the calorimeter on and off) is provided. Only one sample irradiation position is indicated in Fig. 5.5, but several could be provided if necessary to increase capacity and irradiation time and to improve statistics.

Our calculations indicate that count rates of $\sim$2000 cps/g of ^{233}U can be expected from this device with a 1-mg californium source. Los Alamos has constructed similar devices, and their experience indicates that these results are reasonable.[2] Thus, for the sample sizes under consideration and 10-min assay times, adequate counts (of the order of 10^5) should be available. This is sufficient to achieve the required statistical precision.

The second option, the californium multiplier, is sketched in Fig. 5.6. This is a commercially available device. Performance characteristics supplied by the vendor are given in Table 5.2. The device consists of a californium source buried in a subcritical assembly. The surrounding multiplying medium amplifies the thermal flux level over that obtainable from the bare californium source by a factor of approximately 30.

HTGR fuel rods and fuel particles would be assayed in this device by in-core irradiation and removal of the sample for delayed neutron counting. Counting is done by transferring the sample to a chamber containing moderating material (polyethelene) and BF_3 detectors. Operating in this mode and assuming a 10% overall detector efficiency, accumulation of $\sim 10^6$ counts from a single HTGR fuel rod in a 2-min

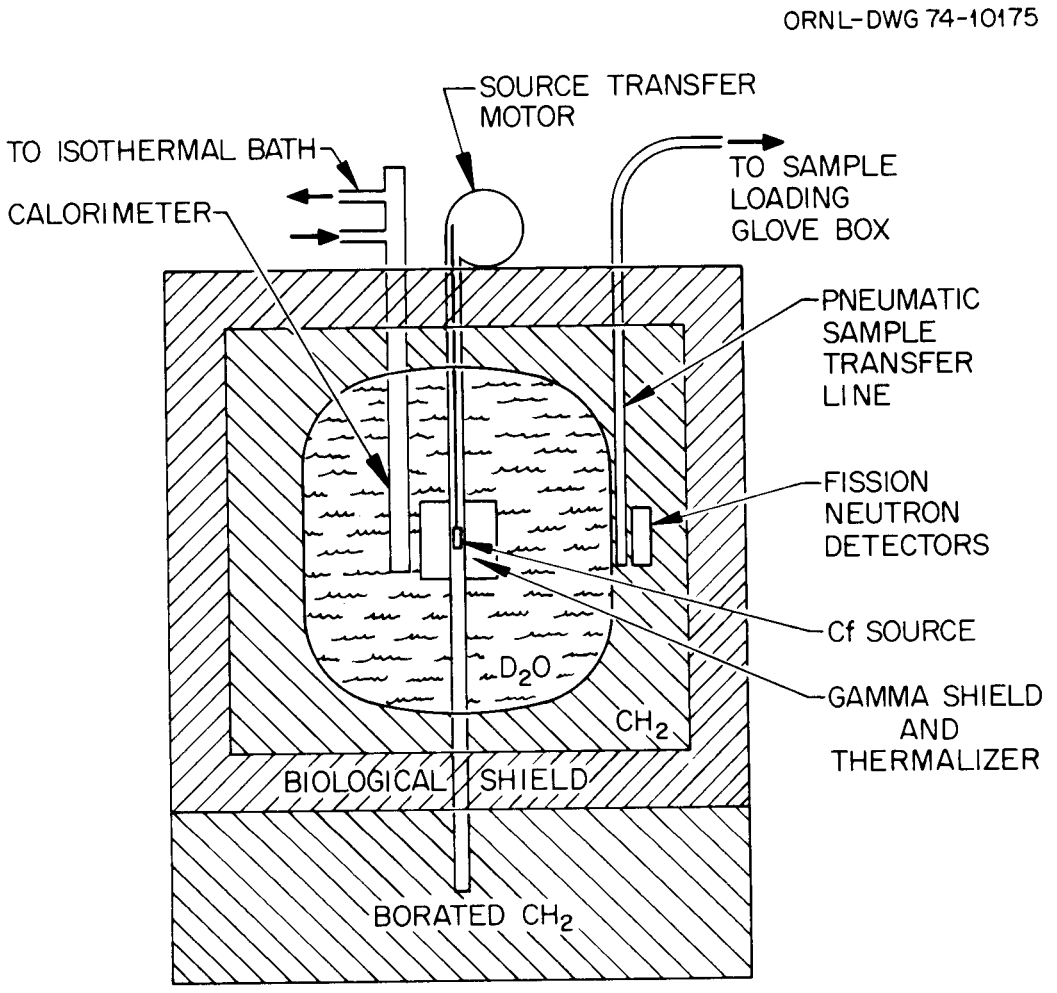

Fig. 5.5. Sample inspection station radioassay unit option 1 — californium-source device.

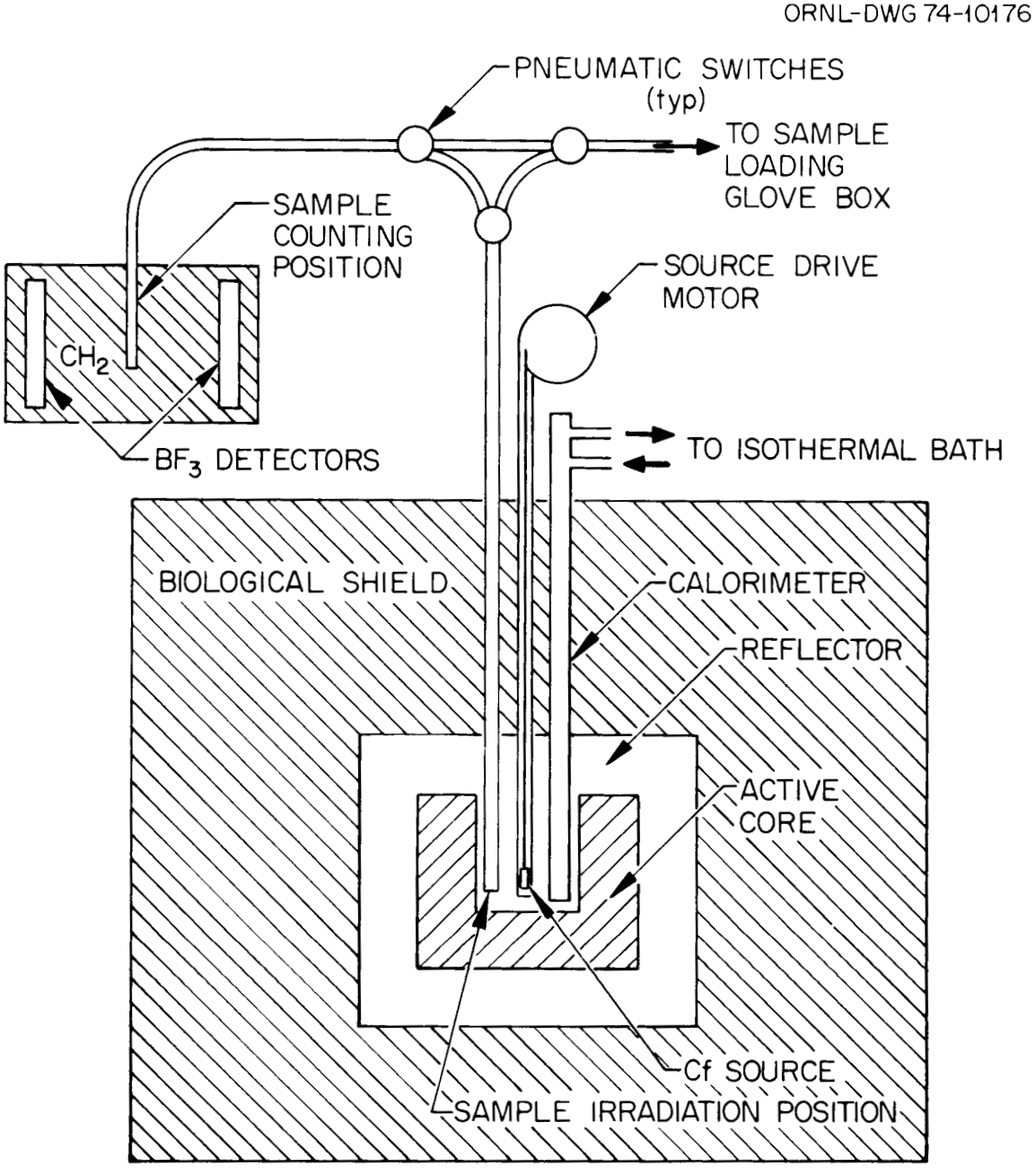

Fig. 5.6. Sample inspection station radioassay unit option 2 - californium-source multiplier device.

Table 5.2. Performance and design characteristics of ^{252}Cf multiplier (CFX)[19]

^{252}Cf source	1 mg
^{235}U loading	965 g
Uranium enrichment	93.4%
Fuel form	Clad metal plates
Moderator	Polyethylene
Maximum k_{eff}	0.990
Δk_{eff} increase for 20-g ^{235}U sample	0.004
Control poison	Cadmium, steel clad
Thermal flux	4×10^8 neutrons cm^{-2} sec^{-1}
Fast flux	6×10^8 neutrons cm^{-2} sec^{-1}
Thermal flux multiplication	33
Equivalent ^{252}Cf source	33 mg
Radiography collimator ratio (L/D)	20 or greater
Thermal flux at film plane	1×10^5 for L/D = 20
Dose rate at shield surface	Less than 10 mR/hr
Fission power level	3.8 W

irradiation, 2-sec transit, and 2-min count cycle appears possible. These high count rates also make it feasible to assay individual fuel microspheres to approximately ±1% precision, in five repetitive 2 min in — 2 min out cycles, a capability that could be used to evaluate uniformity of the resin-loading process.

The multiplier system suffers from the same deficiency as all other thermal-neutron interrogation devices, that is, the requirement for thermal-neutron self-shielding corrections to the assay data. In addition, introduction of a fissile sample perturbs the system multiplication and hence the effective interrogating source strength. We have not been able to obtain quantitative information from the vendor on the magnitude of this effect. However, from statements[20] that it would require ∿100 g of ^{235}U at the sample location to drive the system critical, we estimate that a 0.5-g sample would perturb the thermal flux level by approximately 0.5%. A third (and possibly the most serious) deficiency of the multiplier is its reliance on delayed neutrons as the fissile content indicator. The large difference in delayed-neutron yields between ^{233}U and ^{235}U (see Sect. 3.7) and the fact that the recycle fuel will contain appreciable quantities of the latter (see Tables 2.3 and 2.4) make its application highly dependent on the availability of accurate information on the isotopic content of the fuel.

Both the californium-source device and the multiplier device could serve as drivers for an active assay calorimeter for individual fuel rods or particle samples. Both Figs. 5.5 and 5.6 include a calorimeter as part of the assay system. A sketch of the proposed calorimeter is shown in Fig. 5.7.

The calorimeter is currently envisioned as an isothermal twin-bridge type similar to those designed, built, and operated by the Mound Laboratory.[15,16] In our system both the active sample and the reference sample (nonheat generating sample) are enclosed in a single tube surrounded by an isothermal water jacket and a vacuum insulator. Constant-temperature water is circulated through the system from an external isothermal reservoir. Heat generation in the active sample is measured by detecting the change in resistance in the nickel windings surrounding the active sample relative to that of the reference, the two sets of windings being connected as a Wheatstone bridge. Heater coils are provided around both the sample and reference holders to allow several different types of measurements to be performed.

To make a measurement, a sample is inserted and the calorimeter is sealed. The calorimeter is allowed to equilibrate, and the source is then raised to induce fissions in the sample. The incremental fission heating can be determined by (a) measuring the resistance change in the sample arms of the bridge circuit, (b) feeding a measured amount of power to the reference side heater to balance the bridge circuit, or (c) removing the source and feeding a measured amount of power to the sample side heater to reproduce the previously measured resistance change. All three measurement techniques can be implemented without unsealing or otherwise perturbing the calorimeter.

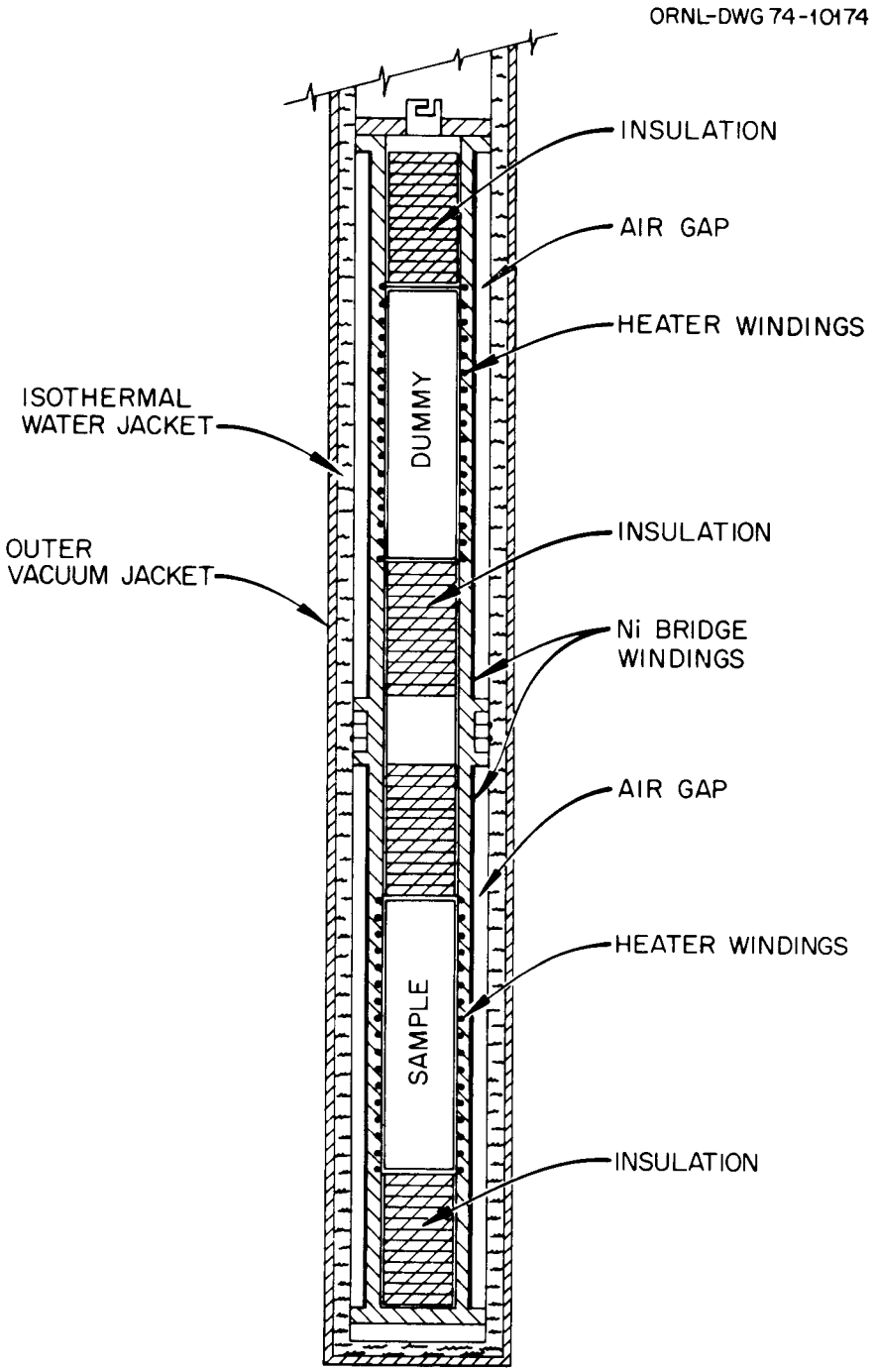

Fig. 5.7. Twin-bridge calorimeter for active HTGR fuel rod assay.

Conversations with Mound Laboratory personnel indicate that a device of the size envisioned should be sensitive to power variations of approximately 1 μW under routine operation.[21] Sensitivities greater than 1 μW should be achievable but only with considerable attention to detail. The problem of thermal-neutron self-shielding is again an unavoidable source of error in this technique (as in particle-counting techniques) and must be corrected for. Differences between gamma heat deposition by gammas from the ^{262}Cf source in the sample and dummy may also introduce errors, but these are anticipated to be <0.1%.

The californium-source device appears marginal as a driver for the active fuel rod calorimeter. A 1-mg californium source produces a thermal flux of $\sim 2 \times 10^7$ in the region adjacent to the source. This flux will result in a fission heat production of from ∿200 μW in an HTGR fuel rod to ∿400 μW in a 1-g sample of loaded dried resin particles. However, inclusion of the calorimeter in the device for development purposes is contemplated because sufficient power is available to develop and test the technique even though the results may not be significantly better than those obtained from the fission-neutron-counting technique.

If the multiplier is selected as the sample inspection station radioassay unit, the active calorimeter immediately assumes a preeminent status. The increased flux levels result in fission heating of from 6 to 12 mW, and, if 1-μW sensitivity is achieved, the calorimeter could serve a primary standard calibration function. Here again, however, corrections for self-shielding and flux-level variations with sample size would be required and would probably be the limiting factors on achievable accuracy.

Some thought has been given to minimizing the thermal-neutron self-shielding problem in both devices. For green and carbonized rods, one would have to rely on calculations supported by measurements on standards constructed from closely sized particle batches. For bare particle samples, the double heterogeneity problem (particles in a sample in a moderating medium) can be reduced to a more analytically tractable form by constructing special rabbits which retain the particles in a regular and calculable array. For example, ∿0.1 g of ^{233}U could be contained in ten 2-in.-long single-particle stacks in holes drilled in a polyethelene rabbit. Such a configuration (see Fig. 5.8) is readily calculable by conventional Monte Carlo techniques.

5.3.5.4 Development program

Scoping calculations on the californium-source device have been completed, and plans have been made to construct and operate such a device for development purposes. Detailed design calculations are under way to determine optimum deuterium tank size, shielding requirements, etc. In addition, experiments are under way in the TURF facility to determine the sensitivities of several types of candidate detectors

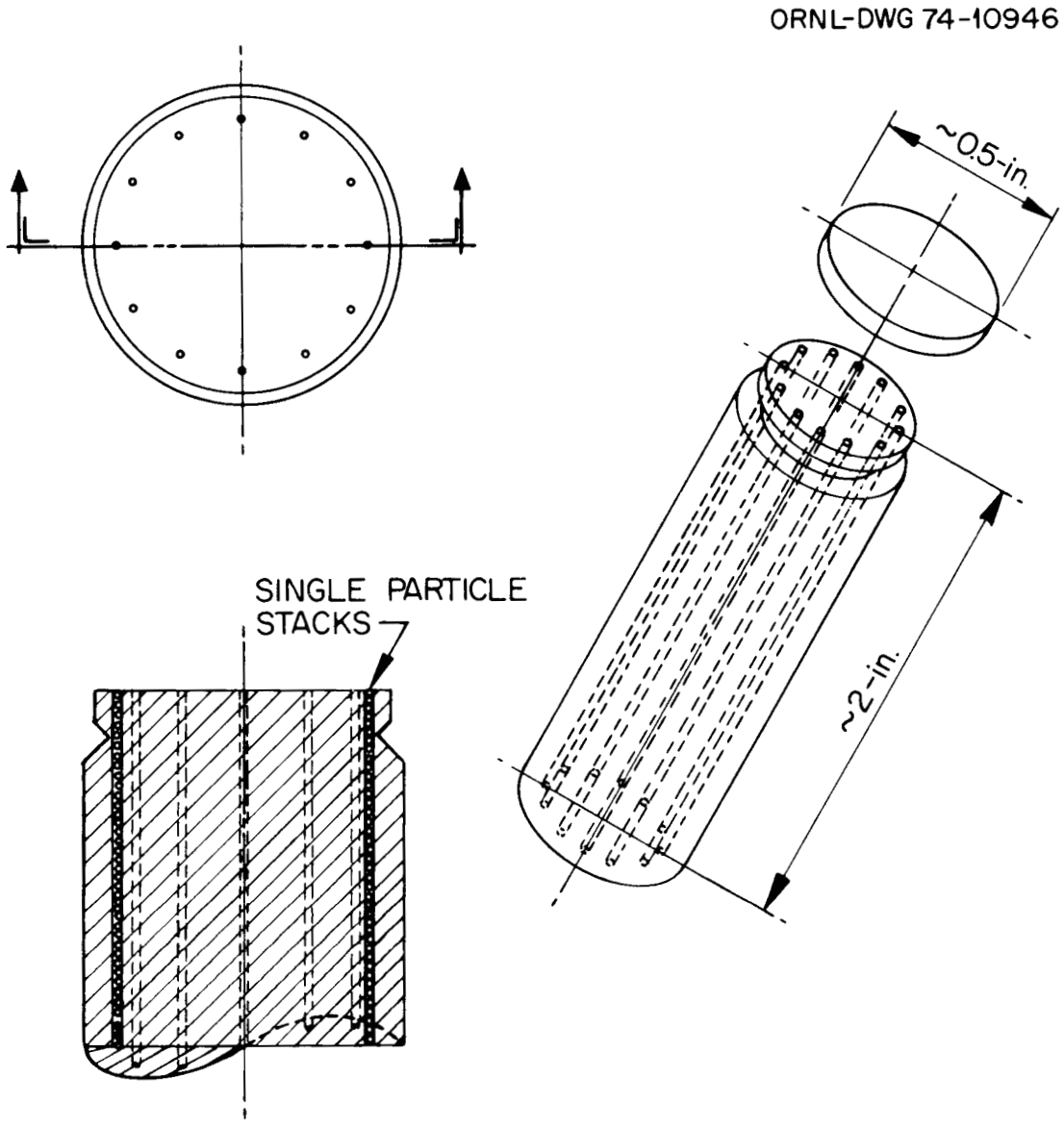

Fig. 5.8. Rabbit for assay of loose particles.

to fast neutrons in the anticipated thermal-neutron and gamma environment. We intend to design the development device with sufficient flexibility to allow continued testing of the various detectors in the device proper and also to allow testing of the techniques more suited for the higher flux levels of the multiplier. Information generated in this experimental program will form the basis for an intelligent decision on which of the two options to choose for the sample inspection station radioassay unit and provide design information for the on-line assay device. The possibility exists of converting the developmental californium-source device for use in the sample inspection station if results from the experimental program indicate this device can fulfill that function satisfactorily.

5.4 STANDARDS

All of the nondestructive techniques and equipment discussed in Sect. 5.3 will rely ultimately on the use of calibration standards to achieve their design accuracies. The construction and verification of standards is therefore a major component of the nondestructive assay program, and the ultimate accuracy achievable by the equipment is limited by the ability to characterize the material used for calibration.

Current destructive chemical assay techniques appear capable of fractional percent precision and approximately 1% accuracies when applied to HTGR fuel materials.[22] A development effort is under way to utilize activation techniques to determine the fissile content of individual fuel microspheres, with the hope that precisions of 0.25% relative to a known uranium metal foil standard or NBS oxide material can be achieved.

Equipment has been developed which will allow exact dispensing of a fixed number of bare or coated microspheres to fabricate loose-particle and fuel-rod standards. Current plans are to construct ^{235}U and eventually ^{233}U standards as part of the assay development program so that the requisite techniques and capability are available when the pilot plant is put into operation.

REFERENCES FOR SECTION 5

1. H. O. Menlove, *Nuclear Safeguards Research and Development, Program Status Report*, LA-4605-MS (1970), p. 12.

2. R. A. Forster, D. B. Smith, and H. O. Menlove, *Error Analysis of a ^{252}Cf Fuel-Rod-Assay System*, LA-5317 (1974).

3. H. R. Lukens, D. M. Fleishman, and R. L. Bramblett, "Determination of U-235 in Highly Enriched Reactor Fuel Sticks," *Conference Internationale Sur Les Tendances Modernes De L'Analyse Par Activation.*

4. H. Kendrick et al., *High Precision Nondestructive Assay of Th-U Fuel Particles and Rods*, Gulf Radiation Technology Report GULF-RT-A10819 (1971).

5. T. L. Atwell, J. E. Foley, and L. V. East, "NDA of HTGR Fuel Using the Random Driver," paper presented at the 1974 meeting of the Institute of Nuclear Materials Management, Los Alamos Scientific Laboratory Report LA-UR-74-977 (1974).

6. H. O. Menlove, R. A. Forster, and D. L. Matthews, "A Photoneutron Antimony-124-Beryllium System for Fissile Materials Assay," *Nucl. Technol.* 19: 181 (1973).

7. Tsahi Gozani, Hans Weber, and Ytzhak Segal, "A Gamma Ray Transmission Gauge for Determination of Heavy and Light Metal Loading of Fuel Elements," *J. Inst. Nucl. Mater. Manage.* 2: 139 (1973).

8. P. Wälti, "Evaluation of Grain Shielding Factors for Coated Fuel Particles," *Nucl. Sci. Eng.* 45: 321 (1971).

9. H. O. Menlove, A. E. Evans, and R. A. Forster, *Nuclear Analysis Research and Development Program Status Report*, LA-5197-PR (1973).

10. *National HTGR Fuel Recycle Development Program Plan*, ORNL-4702, Rev. 1 (August 1973).

11. J. D. Jenkins, *Solid Waste Handling Policy for HTGR-FRPP*, GCR:74-33 (undated).

12. 10 CFR 70.51, Sect. C.5.

13. H. O. Menlove, *Modulated ^{252}Cf Assay System, "Shuffler,"* LA-5675-PR (August 1974), p. 25.

14. H. O. Menlove, personal communication.

15. K. C. Jordan, *Calorimetry at Mound Laboratory*, Internal Mound Document J-121A, paper presented at Sixth Tripartite Instrumentation Conf., Chalk River, Canada (April 1959).

16. F. A. O'Hara, J. D. Nutter, W. W. Rodenburg, and M. L. Dinsmore, *Calorimetry for Safeguards Purposes*, MLM-1798 (Jan. 5, 1972).

17. V. A. DeCarlo, *Design of a System for the Nondestructive Assay of ^{233}U in Waste Drums*, ORNL-TM-4249 (August 1973).

18. *HTGR Fuel Refabrication Pilot Plant Sustem Design Description: Sample Inspection System, System 7*, Document No. Q-11416-EP-035-S1 (Oct. 25, 1974).

19. *The Californium Multiplier (CFX)*, Intelcom Rad Tech, Document No. RT-TB-168 (undated).

20. C. Preskitt, Intelcom Rad Tech, private communication.

21. W. W. Rodenburg and K. C. Jordan, Mound Laboratory, private communication.

22. C. D. Bingham and J. Whichard, *Evaluation of an Inter-laboratory Comparison Involving Pyrocarbon and Silicon Carbide-Coated Uranium-Thorium Carbide Beads*, NBL-269 (November 1973).

6. DATA FLOW AND DATA HANDLING

6.1 HARDWARE DESCRIPTION

The complexity and remoteness of the HTGR fuel refabrication processes dictates that most of the equipment be highly automated through control systems which are located outside of the cells. The HTGR-FRPP conceptual design[1] calls for each of the plant operating systems to be supported independently by a local instruments and control subsystem (LICS) which, depending on the complexity of the specific process system, may include any or all of the following: analog instrumentation, a programmable logic controller(s), and a minicomputer. In addition to LICS functions, overall plant management and data handling functions will be performed by system 8, plant management system (PMS). The PMS, which also utilizes a minicomputer, communicates with all plant process systems through their respective LICS and serves as a central point for data accumulation and reduction. It is apparent that the HTGR-FRPP instrumentation and control philosophy lends itself directly to the implementation of a real-time material accountability system. Accordingly, the assay and accountability system has been designed to take advantage of the available data processing capabilities. The PMS will collect data from various nondestructive-assay machines, store such data in reduced format, and maintain plant fissile inventory records. All data transmitted from any given LICS to the PMS will be made available by each LICS to process-operating personnel. Consequently, plant operation will not be dependent on the availability of the PMS. Each LICS will have the capability to operate its system individually with PMS-related data functions being accomodated through automatic data acquisition (via local minicomputers) or manual data recording from local displays.

The process requirements for LICS-1 through LICS-4 and LICS-9 can be handled by programmable logic controllers and analog instrumentation with no local data reduction capabilities. LICS-5 and LICS-6, because of the complexity of the fuel rod fabrication and fuel element assembly processes, will require more sophisticated configurations and will share a common minicomputer. Data from the on-line assay machine and the gamma scanner, both in system 5, will be processable at the LICS-5 level and only reduced data will be transmitted to the PMS. LICS-7, which supports the sample inspection system, will utilize a dedicated minicomputer and several programmable logic controllers. System 7 will process and correlate data from QA and QC analytical equipment and will also maintain the material balance records for the sample inspection system. Only reduced System 7 data will be transmitted to the PMS.

6.2 Software Description and Data Flow

A schematic of the proposed plant accountability data handling system and the types of data available from each station is shown in Fig. 6.1. Figure 6.2 shows, schematically, the types of processing and software requirements necessary for the on-line assay machine and provides an

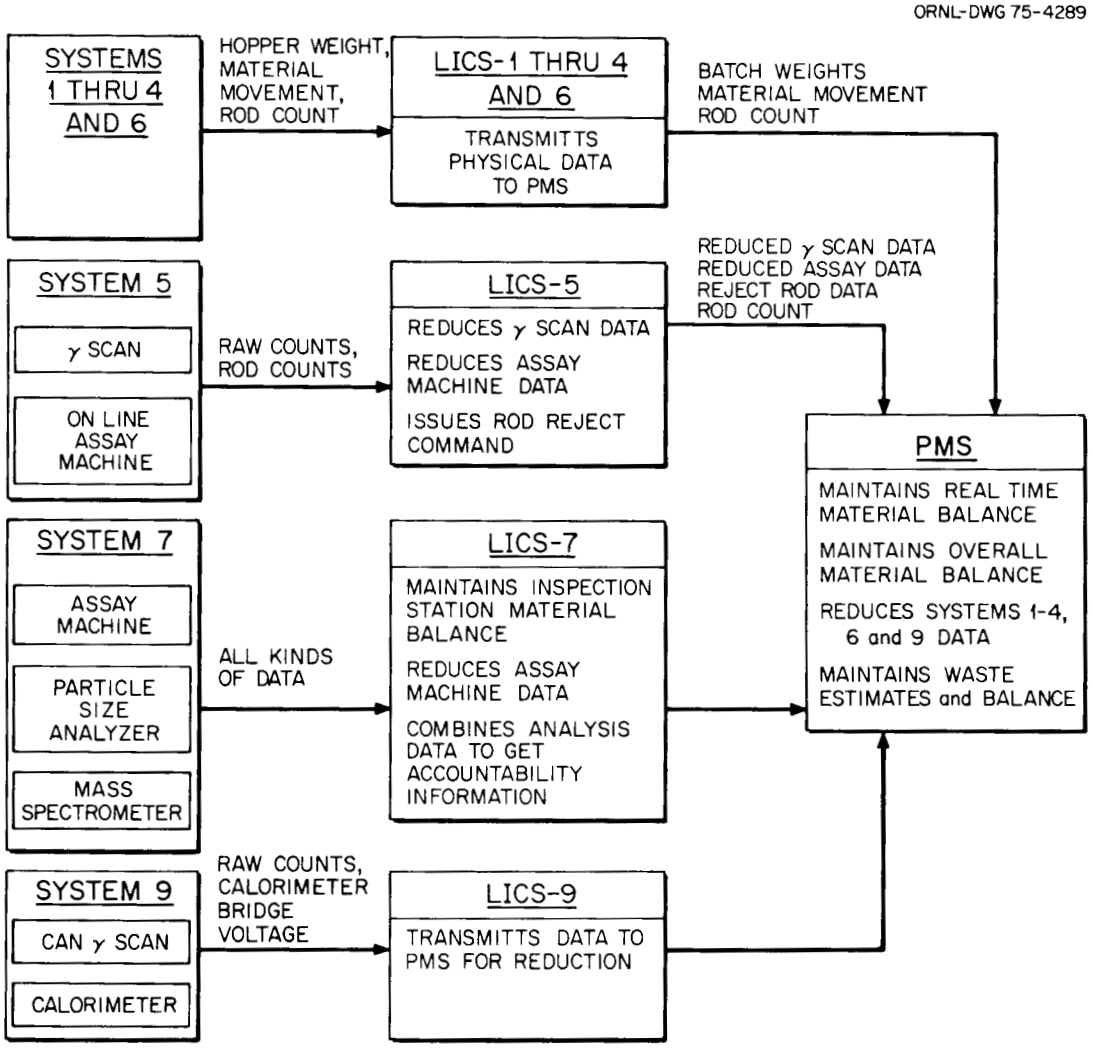

Fig. 6.1. Schematic of the proposed plant accountability data handling system and the types of data available from each station.

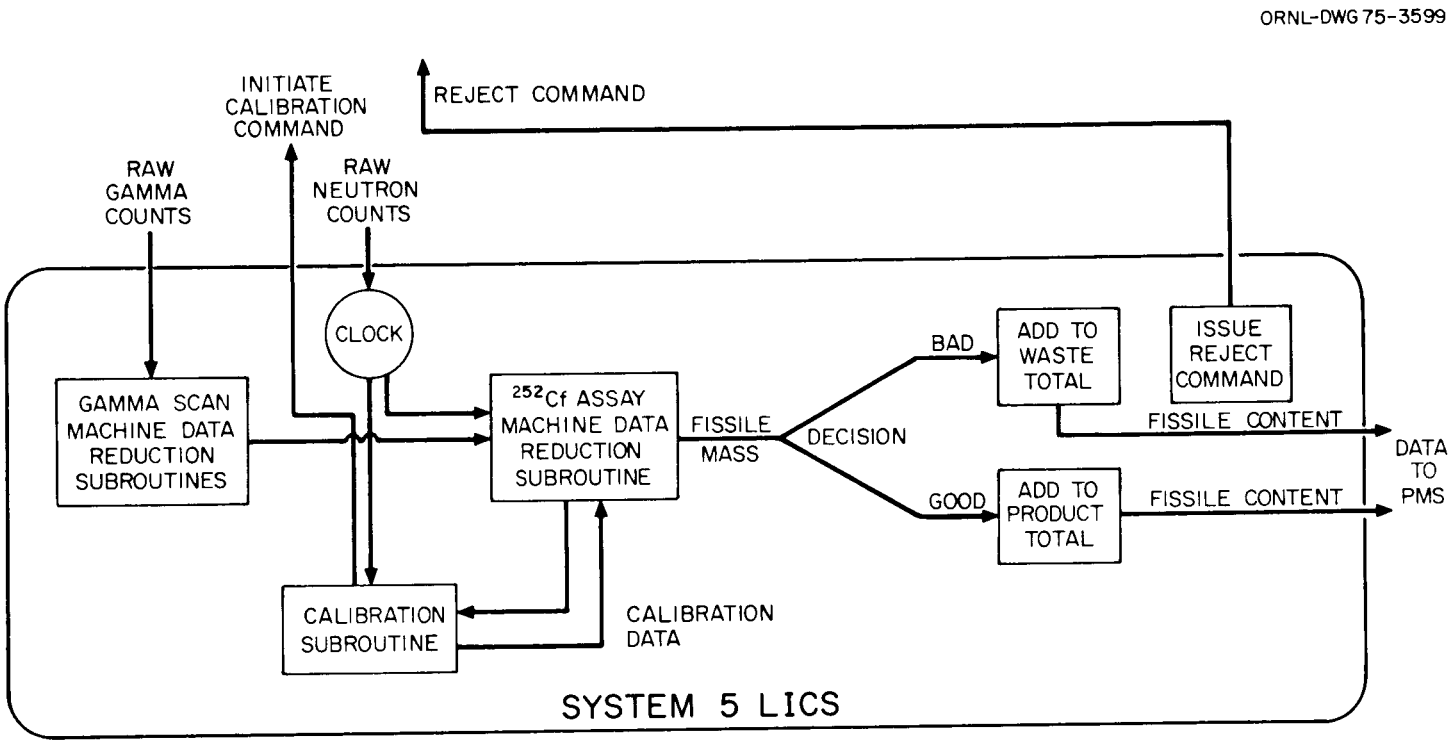

Fig. 6.2. Schematic of on-line assay machine and data flow.

indication of the level of complexity required in LICS-5 to maintain real-time accountability information. Table 6.1 is an example of a proposed material balance sheet that would be available at any time during plant operation at the punch of a button. Note that a number of items in the table must be obtained by differencing the amounts of material flowing into and out of a particular process step. These quantities would be verified at regularly scheduled plant inventory periods at the end of each campaign, at which time all wastes would be consolidated, canned, and assayed. Table 6.2 is a listing of the types of data that will be needed from the in-plant sensors and the use to which that data will be put in computing the items in Table 6.1.

6.3 REAL-TIME DYNAMIC SYSTEM MODEL

Future plans call for the development of a computer program that will model the dynamic behavior of material flows through the refabrication facility. There will be several uses for such a model. During plant operation the program will reside in the plant management system computer and will make estimates of flow rates at various points in the process. If actual measurements differ significantly from these estimates, then this might indicate a diversion of material from the process line. Another use will be to estimate quantities of materials located in nonmeasurement areas and waste streams. A third use of the model will be during system development to study the sensitivity of calculated LEMUF on the precision and location of various measurement devices in the process line. This application will also be useful to optimize the assay system. Here, optimization will be with respect to assay locations, along with the precision of the proposed assay devices.

In light of the above applications, it is evident that a simulation model will be useful as a development tool in the optimization of a system and also as a watchdog for material division, human errors in transfer of material, and as an estimator on unmeasured material flows in an operating plant.

Table 6.1. Proposed material accountability summary data sheet

Material balance as of (time, date)

	Material	Amount (g ^{233}U)
I.	Feed batch JJ	xxx ± xx
II.	Closed totals	
	1. Loaded in block I	xxx ± xx
	I + 1	xxx ± xx
	⋮	⋮
	2. Sealed waste can J	xxx ± xx
	J + 1	xxx ± xx
	⋮	⋮
	3. Sealed waste drum K	xxx ± xx
	K + 1	xxx ± xx
	⋮	⋮
	4. Logged out sample N	xxx ± xx
	N + 1	xxx ± xx
	⋮	⋮
	5. Liquid wastes to storage	xxx ± xx
	Total	xxx ± xx
III.	Total in process (I-II)	xxx ± xx
	Total in process from control instrumentation (running sums)	
	1. Feed batch JJ in	xxx ± xx
	2. Loaded resin in storage	xxx ± xx
	3. Reject resin[a] to waste	xxx ± xx
	4. Carbonization furnace	xxx ± xx
	5. Carbonized resin storage hoppers	xxx ± xx

Table 6.1 (continued)

	Material	Amount ($g\ ^{233}U$)
6.	Reject carbonized resin[a] to waste	xxx ± xx
7.	Coating furnace A	xxx ± xx
8.	Coating furnace B	xxx ± xx
9.	Reject coating run[a] to waste	xxx ± xx
10.	Coated particle storage hoppers	xxx ± xx
11.	Rod fabrication machine feed hoppers	xxx ± xx
12.	In process in rod fabrication machine	xxx ± xx
13.	Gamma-scan rejects to waste[a]	xxx ± xx
14.	Holdup feed to assay machine	xxx ± xx
15.	Rod storage rack	xxx ± xx
16.	Loaded in block	xxx ± xx
17.	Blocks in carbonization furnace	xxx ± xx
18.	Samples in sample inspection station[b]	xxx ± xx
19.	Samples returned to waste[a]	xxx ± xx
20.	Estimate of furnaces' blowover losses to waste[a]	xxx ± xx
21.	Estimate of other losses to waste[a]	xxx ± xx
22.	Archive samples	xxx ± xx
	Total in process	xxx ± xx

[a]The amounts of material destined for the high- and low-level waste cans are maintained as running sums for each can. After a can is filled and sealed it is assayed for total content. A discrepency would be cause for alarm.

[b]A separate subbalance sheet similar to above will be maintained for the sample inspection station.

Table 6.2. Information type and application in calculating accountability data

Information type	Application (numbers refer to Table 6.1 items)
Mass spectrometer analysis of liquid feed solution	All items
Liquid level in storage waste and process tanks	II-5, III-1
Storage and process hopper weights	III-2,3,4,5,6,7,8,9,10,11,20,21
Rod counts	II-1,4; III-12,13,14,15,16,17,19
In-cell gamma-scan count rates	III-13
In-cell assay machine count rates	II-1,4; III-15,16
Sample inspection station assay machine count rates	All items
Sample weights	II-4, III-18,19,22
Particle size analyzer data	All items
Sample count	II-4; III-18,19
Block count	II-1
Waste can gamma-scan count rates	II-2
Waste can calorimeter	II-2
Waste drum gamma scanner (out of cell)	II-3

REFERENCE FOR SECTION 6

1. *HTGR Fuel Refabrication Pilot Plant — Conceptual Design Report*, GCR: 74-30, Volumes 1 through 4 (Nov. 1, 1974).

ACKNOWLEDGEMENTS

The authors wish to acknowledge the contributions of others to this work; in particular W. W. Rodenburg and K. C. Jordan of Mound Laboratory for information on calorimetry techniques; H. O. Menlove, LASL, for information on californium-source interrogation devices; E. V. Weinstock, BNL, for comments on the first draft; and W. L. Pattison for information on low-level ^{233}U waste assay. In addition, the authors thank H. R. Livesey for his artistic contributions, M. H. Wilson and M. E. Smith for typing and final document preparation, R. H. Powell for editing, A. G. Mason for performing many of the calculations, and A. R. Olsen and M. L. Tobias for their critical reviews.

ORNL-TM-4917
UC-77 — Gas Cooled
Reactor Technology

INTERNAL DISTRIBUTION

1-2. Central Research Library
3. Document Reference Section
4-6. Laboratory Records Department
7. Laboratory Records, ORNL R.C.
8. ORNL Patent Office
9. N. J. Ackerman
10. E. J. Allen
11. P. Angelini
12. R. L. Beatty
13. L. L. Bennett
14. A. L. Boch
15. R. A. Bradley
16. R. E. Brooksbank
17. W. D. Burch
18. A. J. Caputo
19. J. A. Carpenter
20. M. M. Chiles
21. J. A. Conlin
22. J. H. Coobs
23. D. Costanzo
24. F. L. Culler
25. F. C. Davis
26. W. P. Eatherly
27. G. G. Fee
28. P. A. Haas
29. W. R. Hamel
30. J. W. Hill
31. C. C. Haws
32. F. J. Homan
33-52. J. D. Jenkins
53. D. R. Johnson
54-56. P. R. Kasten
57. H. T. Kerr
58. R. W. Knoll
59. W. J. Lackey
60. A. L. Lotts
61. R. S. Lowrie
62. J. E. Mack
63-67. S. R. McNeany
68. J. T. Mihalczo
69. F. R. Mynatt
70. K. J. Notz
71. L. C. Oakes
72. A. R. Olsen
73. W. H. Pechin
74. Herman Postma
75. G. L. Ragan
76-80. J. E. Rushton
81. J. D. Sease
82. J. W. Snider
83. I. Spiewak
84. D. P. Stinton
85. W. E. Thomas
86. M. L. Tobias
87. D. B. Trauger
88. W. E. Unger
89. J. E. Van Cleve
90. T. N. Washburn
91. J. R. Weir
92. C. R. Weisbin
93. R. G. Wymer

EXTERNAL DISTRIBUTION

94-95. Director, ERDA, Division of Reactor Research and Development, Washington, D.C. 20545
96. Director, Reactor Division, ERDA-ORO
97. Research and Technical Support Division, ERDA-ORO
98-240. Given distribution as shown in TID-4500 under category Gas Cooled Reactor Technology (25 copies — NTIS)